Master's thesis

NTNU
Norwegian University of Science and Technology
Faculty of Engineering
Department of Civil and Environmental Engineering

Kevin Peter Cruz Sønsterud

Stability of Pipe Walls for Supporting Excavation in Cohesive Material

Master's thesis in Civil and Environmental Engineering
Supervisor: Steinar Nordal
July 2021

NTNU
Norwegian University of
Science and Technology

Kevin Peter Cruz Sønsterud

Stability of Pipe Walls for Supporting Excavation in Cohesive Material

Master's thesis in Civil and Environmental Engineering
Supervisor: Steinar Nordal
July 2021

Norwegian University of Science and Technology
Faculty of Engineering
Department of Civil and Environmental Engineering

NTNU
Norwegian University of
Science and Technology

Preface

This master thesis is written for the Geotechnical Group, Department of Civil and Environmental Engineering at the Norwegian University of Science and Technology (NTNU). The thesis is a continuation of the work done in the introductory report TBA4510 written in 2020.

The first part includes a literature review on pipe walls and the arching effect. In the second part the results of various Plaxis 2D simulations are analyzed. A range of different simulations have been carried out to investigate the stability and significance of soil parameters, soil gap ratio, shotcrete sealing and excavation geometry.

Trondheim, July 2021

Kevin Peter Cruz Sønsterud

Acknowledgments

I would like to thank my supervisor Professor Steinar Nordal for enthusiastic guidance along the way and good advice throughout the process. I would also like to thank Torbjørn Johansen and Kari Tilrem Ørjavik from Geovita for proposing an interesting problem and good discussions, as well as Professor Gudmund Eiksund for great help. Finally, I would like to thank my family and friends for their support, and especially my dear Thea for always being there to support and motivate me. K.P.C.S.

Abstract

A pipe wall is a good construction solution because it is adaptable, and has quick and simple construction stages. It can be bored through hard layers consisting of rocks, moraine and embankments, which is favorable because it is faster and simpler than other retaining solutions that may need preboring. Today, much of the design regarding center distance and the pipe dimension to secure stability is based on experience and engineering judgment. There are no standardized guidelines for cleaning of the pipes and excavation geometry.

In this thesis, various simulations are performed in Plaxis 2D, and different challenges are discussed to obtain an improved understanding of the critical parts of the stability. The simulations can be divided into two main categories, simulations with and without shotcrete. For the simulations without shotcrete, soil parameters such as cohesion and dilatancy are studied, as well as the center distance and the excavation geometry between the pipes. For the simulations with shotcrete, the geometry and placement of the shotcrete used to support the soil gap are studied, as well as the shotcrete adhesion to the steel pipes and center distance.

The results show that cohesion has a significant influence on developing the arching effect in the soil. The arching effect is crucial for obtaining stability before shotcrete is applied. The main objective for applying shotcrete is to secure long-term stability of the wall, which is necessary because the cohesion will be reduced over time. Therefore, the load on the concrete will increase over time. The concrete will ensure that the arching effect is maintained by supporting the soil so it does not loosen up and loose all the cohesion, as well as reduce erosion of fine-grained soil material and fallout of soil which would have led to further weakening of the arching effect. The majority of the cohesion in the soil comes from cementation of the soil where this solution usually is applied, and this will be reduced due to unloading from excavation.

High safety factors are obtained if the shotcrete comes on the inner side of the center point of the pipes, the challenge is if it only sticks to the unfavorable outer side of the pipes, because here it will essentially depend on the adhesion which is difficult to predict and is highly dependent on enough clean surface area on the pipe. The results from the parametric study of the adhesion shows that a sufficient stability is achieved with rather small values of adhesion strength.

The results from the investigation of soil squeezing under the excavation floor when the pipes end in soft to medium firm clay, show that as long as the pipes are not very short, the stability under the excavation floor is usually not critical.

The thesis concludes with a set of guidelines for preparing the soil pipes and soil gaps before applying the shotcrete in order to enhance the adhesion and shotcrete location between the pipes.

Sammendrag

En rørvegg er en anleggsteknisk god løsning, den er tilpasningsdyktig, og rask og enkel å gjennomføre med lite omfattende byggetrinn og uten behov for betydelig rigging. Rørene kan bores rett gjennom harde lag bestående av morene, steinfyllinger og blokkrik jord, noe som er gunstig ettersom det kan gjøres raskere og enklere enn andre støttekonstruksjoner som også kanskje trenger forgraving. En stor del av rørveggdimensjoneringen, med tanke på rørdimensjon og senteravstand for å sikre stabilitet under og over gravenivå, blir i dag basert på erfaringer og ingeniørmessig skjønn. Det er ingen standardiserte løsninger for rengjøring av rør, og omfang og geometri av utgraving mellom rørene.

I denne masteroppgaven blir ulike Plaxis 2D simuleringer utført og ulike problemstillinger diskutert for å øke forståelsen av de kritiske momentene ved stabiliteten til veggen. De utførte simuleringene kan deles inn i to hovedkategorier, simuleringer med og uten sprøytebetong. For simuleringene uten sprøytebetong har jordparametere som kohesjon og dilatans blitt undersøkt, i tillegg til senteravstanden og utgravingsgeometrien mellom rørene. For simuleringene med sprøytebetong har geometrien og plasseringen til betongen som støtter opp lysåpningen blitt studert, i tillegg til senteravstanden og heften mellom betongen og stålrørene.

Resultatene viser at kohesjonen har mye å si for å utvikle buevirkningen i jorden. Buevirkningen er helt avgjørende for å sikre stabilitet før sprøytebetongen påføres. Hovedgrunnen til å benytte sprøytebetong er for å sikre en langtidsstabilitet av veggen; den er nødvendig fordi kohesjonen vil reduseres med tiden og da vil spenningene løpe på betongen over tid. Betongen vil sørge for å opprettholde buevirkningen i jorden ved å redusere erosjonen av finstoff og utfall av jord som ville ha ført til svekkelse av buevirkningen, samt sørge for at jorden ikke løsner opp og mister all kohesjon. Kohesjonen i materialet kommer i hovedsak fra sementeringen som er mellom kornene i materialet.

Svært høye sikkerhetsfaktorer er oppnådd fra simuleringer der betongen kommer på innsiden av rørene slik at den kiles fast. Utfordringen blir når den ikke kommer forbi midtpunktet av rørene og må avhenge av heften for å henge på yttersiden av rørveggen, ettersom heftstyrken er vanskelig å forutse og veldig avhengig av ren overflate for å feste seg. Resultater fra parameterstudiet på heften viser at en oppnår tilstrekkelig stabilitet selv med forholdsvis lav heftstyrke.

Resultatene fra undersøkelsene gjort på skvising under gravenivå i bløt til middels fast leire viser at så lenge pelene ikke har en veldig kort forankringslengde ned i leira, så vil vanligvis ikke stabiliteten under gravenivå være dimensjonerende for lysåpningen.

Oppgaven konkluderer med et sett retningslinjer for forberedelser av rørene og lysåpningen før påføring av sprøytebetong, for å sikre heft og betongplassering mellom rørene.

Contents

Chapter 1

Introduction

1.1 Motivation

The demand for deep excavation for basements of high-rise buildings and tunnel stations is increasing and has been growing over the years due to urbanization [1]. Urbanization has increased the cost of land, and it is therefore necessary to excavate deeper to create underground floor space and parking space for multi-story buildings. Pile retaining walls are an excellent choice for deep excavation. A contiguous wall is a bored pile retaining wall option. Compared to other types of pile walls, the contiguous wall has the advantage of being more adaptable in the construction phase, quicker, and with simpler construction stages, which makes it fit well in urban areas. It is also a good solution considering that it is possible to drill through embankments and concrete slabs, which is common in urban areas.

The method of pile retaining walls is a good construction solution; however, it is expensive. Today, the engineering of the center distance and pipe dimension is mostly based on experience and engineering judgment because no practical calculation methods for this type of problem are available. The reason to study this problem is to ensure safety not only based on experience and engineering judgment and to get a better impression of the mechanics of the problem. This is achieved by simulating different scenarios and by performing a parametric study. With this information, some general guidelines can be formulated in order to help engineers with the calculations. Another important aspect of the study is to optimize the existing solutions, which may have significant economic potential considering the expenses of the retaining wall method. The method is frequently used in Norway.

1.2 Scope of the Thesis

A substantial part of the work done in this thesis has consisted of gathering knowledge from relevant literature, in addition to experience-based information from contractors and geotechnical consultants. This information forms a basis for discussions with the industry and academic supervisors on how to establish a suitable numerical model of the problem at hand. This interplay proved to be extremely valuable and deepened the problem understanding considerably. In any geotechnical structure, the coordination between theoretical aspects and practical considerations is crucial.

Through fruitful interdisciplinary discussions, a much more complete understanding of the problem was obtained.

In this thesis, the stability of the soil gap in a pile wall is investigated for a sandy material. It is of interest to investigate the effect of the concrete sealing in the soil gaps, and parameters such as soil gap ratio, cohesion and dilatancy. The effect of cohesion and dilatancy in the sand material has been studied along with the shotcrete sealing, and the soil gap ratio. The investigation is interesting because there are few parameter studies done of contiguous pile walls used in combination with shotcrete. The soil arching has been accounted for in the stability of the wall without concise information about the required spacing of the piles, based on experience. The stability the reinforced shotcrete provides by taking tensile stresses has previously not been considered. The lack of information requires the engineer to be more conservative than may be necessary. This results in more construction stages, a smaller distance between the piles than necessary and the use of reinforcement mesh where it may not be needed. In this thesis, the effect of soil arching and shotcrete is simulated and examined in Plaxis 2D to see how much they contribute. Results can be used to compare results and assumptions when designing contiguous pile walls and would therefore be of interest to consultants in the geotechnical field.

In this report, four central questions are investigated:

- What is the effect of the shotcrete?
- How does the soil gap ratio between piles affect stability?
- How much do cohesion and dilatancy affect stability?
- How does the geometry of the excavation and shotcrete sealing affect stability?
- How to avoid squeezing of clay under excavation floor?

1.3 Outline

First, relevant theory is presented in Chapter 2 with emphasis on the arching effect and the bearing capacity. This chapter covers different arching effect theories and examples. This will serve as a foundation to understand the mechanism that retains the soil behind the pile wall.

A literature review is then done in Chapter 3. The chapter covers literature on the wall and the wall construction. It includes some examples of different projects where contiguous pile walls have been used, which show the variety of application areas for the wall.

Chapter 4 is based on discussion with consultants and contractors from the field. Particular solutions and challenges both with construction and modeling are presented and discussed. From the discussions, guidelines to secure structure stability are formed.

Next, Chapter 5 covers the model, discussing boundary conditions and idealization of the problem, along with the simulation steps.

Finally, results from several simulations of the construction sequence are presented in Chapter 6, with further discussion in Chapter 7. The conclusion and further work are presented in Chapter 8.

Chapter 2

Theory

2.1 Lateral earth pressure

Earth pressure is an expression for the stress components, normal stress and shear stress, that works in the interface between structure and soil [2]. The effective stress is not the same in all directions; the vertical effective stress in the soil can be obtained from γZ, where γ is the unit weight of the soil and Z is the depth of the soil. The vertical stress is denoted σ'_v and is handled as principal stress. The horizontal stress, σ'_h, is given by $K\sigma'_v$. K is the coefficient of earth pressure and is used to relate the vertical stress to the horizontal stress. For a vertical wall this coefficient is $K = \frac{\sigma'_h}{\sigma'_v}$. The amount and type of movement of the wall have a major effect on the horizontal stresses developed. When there is no movement at all, the ratio of the stresses is given by the coefficient at rest K_0.

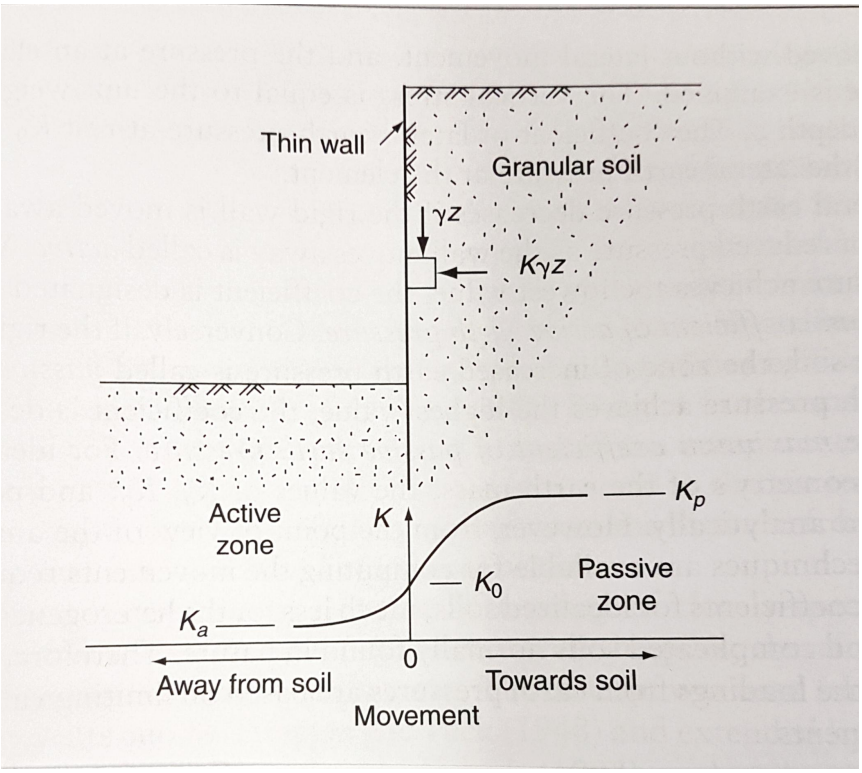

Figure 2.1.1

Estimating the earth pressure distribution is essential when designing a retaining wall. Different theories are available; Coulomb and Rankine are presented in this section. Both theories are based on the assumptions of a cohesionless, homogeneous and drained soil.

Various factors determine the horizontal stress acting on the wall, such as the wall flexibility, bracing and wall friction. The Rankine theory assumes a smooth surface, but in reality, it is usually rough. Friction between the wall and soil is produced by shear stress caused by movements. Contiguous bored pile walls are more rigid than steel sheet pile walls, deformation in a retaining wall due to lateral stress gives a redistribution of stresses because of stress transfer and arching [3]. This redistribution of stress increases as the wall deforms more. If the top part of the wall is braced with a prestressed anchor or strut and the prestress is large enough, the pressure behind the wall increases and could reach the passive pressure. The deflection is smaller at the bottom of the wall because of the passive resistance behind the wall at its toe.

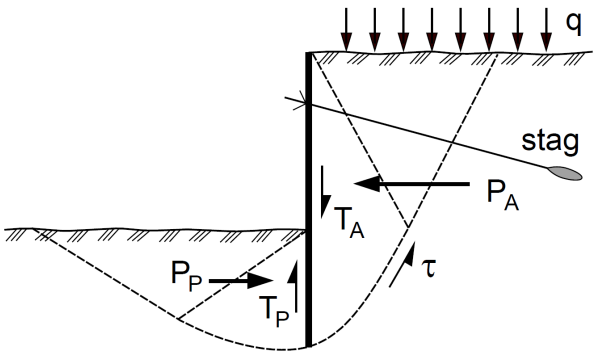

Figure 2.1.2: Earth pressure against a retaining wall with resultant forces and stress zones, taken from [4]

.

The stability problem for a retaining wall consists of the loads that keep the wall in equilibrium and the resulting stresses in the neighboring soil. The forces come from the bracing and the earth pressure, which depend highly on the shear strength of the soil. The shear strength also dictates the wall's ability to be stable without a bracing system. However, deep excavations are only possible when using bracing systems, or when the supporting structure is driven far into the ground. The retaining wall is usually designed with a bracing system denoted "stag" in Figure 2.1.2, in this case with a tension anchor, in order to reduce the dimensions of the structure. The dimension of the retaining wall, anchor force and installation depth of the structure need to be designed in order to take care of the stability and fulfill other guidelines such as ensuring that the deformations are within the requirements.

2.2 Dilatancy

The dilatancy can be explained through the analogy in Figure 2.2.1 shown below. The figure shows dense sand illustrated as densely packed spheres. To the left, shear strains are applied, and as illustrated, these strains demand an increase in volume. The shear strains make the soil (spheres) move, and the only way to move is to climb above each other. Thus, the increase in volume is given by a dilatancy angle, ψ. It is, therefore, reasonable to consider dilatancy as an addition to shear strain resistance [5].

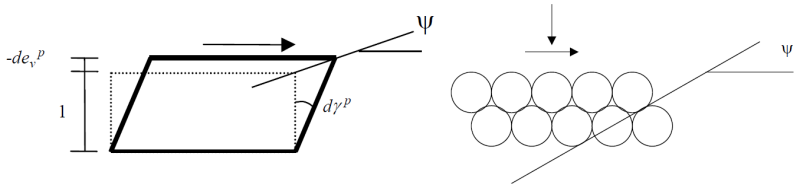

Figure 2.2.1: Densely packed grains (spheres) with a dilatancy angle. Dilatancy occurs when shear strains makes the grains climb above each other in order to move. Taken from [5]

.

The way that dilatancy works in drained Mohr-Coulomb is that it reacts to a confining pressure

by making the material stiffer. Under a foundation, dilatancy increases the strength since the soil can withstand more deformations. This is because the dilatancy causes a volume expansion which is restrained under the foundation, so the soil gets stiffer. This is described by the term confining pressure. At the edge of the foundation, the dilatancy will have no effect and does not contribute to the stiffness of the material, since volume expansion is not restrained, but the material has the possibility to dilate/expand outwards. The soil in an oedometer has the urge to expand because of the dilatancy but is restrained by the vertical pressure from the non-deformable steel ring that encloses the soil specimen. Therefore, the soil becomes stiffer, and the strength increases since it can withstand more deformations.

The stiffness dictates the relationship between deformation and stresses. With the extra confining pressure from the dilatancy, less deformation is achieved when applying the stress. The strength of the material dictates how much load the material can withstand before failure, the shear stresses in the soil need to be smaller than the shear strength. With an increased confining pressure, the soil shear strength increases, the same way it does in a triaxial test. In the Plaxis model, horizontal deformations are restrained, and the only deformation that is made possible by the model is through the steel pipes, which is similar to an oedometer test. As it does in an oedometer test, the dilatancy can have a favorable effect on the strength by increasing the confining pressure when plastic deformations occur. It is therefore interesting to study the dilatancy, but it is reasonable to have some caution since it can be nonconservative, as explained in Section 5.1.1.

2.3 Failure criterion

There are several failure criteria with different applications that are suitable for different uses and materials. Mohr-Coulomb and Rankine are used for brittle materials, while for ductile materials, the Von Mises and Tresca criteria are frequently used. Soil is defined as a brittle material. A failure criterion is a mathematical equation for the strength of a material and is expressed in terms of stress components and material properties [5].

2.3.1 Mohr-Coulomb

The Mohr-Coulomb criterion, often referred to as the Coulomb criterion, is probably the most important criterion for the strength of soil. The MC material model is used for modeling the soil. The basic formulation of the Coulomb criterion is in the $\tau - \sigma'$ plane see Figure 2.3.1a, and include parameters such as a $(attraction)$, c $(cohesion)$, and $tan\phi$ $(friction\ coefficient)$ where ϕ is the friction angle [5]. Cohesion is expressed by $c = a \cdot tan\phi$. The soil model's failure criterion is based on deviatoric stresses and mean stresses, and is known as a pressure-sensitive material model [6]. This main idea for pressure sensitive material models is that larger deviatoric stresses are allowed for larger mean stresses.

The strength limit for the material is represented by the failure envelope in Figure 2.3.1a, the definition of τ_f comes from Coulombs law (Coulomb, 1773):

$$\tau_f = c + \sigma' tan\phi = (\sigma' + a) \cdot tan\phi \tag{2.3.1}$$

In Figure 2.3.1b the criterion in the major and minor principal stress space is shown. The Coulomb line is defined by the attraction and the inclination N. The transformation to principal

stresses is based on Figure 2.3.1a from where the radius of the Mohr-circle is expressed by:

$$R = \frac{1}{2}(\sigma_1' - \sigma_3') = \left(a + \frac{1}{2}(\sigma_1' + \sigma_3')\right) sin\phi \tag{2.3.2}$$

which can be rewritten to:

$$(\sigma_1' + a) = N(\sigma_3' + a) \tag{2.3.3}$$

$$N = \frac{(\sigma_1' + a)}{(\sigma_3' + a)} = \frac{(1 + sin\phi)}{(1 - sin\phi)} \tag{2.3.4}$$

$'_3$ Where σ_1' is the maximum principal stress and σ_3' is the minimum principal stress. The inclination N will be in the range 1 to 5,8 for ϕ from 0° to 45°.
With a $\rho = 30° \rightarrow N = 3$. A useful relationship between the friction angle, ϕ, and the inclination, N, of the Coulomb line is:

$$\phi = asin\left(\frac{N-1}{N+1}\right) \tag{2.3.5}$$

The line tangent to the MC circle in Figure 2.3.1a is the reduced strength criterion. This gives a factor against failure. The attraction is left unchanged, so the reduced criterion is here defined by the mobilized strength $tan\rho$ showed in Equation (2.3.7), called mobilized friction. The reduced strength corresponds to a degree of mobilization f showed in Equation (2.3.6) [5]. Mobilized friction f may be seen to control the development of plastic shear strains developing when loading towards shear failure in elasto-plastic soil models based on the Coulomb criterion [5]. This happens because of the increase of plastic shear strains when approaching the Coulomb failure criterion, as illustrated by the degree of strength mobilization f:

$$f = \frac{\tau}{\tau_f} = \frac{(\sigma' + a) \cdot tan\rho}{(\sigma' + a) \cdot tan\phi} = \frac{tan\rho}{tan\phi} \tag{2.3.6}$$

$$tan\rho = f \cdot tan\phi = \frac{tan\phi}{F} = \frac{tan\phi}{\gamma_m} \tag{2.3.7}$$

where F is the safety factor and γ_m is the material factor.

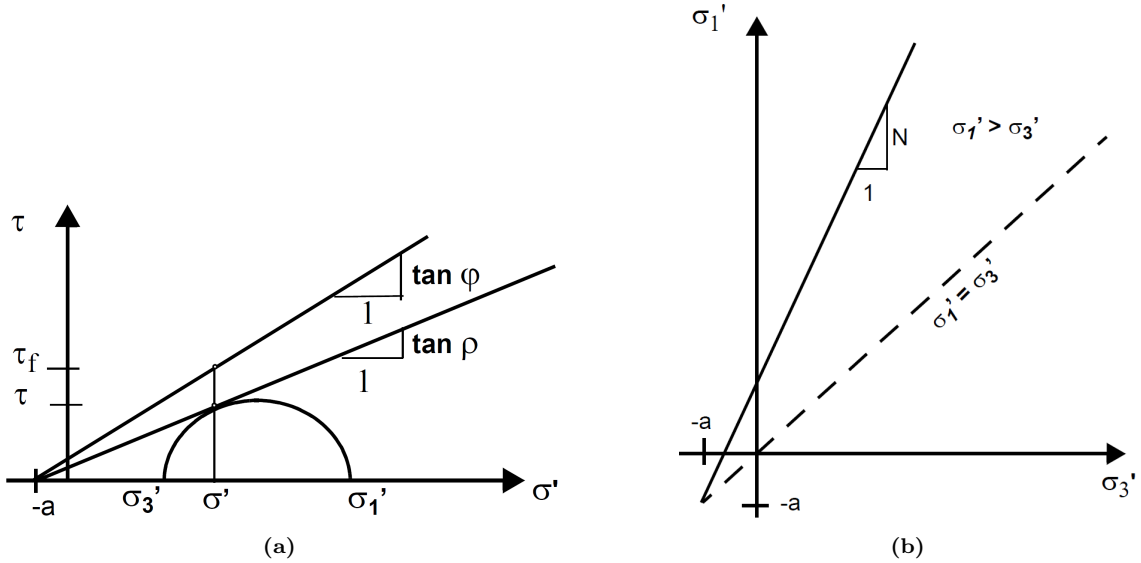

Figure 2.3.1: **a** Coulomb criterion in $\tau - \sigma'$ plane, the strength of soil is controlled by effective, normal stresses (σ'). The plot shows the mobilized strength $tan\rho$. Taken from [5]. **b** The Coulomb criterion in $\sigma_1' - \sigma_3'$ stress space, taken from [5]

Experiments have verified that the strength of soils is determined by the σ', and parameters c and $tan\phi$ should be considered as curve-fitting parameters to roughly fit a straight line to experimental results. The attraction indicates that tension stress is allowed, $\sigma' < 0$. Tension in real design is not accepted, c and a are both curve-fitting parameters and should not be viewed as some real cohesive or attractive (tensile) capacity [5].

The Mohr-Coulomb model is linear-elastic, perfectly plastic, and does not have a separate yield and failure criterion, which means that all the strains are elastic until the failure surface is reached, and then permanent plastic strains develop. When the stress state reaches the Coulomb failure envelope, unlimited plastic strains may occur. This is because the "plastic stiffness" is zero at this state [5]. The stress-strain relationship at failure will be flat as shown in Figure 2.3.2, but there will be a non-associated plastic flow controlled by the dilatancy ψ [5]:

$$\frac{d\epsilon_v^p}{d\epsilon_1^p} = \frac{-2sin(\psi)}{1 - sin(\psi)} \tag{2.3.8}$$

This will give a volume change of the soil when the soil has plastic strains as explained in Section 2.2. As mentioned in Section 5.1.1, the ψ is set to zero for the majority of the simulations, but some simulations with $\psi = 5°$ are performed, which from experience often may be a realistic value.

The stiffness is set by Hooke's law, which has a constant stiffness and is isotropic. In practice, soils may have anisotropic stiffness behavior and may experience stress and/or strain-dependent stiffness. The MC model does not account for this, and the chosen stiffness is an average value, see Figure 2.3.2. This model is competent for numerical simulations aiming for ultimate loads such as bearing capacity.

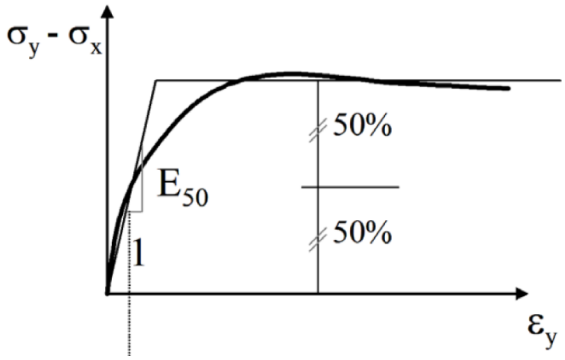

Figure 2.3.2: The stiffness used in the MC model, E_{50}, is an average value of the soils stiffness. Taken from [5]

2.3.2 Norwegian soil parameters

Some average values for the Coulomb strength parameters, a and $tan\phi$, for Norwegian soil are presented in Table 2.3.1.

The purpose of the table is to illustrate what the typical strength parameters are for Norwegian soils, which is interesting for a parameter study of the soil parameters. The values are only indicative and useful for a parameter study, but they are not exact and must not be used instead of sufficient soil investigations and experimental parameter determination in practice. Due to several factors such as stress level and mineralogy, large variations occur for the parameters [5]. As mentioned in

Section 2.3.1, attraction is a curve-fitting parameter that for low stresses has a significant effect on the results, and may not be valid at low levels. The approximated line deviates from the curve made from experimental results, both for low and high stress levels as shown in Figure 2.3.3. Therefore, one must be careful to use high values for the attraction at low stress levels.

Table 2.3.1: Some typical values for effective stress parameters, according to Norwegian experience. Values from [5]

Soil	**Attraction, a [kPa]**			**Friction angle, φ**		
Clay	5-10	15-25	30-60	21,8	26,5	31
Silt	0	0-10	10-20	26,5	31	35
Sand	0	0-15	15-40	31	35	38,6
Condition	Loose	Medium	Dense	Loose	Medium	Dense

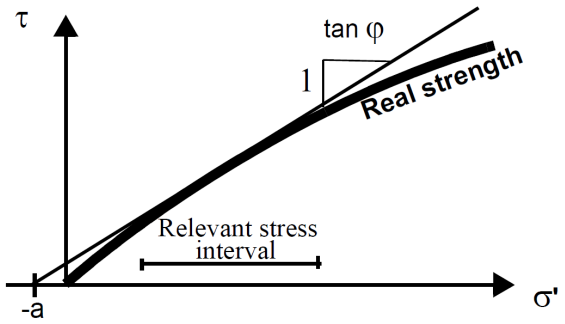

Figure 2.3.3: Real strength form experimental results approximated by a straight line with curve fitting parameters a and $tan\phi$. Taken from [5]

2.3.3 Tresca-criterion

The Tresca-criterion is used as the failure criterion for the shotcrete in the Plaxis model. It is modeled using a linear elastic, perfectly plastic material curve and is formulated using the coulomb-criterion. This is done by setting the value of $\sin\phi = 0$. The failure line in a principal stress plot for a Tresca-criterion is horizontal, and it cuts the σ_1-axis for a stress equivalent to $2c$, c is the cohesion parameter. A B20 concrete is utilized and has a uniaxial compressive strength of 20 MPa; more about the concrete can be found in Section 4.2. 20 MPa is the diameter in the Mohr circle, and the radius becomes the cohesion of $c = 10MPa$.

The failure line in Figure 2.3.4 intersects the σ_1-axis at $2s_u$ and at this point $\sigma_3 = 0$, this is the situation that can be found in a uniaxial stress apparatus used to find the undrained strength of soil, [2]. Figure 2.3.4 also shows that if the major and minor principal stress axes changed place, a similar failure line intercepting the abscissa in the $2s_u$-point would occur. The plot illustrates an upper and lower limitation, independent of the principal stress σ_2, for the allowed stress deviation between the principal stresses. The Tresca-criterion in a three-dimensional stress space can be shown if the intermediate principal stress σ_2 is included [2]. The Tresca-criterion in three dimensions is illustrated in Figure 2.3.5 with the principal stresses as the axes.

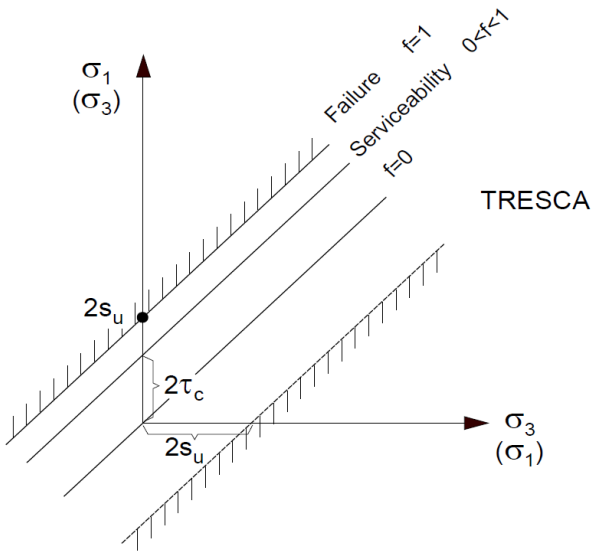

Figure 2.3.4: Tresca-criterion in a principal stress diagram, the line with a 45° angel and intersecting the σ_1-axis at a stress level $2s_u$ shows the failure criterion, taken from [2]

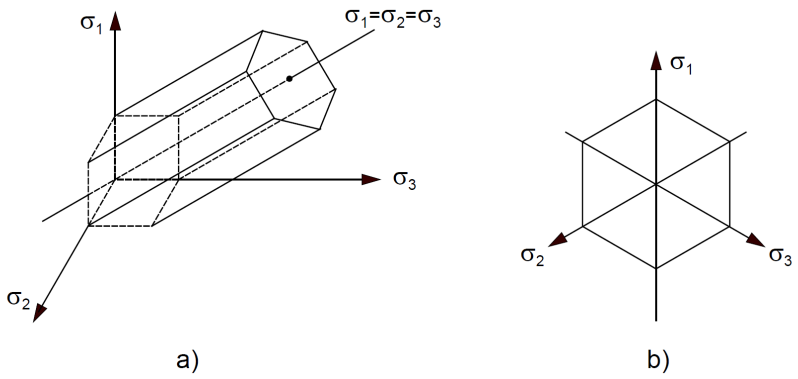

Figure 2.3.5: (a) Tresca-criterion in a three-dimensional stress space, taken from [2]. The isotropic stress condition is locates along the central line in the hexagon shaped surface made by the Tresca failure lines. (b) Tresca criterion in the π-plane

The lines shaping the hexagon surface in Figure 2.3.5 are the limit for allowed stress combinations. The figure shows that according to the criterion, the material has the same shear capacity in tension, which is not the case for soil material, as most soils have an insignificant capacity in tension. In the Plaxis software, the "tension cut-off" function found in material settings may be used to introduce a tensile strength to the material. As explained in the Material Models Manual from Plaxis [7], for the Mohr-Coulomb model, the tension cut-off is, by default, selected with a tensile strength of zero. In some practical problems, tensile stresses may develop, and according to the Coulomb failure line shown in Figure 2.3.6 this is allowed when the shear stress is sufficiently small. The soil may fail in tension instead of in shear and can be handled in Plaxis by selecting an appropriate tension cut-off value, often zero.

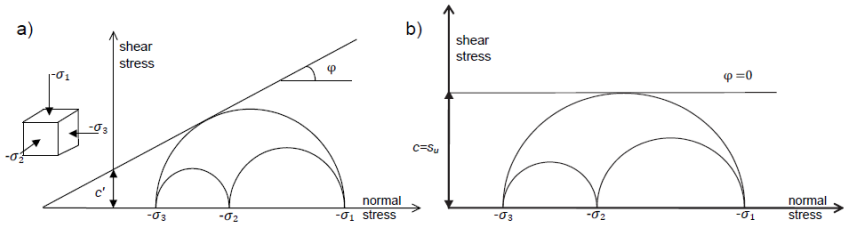

Figure 2.3.6: (a) Shows a stress circle at yield utilizing Mohr-Coulomb effective strength parameters. (b) Tresca-criterion using undrained strength parameters, by setting the cohesion equal to the undrained shear strength and $\phi = 0$, from Plaxis Material Models Manual [7]

2.4 Arching effect

2.4.1 Definition of arching effect

Arching in geotechnics is the phenomenon of stress transfer through the mobilization of shear strength. The arching effect will reduce the stress in the yielding parts of soil mass and transfer this to adjacent stationary soil mass or restrained parts of the soil mass [8]. In 1943 Terzaghi described the phenomenon of pressure transfer from a yielding mass of soil to the adjacent rigid boundaries by a trap door test, explained in Section 3.1. The shear stresses in the transition zone between the moving and the stationary soil masses will support the yielding part since shearing resistance tends to maintain the moving soil in its original position. The shear stresses are created by the relative displacements of the two masses. Because of this, the yielding mass has a reduction of pressure which is transferred to the stationary part. The pressure transfer explained here and found in Terzaghi's experiment is called the arching effect, and the soil is said to arch over the yielding part of the support. This effect occurs when there is a localized displacement along with any restraining structure which confines a soil mass [9]. This happens both in the horizontal and vertical directions.

In practice, examples of soil arching may be found on tunnels and pipes, originating from vertical soil movement. Atkinson and Potts (1977) [10] and Bolton (1979) [11] studied soil arching in connection with the stability of tunnels, and between adjacent piles in a pile wall, used as either retaining wall for a construction pit or slope stabilizing. Slope stabilizing pile walls are further discussed in Section 3.2 and Section 2.4.2. For this situation, the arching is caused by horizontal soil movement and was found to occur when the soil attempted to squeeze through the fixed piles [9]. The arching transfers the stresses from the yielding soil in the soil gap to the restrained piles on the sides.

2.4.2 Arching in pile walls

In contiguous pile walls, the adjacent piles' gap can be freely exposed without sealing and still be stable, which is possible with a relatively small soil gap (S). Therefore, the gap ratio:

$$\frac{S}{D} = \frac{soil\ gap}{diameter\ of\ pile} \tag{2.4.1}$$

becomes a crucial factor that influences the short-term performance of the pile wall. The mechanism that makes this possible is the arching effect that occurs in the soil between the piles. This is

produced in the gap between the piles and is acting against a lateral earth pressure. For designing a retaining wall system, the most important aspects are the estimates of the limiting pressure behind soil gaps and the lateral force acting on the piles.

In the article Centrifuge Study of Soil Arching in Slope Reinforced by Piles from Lei et al. [12] the soil arching in a piled sandy slope is modeled in a centrifuge, and its role in slope stability is analyzed. A series of centrifuge tests are conducted of a 90° slope reinforced by piles with different spacing. Figure 2.4.1 shows the dimensions of the model. From the results of the tests, it was observed two failure modes of soil arching. Firstly, the soil arch tends to fail at the dome when the pile spacing is large. Secondly, the soil arch tends to fail at the pile-soil contact when the pile spacing is small. The slope went through a plane sharing failure, which produced a wedge-shaped moving mass that is divided into three soil zones.

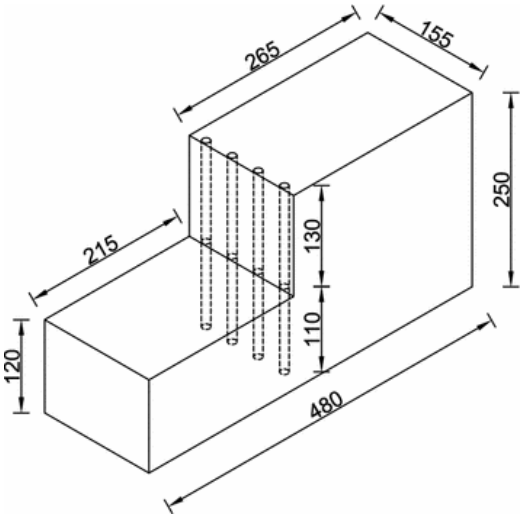

Figure 2.4.1: Geometry of the centrifuge model, taken from[12]

As can be seen in Figure 2.4.3, three soil zones are defined in the soil behind the piles. The soil in zone 1 is barely supported by the piles. In zone 2, the friction between the soil and the pile surface is what mainly reinforces the soil, corresponding to frictional soil arching. In zone 3, the main soil arching is formed, according to Li et al. [13]. In the tests performed in the article, it was shown that zone 1 failed early, then zone 2 failed, and lastly, zone 3 failed. It is seen that the failure of zone 3 implies a complete failure of the soil behind the wall. Zone 3 contributes the most to the arching effect and thus is the most interesting area. Assisting the existence and integrity of zone 3 by shotcrete will therefore be very beneficial.

The Figure 2.4.2 shows the failing process from above and how the failure of the different zones looks. The piles have a gap ratio of 3,88. It can be observed that there is a big influence from the friction of sidewalls on the soil behavior, making the failure first occur in the middle.

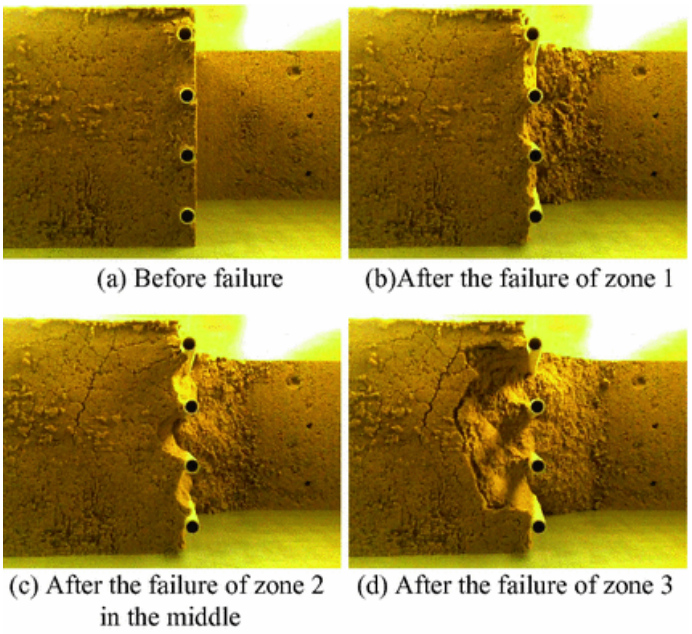

Figure 2.4.2: Failure process of a reinforced slope with soil gap ratio $\frac{S}{D} = 3,88$. Taken from [12]

Adachi et al. [14] did an analysis on the preventive mechanism that occurs in landslide stabilizing piles and made a drawing of the problem definition with results, see Figure 2.4.3 [12]. In the paper, the development of arching in granular material is explained, and they found that the soil in the points B, C and D, inside the arching zone is not affected by the pressure from the slope against the piles. These points are within zone 1 and 2, and thus the end-bearing soil arching in zone 3 takes the most load, Li et al. [13] did also conclude with this, and numerical studies by Chen et al. [8] and Liang et al. [15] have shown that zone 3 contributes the most to the arching effect, by a big rotation of principal stress directions in this zone.

Lei et al. [12] found that even though zone 3 contributes the most to arching, losing the confinement of soil in zone 1 and zone accelerates the failure of zone 3.

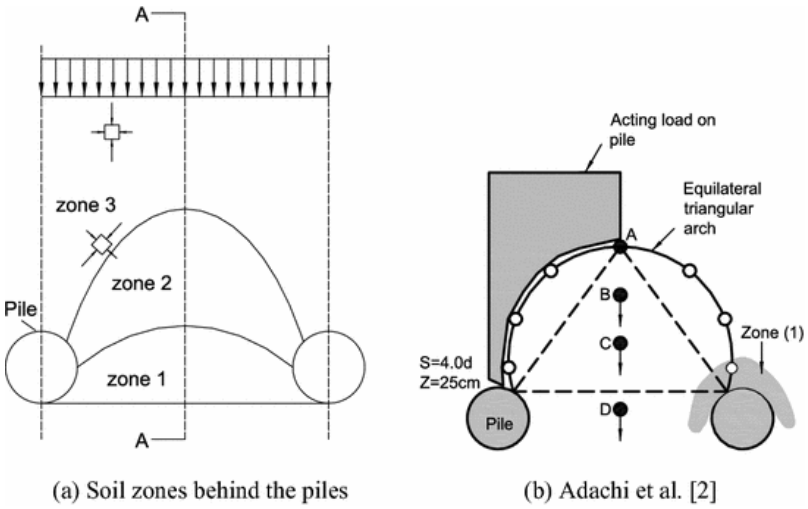

Figure 2.4.3: Division of arching effect zones, according to [12]

2.5 Bearing capacity

A classic bearing capacity failure occurs if a foundation of limited dimensions is subjected to a sufficiently large load. This will cause shear failure under the foundation. Further, the foundation will enter the soil, and the soil masses will be pushed up on the sides of the structure. The bearing capacity for a structure is the greatest response that the system can resist. The bearing capacity is characterized by three different stress zones: the active and passive Rankine zones and the Prandtl zone. In Figure 2.5.1a a combination of these critical shear zones is shown. The bearing capacity is obtained when these three stress zones are combined, together with boundary conditions.

The greatest development of shear strain is along the lines enclosing the stress field in Figure 2.5.1a. This is where a potential failure will occur. The stress field must be able to give a reaction from the soil that is in equilibrium with the actions from the load.

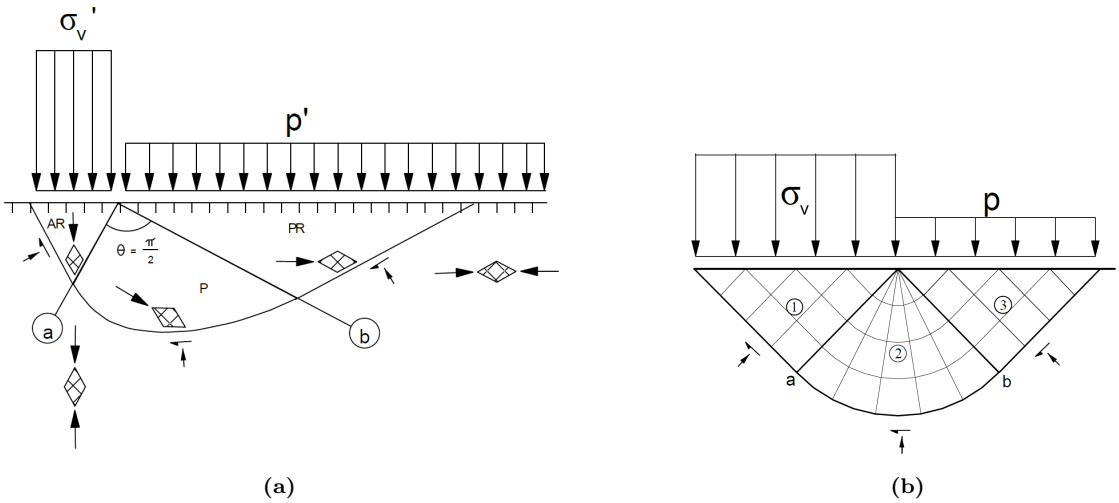

(a) **(b)**

Figure 2.5.1: **(a)** Combination of shear zones for bearing capacity for an effective stress analysis. taken from [2]. **(b)** Combination of shear zones for bearing capacity, centred vertical load, for a total stress analysis. Taken from [2].

2.5.1 Undrained shear strength Su analysis

Under the foundation there is an active Rankine zone; it is connected to a Prandtl-zone which links it to a passive Rankine zone outside the foundation, see Figure 2.5.1b. If there is a load p on the side of the foundation as shown in Figure 2.5.1b, the difference between the foundation stress σ_V and p gives the shear stress in the soil. Combining these zones for a Su analysis the bearing capacity formula is obtained:

$$\sigma_V - p = N_c \cdot \tau_c \rightarrow \sigma_v = N_c \cdot \tau_c + p = 5,14 \cdot \tau_c + p \tag{2.5.1}$$

N_c is the bearing capacity factor for total stresses.

2.5.2 a-ϕ analysis

The relation between the major principal stress σ_v and the smaller vertical stress p' is derived by combining the equations for the three stress fields from Figure 2.5.1a. The bearing capacity formula for an effective stress analysis:

$$\sigma_v + a = N_q(p' + a) \tag{2.5.2}$$

The bearing capacity factor N_q for vertical load is given by:

$$N_q = N.e^{\pi tan\rho} \tag{2.5.3}$$

2.6 Reversed bearing capacity

In figure 2.6.1, a fundamental drawing of the stability problem is shown; it is a reversed bearing capacity problem. The bearing capacity q can become great even if the p' is rather small. The

support of the exposed soil gap produces the load p'. The reason is that the p' is multiplied by the N_q factor. The effect of cohesion is seen from

$$a = \frac{c}{tan\phi} \tag{2.6.1}$$

and the attraction will contribute to the initial stresses necessary to initiate and obtain a developed arching effect, where the attraction is included in Equation (2.6.2). The p' comes from the sealing of the soil gap, either with shotcrete or steel plates as explained in Section 4.1. The q is provided by the piles. When q increases, the sand pressure acting on the shotcrete arc increases, making the p' increase. The p' represents the load on the shotcrete, and if this becomes too high, the shotcrete may fail.

The excavation is mostly done in friction material, and a small p' will increase inwards in the stress fields because of the log spiral see Figure 2.6.2, which is the factor $e^{\theta \cdot tan\rho}$ in Equation (2.6.3). The initial stress p' has an considerable effect because it is accelerated through a friction system. This is the same effect which helps a person to hold back a boat at the dock with the help of a puller. The rope is laid around a puller a few times, and because of the friction between the rope and the puller, the initial force holding back the boat is multiplied and becomes a large force. Between the pipes a little initial stress p' might be enough to initiate arching and this will increase by itself. The same effect is found in tunnels. For some projects a thin layer with reinforced shotcrete is used as protection and sprayed around the surface, this gives a rather small initial stress at the surface. This initial stress is then built up inwards in the stress field, and makes the tunnel stable.

$$(q + a) = N_q \cdot (p' + a) \tag{2.6.2}$$

$$N_q = N \cdot e^{\theta \cdot tan\rho} \tag{2.6.3}$$

For undrained condition, p was added to the bearing capacity, see Equation (2.5.1). For drained friction material the p' is multiplied with Nq. p' is accelerated through the stress field and increases the capacity significantly. In Figure 2.6.1 a principal drawing of the model from Plaxis is shown.

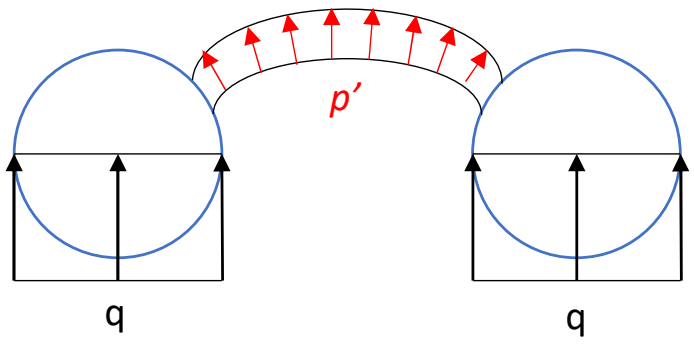

Figure 2.6.1: The bearing capacity problem.

Figure 2.6.2 shows different log spirals for different values of $tan\rho$, and it shows that the spiral becomes a circle for $tan\rho = 0$. Increasing the value of $tan\rho$ opens up the spiral, which means that stress fields of log spiral shape will gradually open up with increasing mobilized friction.

For s_u-analysis the Coulomb criterion in Section 2.3.1 is used, and the friction angle is set to zero $\phi = 0$ as explained in Section 2.3.3. Since $\phi = 0$ for this situation the log spiral produces a circle and therefore the Prandtl zone becomes a circle as seen in Figure 2.5.1b.

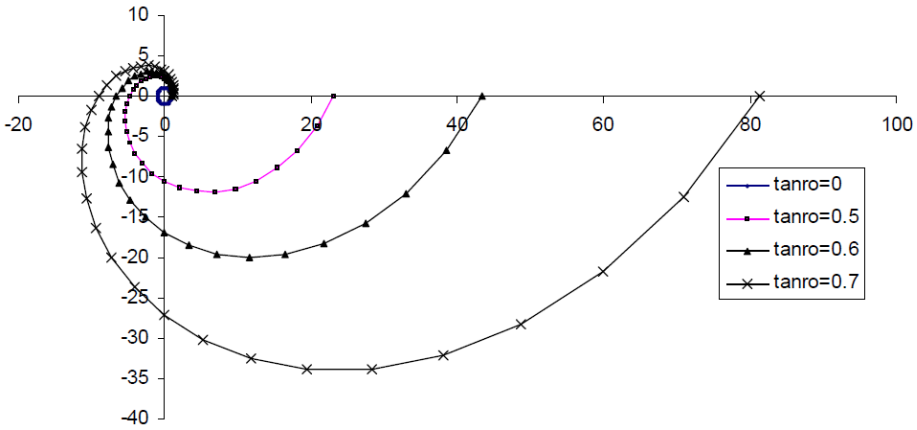

Figure 2.6.2: Plot of the log spiral with different values of $tan\rho$. It has an initial radius r=1. Taken from [2]

N_q is a function of the shear mobilization $tan\ \rho$ and roughness number r between the soil and surface. As explained in the compendium for the course *Geoteknikk beregningsmetoder* [4], the connection between the foundation stress and the vertical stress on the side of the foundation is given by the bearing capacity factor N_q. In the figure 2.6.3a a diagram of N_q is illustrated, as well the N_c factor for undrained conditions.

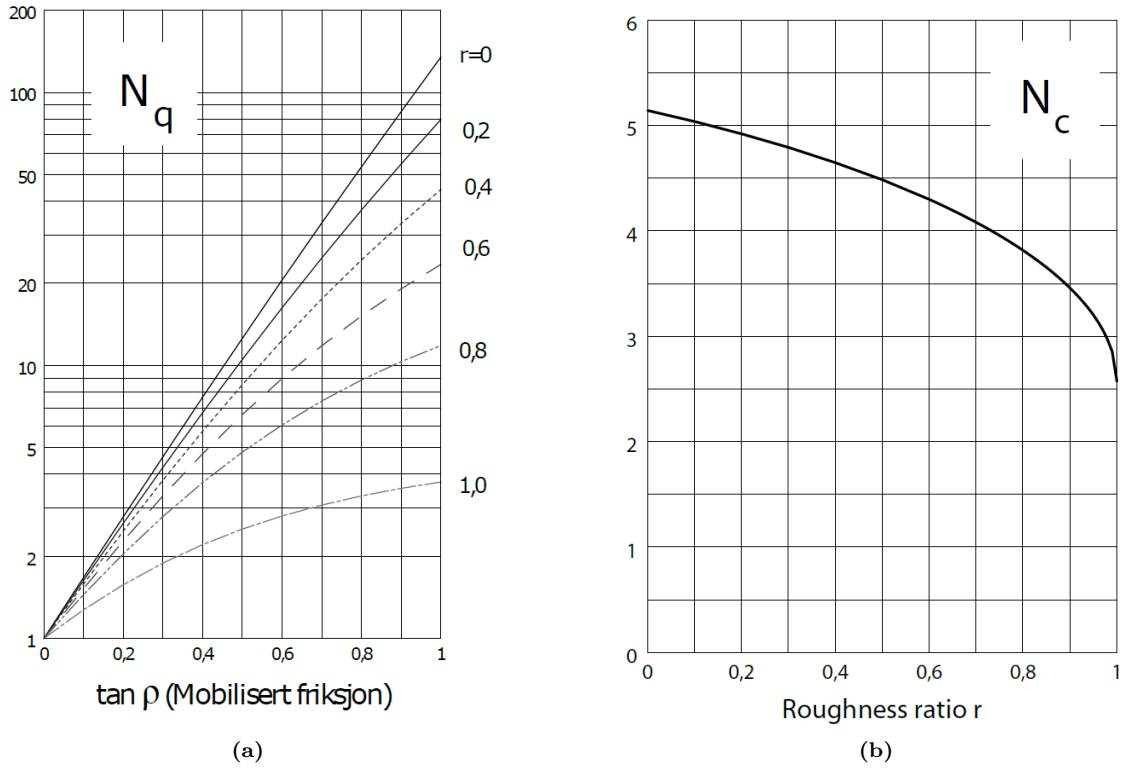

Figure 2.6.3: **a** Bearing capacity factor N_q for $a\phi - analysis$. N_q is a function of the shear mobilization $tan\phi$ and the roughness ratio r between the soil-structure interface. **b** Bearing capacity factor N_c for $s_u - analysis$ becomes a function of the roughness ratio r. Taken from [2]

The drawing of the problem shown above, with the location of q and p', has similarities to the ultimate bearing capacity of strip foundations with Terzaghi's theory. The failure mechanism can also be seen to be similar to the failure mode of Terzaghi's shallow strip foundation [16] in figure 2.6.4 shown below.

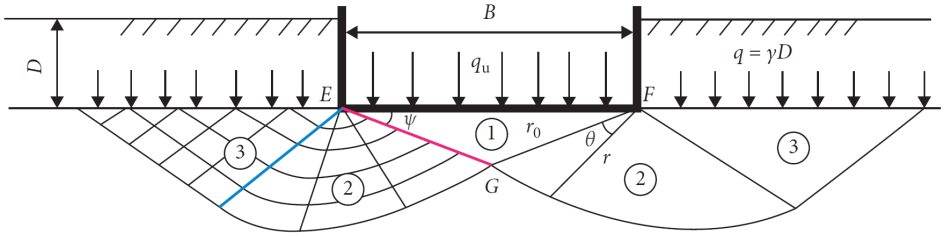

Figure 2.6.4: Failure mode of strip foundations based on Terzaghi's theory, taken from[16]

2.7 Calculation of collapse loads

In order to provide safe designs, it is vital to know the capacity to make sure the loads do not exceed this. This capacity is often denoted collapse loads and has traditionally been calculated by some limit equilibrium method [5]. The Finite Element Method (FEM) is a powerful tool and is an alternative way to calculate collapse loads. More details about the FE software are found in Section 2.8. Usually, the FEM finds a collapse load by increasing the load until large deformations occur, assuming this means failure. The results are approximate, and it is therefore essential to know how accurate they are if the method is going to be safe to apply [5]. Exact limit load solutions may be used to verify the accuracy of FEM simulations.

2.8 Plaxis Theory

Plaxis is a finite element software employed for geotechnical problems. The FEM is an approximate numerical method that can be applied to solve numerous different engineering problems. The theoretical method called the displacement method is applied when using the FEM for geotechnical problems. This theory involves loading a structure or a soil body and then study the response in terms of displacements or deformations. Plaxis was developed at TU Delft in the Netherlands in the 1980s, while the initial use of the FEM in geotechnical engineering took place towards the end of the 1960s, with the further theoretical development of the method in the '70s and '80s. The development continues today.

In Plaxis 2D, which is utilized for the simulation in this investigation, there are two different types of elements to choose from, the 6-noded element and the 15-noded element. For every simulation, the 15-noded element has been used, which provides the highest order of integration and gives the highest accuracy. The 15-noded elements have shown to capture failure conditions better than the 6-noded elements [17]. In Plaxis 2D, the 15-noded element is also the default choice.

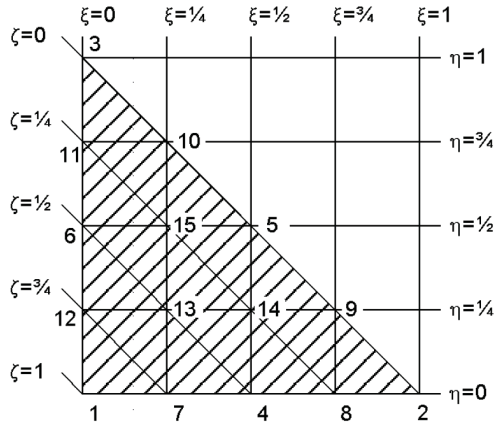

Figure 2.8.1: 15-node triangular element with local numbering and arranging of nodes. Taken from Plaxis Reference manual [18].

The obtained results from the FEM calculations are not exact, and the method gives approximate solutions. Nevertheless, it can provide excellent estimates, and many of the problems do not

have an exact solution. The quality of the results obtained from FEM simulations is also affected by simplifications and adjustments made when modeling the actual problem, such as soil properties, geometry, and boundary conditions. It is important to have a good problem definition so that the simplifications made when modeling are realistic, as well as input parameters and soil model. Various elements can be assessed to enhance the accuracy of the Plaxis results, such as appropriate use of interface elements and value (R_i), selecting the right element for the problem and the extent of the soil volume modeled, S. Nordal [5].

2.8.1 Calculations

To run a simulation in Plaxis, a process including modeling the geometry with the acting forces, generating the appropriate mesh with required refinements, and defining the construction stages has to be done. Each of these calculation phases is generally divided into several steps. This is because the non-linear behavior of the soil requires that the load is applied in small steps. Plaxis is able to do an appropriate sub-division automatically. The loading is then applied in small steps, and the calculation is divided into steps in order to successfully complete the phase [17].

In the simulations, the first calculation phase (initial phase) calculates the initial stress field for the geometry by performing a K_0 procedure. The subsequent phases and calculation types are defined by the user. For the following phases, the staged construction loading type is selected, and in the last phase, a $c - \phi$ reduction safety calculation is done. The staged construction loading type makes it possible to specify a new state that is to be reached at the end of the calculation phase (Plaxis reference manual) [17]. This calculation is performed by using the Load advancement ultimate level procedure, which is controlled by a total multiplier ($\sum Mstage$). At the beginning, the multiplier starts at zero and is expected to reach 1 during the calculation, which means that the calculation has properly finished. If the multiplier does not reach 1 it means the calculation is not properly finished and that the out-of-balance force is still unresolved. There are several reasons why this could happen:

- The $\sum Mstage$ value is set less than 1.
- The maximum number of loading steps was not enough.
- During the calculation a failure occurred in the soil body.

One reason to set the total multiplier to less than zero in the pipe wall case is to let the soil arching take up stresses before the rest of the stresses are taken up by the concrete. This in one of several ways to simulate the situation where the stresses are gradually transferred to the concrete, further explained in Section 5.2. If the value is set to 0,5, then at the end of the phase, 50% of the unbalanced forces is solved. Then in the following phase, the support is activated, and the total multiplier is set to 1 so that 100% of the remaining unbalance is solved. With the following equations, it is possible to estimate the load that has actually been applied:

$$f_{applied} = f_0 + \sum Mstage(f_{defined} - f_0) \tag{2.8.1}$$

where $f_{applied}$ is the applied load, f_0 is the load at the beginning of the calculation phase, which comes from the previous phase. The $f_{defined}$ is the total load that is defined for the phase [17].

To calculate the global safety factor, Plaxis offers a safety calculation by performing a $c\phi - reduction$. This method provides safety factors consistent with requirements in the design codes. A new phase needs to be added, and the calculation type needs to be changed from Plastic to Safety. To reach failure of the modeled problem, the tensile strength and the shear strength parameters $\tan\phi$ and c are continuously reduced until failure.

The safety calculation is executed using the Load advancement number of steps process, which utilizes the incremental multiplier M_{sf}. The M_{sf} determines the increment of the strength reduction of the first calculation step. The default for Plaxis is $M_{sf} = 0,1$, and this value is used for the simulations. The Plaxis reference manual has concluded that it is a generally good starting value. When a safety calculation is performed, the total multiplier $\sum M_{sf}$ is utilized to find the value of the soil strength parameters at that given phase in the simulation. The parameters with the subscript "*input*" in the equation below are the input parameters from Material sets. The parameters denoted with the subscript "*reduced*" are the reduced values in the calculation. When Plaxis starts calculating, the reduced parameters are the actual input values for the material strength, which gives $\sum M_{sf} = 1$. Then the strength parameters are reduced until Plaxis finds a mechanism that provides a failure, resulting in a $\sum M_{sf} > 1$.

The way Plaxis finds the failure mechanism is by running a $c\phi - reduction$ calculation, where the strength parameters are lowered. Then some stresses will violate the reduced failure criterion, so that the surrounding elements that still have capacity will take up stresses from the parts with overextending stresses. This is an iteration process that will go on reducing the stress incrementally until a certain soil area is fully plastified and creates a failure mechanism. Stresses can then no longer be redistributed, and the stiffness of the kinematic failure mechanism turns zero, S. Nordal [5]. Deformations will increase dramatically towards the end of the $c\phi - reduction$ calculation. The MSF (multiplier for safety factor) is the ratio between actual strength and reduced strength, and it is equal to "factor of safety" (SF).

$$\sum M_{sf} = \frac{\tan(\phi_{input})}{\tan(\phi_{reduced})} = \frac{c_{input}}{c_{reduced}} = \frac{s_{u,input}}{s_{u,reduced}} = \frac{Tensile\ strength_{input}}{Tensile\ strength_{reduced}} \tag{2.8.2}$$

To obtain a well-developed plastic failure mechanism and a safety factor, it is important to check if the calculation has converged to a solution. If it has not converged, then Plaxis needs to be allowed to continue calculating until it has a well-developed failure mechanism. This sometimes demands a considerable amount of calculation steps.

2.8.2 Mesh generation

The geometry needs to be divided into finite elements (FE), and this construction of FE is called a mesh. The mesh should be fine enough to obtain accurate numerical results, but not exaggerated, this leads to immoderate calculation time. Plaxis has an automatic generation of FE meshes, based on a triangulation procedure [17]. The process accounts for boundary conditions, structural objects and loads included in the geometry. Mesh refinements are available, and it is favorable to have a fine mesh in areas where there are plastic deformations and occurring failure mechanism.

Deformed mesh

The deformed mesh is a plot of the finite element model in the deformed shape. By default, the deformations are scaled up to give a plot that may be conveniently read. If it is desired to view the deformations on the true scale, then the scale option may be used. The deformed mesh plot may be selected from the Deformations menu.

2.9 Interfaces

Interfaces are utilized around the piles in the model, which is necessary to allow for accurate modeling of soil-structure interaction and give it the right friction. They are, for example, used to simulate the thin zone of intense shearing between a plate and the adjacent soil. Interfaces in Plaxis are joint elements inserted next to plate elements or between two soil volumes. The connection to soil elements is shown in Figure 2.9.1 below. The interface element has zero thickness, and as shown in Figure 2.9.1, the elements are defined by five pairs of nodes when connected to 15-node elements. The interfaces are used to specify a lower shear capacity along a structural surface than in the neighboring soil. This is done by defining a roughness number:

$$R_{inter} = \frac{(shear\ stress\ capacity\ on\ the\ interface)}{(shear\ stress\ capacity\ in\ neighboring\ soil)} \tag{2.9.1}$$

in the material definition. The strength reduction factor (R_{inter} is used to choose the roughness of the modeled interaction. Another reason to use interfaces is that it is recommended as an efficient alternative to extreme mesh refinement in the soil close to structural elements.

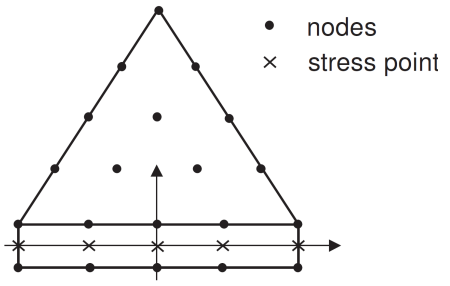

Figure 2.9.1: Connection between 15-node soil element and interface element, and distribution of nodes and stress points in interface elements. Taken from [17]

The soil and pipe are tied together if an interface is not applied between them. When they are tied together, there will be no relative displacement (slipping/gapping) between structure and soil. It is called slipping when there is relative movement parallel to the interface, and gapping when there are relative displacements perpendicular to the interface. Both slipping and gapping could be expected when the interface is elastic. The size of the interface displacements according to Plaxis reference manual [17]:

$$Elastic\ gap\ displacement = \frac{\sigma}{K_N} = \frac{\sigma t_i}{E_{oed,i}} \tag{2.9.2}$$

$$Elastic\ slip\ displacement = \frac{\tau}{K_s} = \frac{\tau_i}{G_i} \tag{2.9.3}$$

All the variables in Equation (2.9.2) and Equation (2.9.3) are interface parameters. The t_i is the virtual thickness, K_N is the elastic normal stiffness, K_S is the elastic shear stiffness, G_i is the shear modulus and $E_{oed,i}$ is the one-dimensional compression modulus of the interface [17].

As can be seen in Figure 2.9.1, node pairs are created at the interface where one node belongs to the soil and the other to the structure. The interaction between these two nodes consists of two elastic-perfectly plastic springs, one to model the gap displacement and one to model the slip displacement [19]. In Figure 2.9.2 a soil-structure connection is showed, with and without interface.

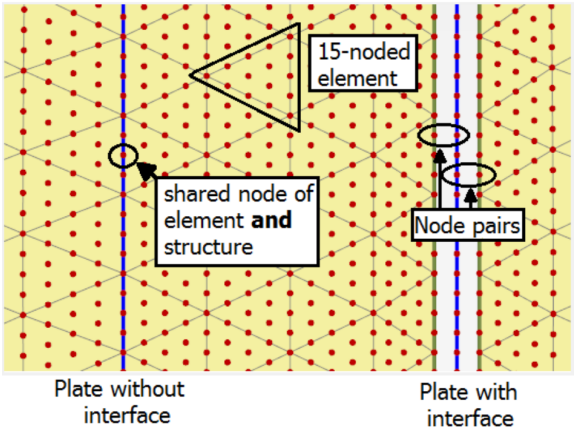

Figure 2.9.2: Connectivity plot of node pairs, showing the connection between soil element and structure element, with and without interface element. and distribution of nodes and stress points in interface elements. Taken from [19]

2.9.1 Strength and stiffness properties of the interface

The interface strength is the achieved friction and adhesion. The strength properties for the material and its corresponding R_{inter} value are directly in control of the level at which plastic slipping happens. The Coulomb criterion is used to distinguish between elastic behavior (small displacements can occur) and plastic behavior (where permanent slip may occur). The required parameters are, by default, taken from the material in the neighboring soil cluster. The R_{inter} relates the interface strength and stiffness to the strength and stiffness of the soil. However, it is also a possibility to choose a material set for the interface, which allows direct control of the strength properties without changing the properties of the adjacent soil cluster [17]. To keep the interface in the elastic domain, the shear stress τ needs to be less than:

$$|\tau| < -\sigma_N \, tan\phi_i + c_i \tag{2.9.4}$$

where σ_N is the effective normal stress, and c_i and ϕ_i are the cohesion (adhesion) and friction angle of the interface [17]. Plastic behavior is obtained when τ is:

$$|\tau| = -\sigma_N \, tan\phi_i + c_i \tag{2.9.5}$$

The reduced strength properties of the interface are calculated from the R_{inter} and the soil parameters, as shown below:

$$c_i = R_{inter} \, c_{soil} \tag{2.9.6}$$

$$tan\phi_i = R_{inter} \, tan\phi_{soil} \leq tan\phi_{soil} \tag{2.9.7}$$

$$\psi_i = 0^\circ \; for \; R_{inter} < 1, \; otherwise \; \psi_i = \psi_{soil} \tag{2.9.8}$$

The tension cut-off criterion also applies to the interface and is reduced if not deactivated. For undrained condition (C), the calculation is performed with undrained strength parameters. The undrained shear strength of the interface is calculated from the undrained shear strength of the soil with an R_{inter} as follows:

$$s_{u,i} = R_{inter} s_{u,soil} \tag{2.9.9}$$

The calculation of the elastic shear and normal stiffness of the interface springs are based on the stiffness of the interface, and those properties are also, by default, taken from the adjacent soil. The program chooses the stiffness so that numerically instability is avoided and elastic deformations are negligible [19]. A material set may also be applied directly to the interface in this case, which gives the possibility to influence the stiffness of the interface directly. The R_{inter} affects both the strength and the stiffness properties.

Interfaces usually have a lower shear capacity than the adjacent material, at least for the soil-structure interfaces and the concrete-steel interface in this project. Especially when modeling the contact and adhesion between the shotcrete and the steel pipes the *Rinter* can become very low. If the R_{inter} value is very low, the interface stiffness may be reduced to the extent where it becomes so low that possibly unrealistic gapping between soil and structure occurs. The stiffness becomes so low because it has a quadratic dependency of R_{inter}.

2.9.2 Choosing the R_{inter} value

The friction between soil-structure elements is an intermediate between smooth and fully rough. To obtain the desired behaviour, the material properties of an interface have to be chosen. In the program, there are two available options, "From adjacent soil", and "Custom". For the first option, the surrounding material must have a specified strength reduction factor, see Equation (2.9.1). In practice, the real soil-structure interaction is weaker and more flexible than the surrounding soil [17]. R_{inter} should therefore be less than 1, and in cases where suitable values are not available, it may be assumed an R_{inter} in the order of $\frac{2}{3}$ [17]. If the value of R_{inter} is very low, the stiffness may become so low that it could result in unrealistic gapping between soil and structure.

2.10 Deconfinement and β-method

The β-method in Plaxis is originally used to simulate tunnel construction with a shotcrete lining. These types of tunnels are constructed following the New Austrian Tunneling Method (NATM). It is a way to simulate the shotcrete layer between the piles, described in Section 5.2.1. For tunnel construction, it helps simulate the construction process by accounting for the three-dimensional arching effect and the deformations that occur in the soil surrounding the unsupported tunnel face. The method is called Converge confinement method (Schikora & Fink, 1982).

The method divides the initial stresses p_k acting around the construction area into two parts. The first part $(1-\beta)p_k$ is applied to the unsupported tunnel and the second part βp_k is applied to the shotcrete support. A schematic representation of the process is given in Figure 2.10.1.

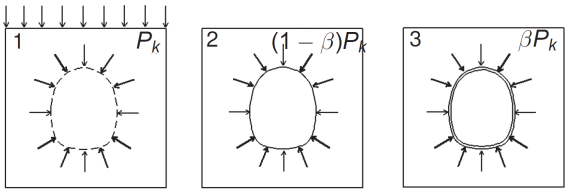

Figure 2.10.1: The figure shows the surface of a NATM tunnel. The initial stresses are shown step 1, which are divided, and taken by arching in the surrounding soil (step 2) and at last the tunnel support (step 3). Taken from [17]

.

The program retains a part of the stresses (β) as support pressure in the soil cluster that will be removed (inside the tunnel) while it is deactivated. In the next phase, this supporting pressure is taken away or reduced.

2.11 The Poisson ratio and K_0'

In oedometer conditions, the Poisson ratio controls the lateral stress coefficient K_0. This relation comes from the Poisson's ratio ability to control the tendency of traversal expansion (S. Nordal) [5].

In an oedometer the increase of stress in the horizontal direction from vertical loading is given by the requirement:

$$\Delta\epsilon_3 = \frac{1}{E}(-\nu\Delta\sigma_1' - \nu\Delta\sigma_2' + \Delta\sigma_3') = 0 \tag{2.11.1}$$

when $\Delta\sigma_2' = \Delta\sigma_3'$:

$$-\nu\Delta\sigma_1' + (1-\nu)\Delta\sigma_3' = 0 \tag{2.11.2}$$

The resulting horizontal stress becomes:

$$\Delta\sigma_3' = \frac{\nu}{1-\nu}\Delta\sigma_1' \tag{2.11.3}$$

The K_0 is defined by $\frac{\Delta\sigma_3'}{\Delta\sigma_1'}$, and the relation between coefficient at rest and Poisson's ratio is therefore:

$$K_0' = \frac{\nu}{1-\nu} \tag{2.11.4}$$

Chapter 3

Literature study

This chapter includes a literature review of slope stabilizing contiguous pile walls, the arching effect, and lateral resistance of laterally loaded piles in undrained conditions. In addition, a general literature review is done of the construction of contiguous pile walls, with emphasis on the most common small diameter steel pipes used in Norwegian pipe walls, see Section 3.3, and pipe wall solutions used in Norway, see Section 3.3.1. A review of bracing systems that may be used is also performed, see Section 3.4.

3.1 Calculating undrained limiting pressure behind soil gaps and lateral force acting on a pile in pile walls

In the paper from (S. Keawsawasvong et al.) [1], a finite element limit analysis (FELA) software, with plane strain conditions, is used to determine the upper and lower bound solutions of the undrained limiting pressure factor $\left(\frac{p}{s_u}\right)$ behind soil gaps and lateral force factor $\left(\frac{F}{s_u D}\right)$ acting on a pile per unit length in a contiguous pile wall. A parametric study of the soil gap ratio $\left(\frac{S}{D}\right)$ and adhesion factor (α) at the soil-pile interface is done to cover practical ranges of this problem. The $\frac{S}{D}$ factor is varied between 0.1–3 and α is varied from 0 (smooth) to 1 (rough). A closed-form approximate equation is also proposed for a convenient and accurate prediction of $\frac{p}{s_u}$ and $\frac{F}{s_u D}$ for a contiguous pile wall in practice [1].

In the figure below, a problem definition of undrained limiting pressure behind soil gaps in a contiguous pile wall is shown. The clay in this study [1] has an isotropic and constant undrained shear strength (s_u) and is assumed to behave as a perfectly plastic Tresca material following an associated flow rule.

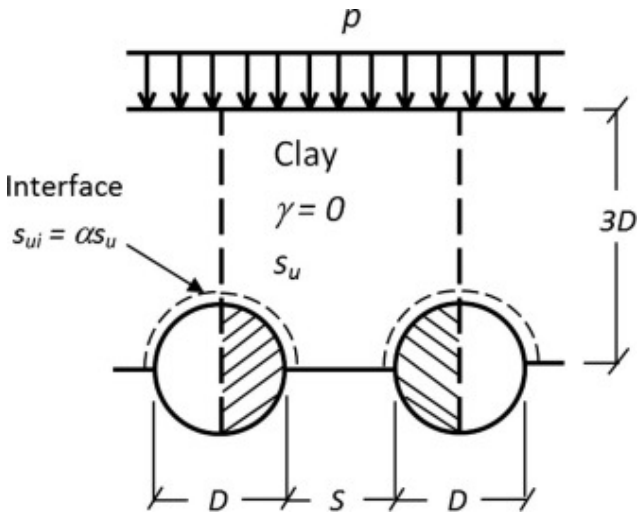

Figure 3.1.1: Problem definition of undrained limiting pressure behind soil gaps in contiguous pile walls from [1]

The adhesion factor (α) at the soil-pile interface is considered in the same study [1]. The definition of α is:

$$\alpha = \frac{s_{ui}}{s_u}[1] \tag{3.1.1}$$

where s_{ui} = undrained shear strength at soil-pile interface
s_u = undrained shear strength of surrounding soil

The α is what is refereed to as R_{inter} in Section 2.9.

The applied pressure p in Figure 3.1.1 represents the earth pressure that comes from the weight of the soil. The soil is considered weightless in the analysis because of the assumption of plane strain that is applied to the direction of pile depth. The goal is to determine the undrained limiting pressure p that causes failure in the soil gaps, and this pressure p can be expressed as the dimensionless parameters [1]:

$$\frac{p}{s_u} = f\left(\frac{S}{D}, \alpha\right) \tag{3.1.2}$$

where

$\frac{p}{s_u}$ = undrained limiting pressure factor behind soil gaps

$\frac{S}{D}$ = soil gap ratio

The lateral force per unit length (F) of one pile can be calculated with vertical force equilibrium. From the product of the limiting pressure (p) and the corresponding width of the free body diagram ($S + D$), a dimensionless relation between F and p can be find:

$$\frac{F}{s_u D} = \left(\frac{p}{s_u}\right)\left(\frac{S}{D} + 1\right) \tag{3.1.3}$$

where
$\frac{F}{s_u D}$ = lateral force factor acting on a pile per unit length in a contiguous pile wall [1].

The arching effect problem, in this case, might be partly similar to the active trapdoor test first studied by Terzaghi [20]. The boundary conditions in this study and the undrained active trapdoor test are significantly different, so the existing solutions can not be used for this problem.

The model of Terzaghi's original trapdoor experiment is shown in Figure 3.1.2. The shearing resistance along the slip surface (ac and bd) is mobilized against the downward movement when the trapdoor is lowered. The slip surface is the border between the yielding and the stationary soil. This mechanism will reduce the pressure acting on the trapdoor since the mobilized shearing resistance tends to keep the yielding mass in its original position. This pressure reduction due to shearing resistance is known as soil arching [20]. It can be seen in Figure 3.1.2 that the two sliding surfaces begin at an angle of $45 + \frac{\phi}{2}$ degrees from the outer edges of the base and end at a 90° angle when reaching the top surface.

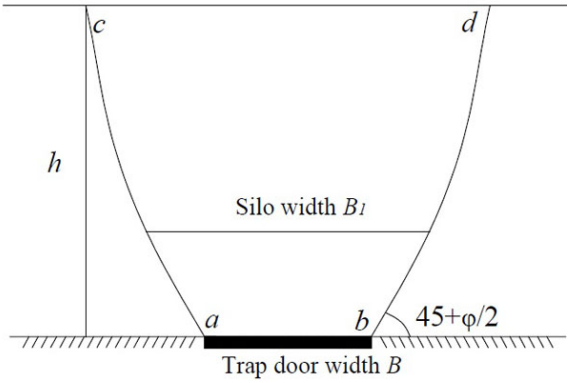

Figure 3.1.2: Terzaghi's soil arching model using the trapdoor test, taken from [21].

Ito and Matsui [22] studied the arching effect between a row of stabilizing rigid piles, see Figure 3.1.3. They employed the limit equilibrium method with a postulated failure mechanism to predict the lateral force acting on a pile per unit length for cohesive-frictional soils. Their expression for $\frac{F}{s_u D}$ with cohesive soil is:

$$\frac{F}{s_u D} = \left(1 + \frac{S}{D}\right)\left(3log\left(1 + \frac{D}{S}\right) + \frac{D}{S}\tan\frac{\pi}{8} - 2\right) \tag{3.1.4}$$

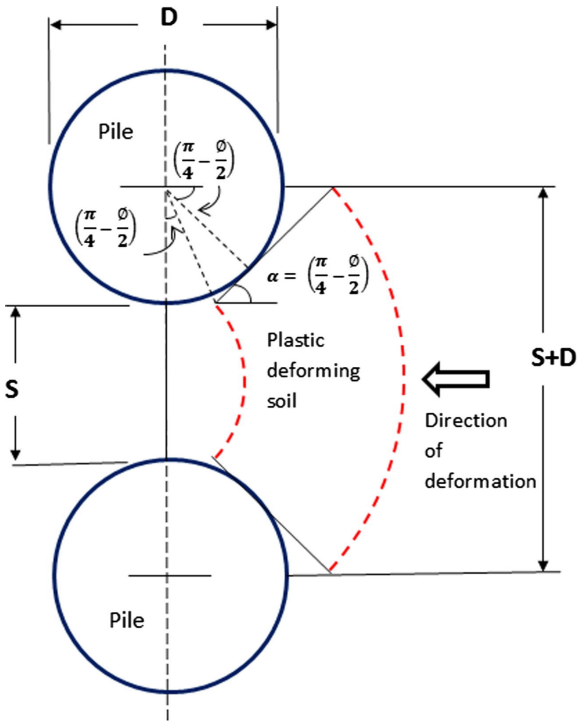

Figure 3.1.3: The postulated failure mechanism in the limit equilibrium calculation by Ito and Matsui [22]. The plastic deformation of the soil between the piles comes from the arching effect produced by the stabilizing piles.

There have been done several studies on the arching effect in soils. Examples are in [23, 8, 9, 22, 12]. Nevertheless, no plasticity solution for limiting pressure behind soil gaps in contiguous pile walls has been found [1]. To compare the results for $\frac{F}{s_u D}$ and $\frac{p}{s_u}$ done in this study [1], three relevant existing solutions are used for comparison [22, 24, 25].

In the study from Haema and Tanseng [25], which is one of the solutions that are used to compare the results in [1], a physical model was used to study the failure of soil gaps. High-quality block clay samples were used in the experiment.

From observations of the failure mechanism in the experiments, the limit equilibrium solution of $\frac{p}{s_u}$ was derived, see Equation (3.1.5).

$$\frac{p}{s_u} = \frac{1}{S}\left(S + D + \frac{\alpha D \pi}{2\sqrt{2}}\right) \tag{3.1.5}$$

The FELA software OptumG2 is used to perform the simulations. The model is symmetrical and consists of only one quarter of the rigid circular pile and one half of the soil gap. The piles are rigid, and interface elements are defined along the pile surface. The sides are fixed horizontally, the bottom is a free surface and a pressure p is applied on the top boundary.

For the cases with a rough pile with $\alpha = 1$, the failure mechanisms are evident and changing for different soil gap ratios, from $0,1 - 3,0$. For $\frac{S}{D} = 0,1$, the shear band behind the pile is circular and intersects the other pile. For $\frac{S}{D} = 0,5 - 1,0$, the shear zone behind the gap is more triangular,

and the shear band still intersects the other pile but is more curved due to the enlargement of the shear zone. For larger soil gaps, the shear bands intersect the bottom line. The arching effect is revealed by the direction of the major principal stresses, which curves from one pile towards the other for small soil gaps and that travels to touch the bottom line for bigger soil gaps. The plots of the major principal stress path form an arch-shape.

The soil gap ratio has a significant influence on $\frac{p}{s_u}$, see Figure 3.1.4. In the same figure, the influence of α can also be noted. For smaller soil gap ratios, the adherence factor has a large significance on $\frac{p}{s_u}$. For larger $\frac{S}{D}$, the α has less effect, and for $\frac{S}{D} = 0,1 - 0,3$, the difference for $\frac{p}{s_u}$, between smooth and rough piles, are found to be 29–76%.

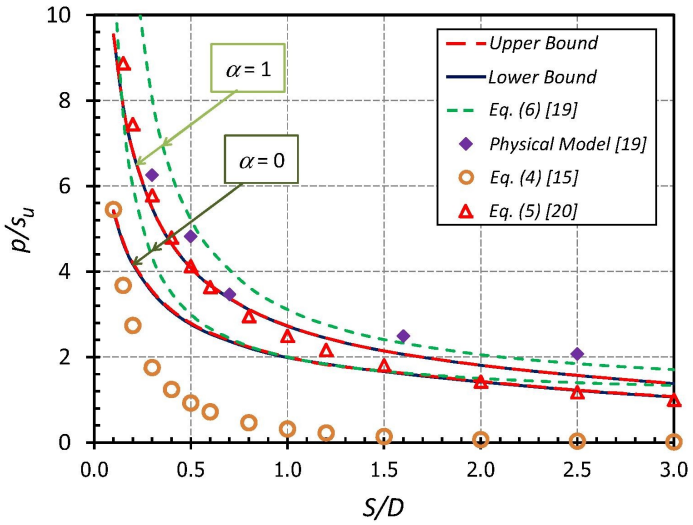

Figure 3.1.4: Undrained limiting pressure factor $\frac{p}{s_u}$ as a function of soil gap ratio, for different adhesion factors (α). $\frac{p}{s_u}$ obtained from FELA is compared to other existing solutions. Taken from [1]

For the undrained limiting lateral pile force factor $\frac{F}{s_u D}$, larger values are obtained for small soil gaps. It is rapidly reduced when increasing the soil gap and becomes constant for $\frac{S}{D} > 2$, as presented in Figure 3.2.1.

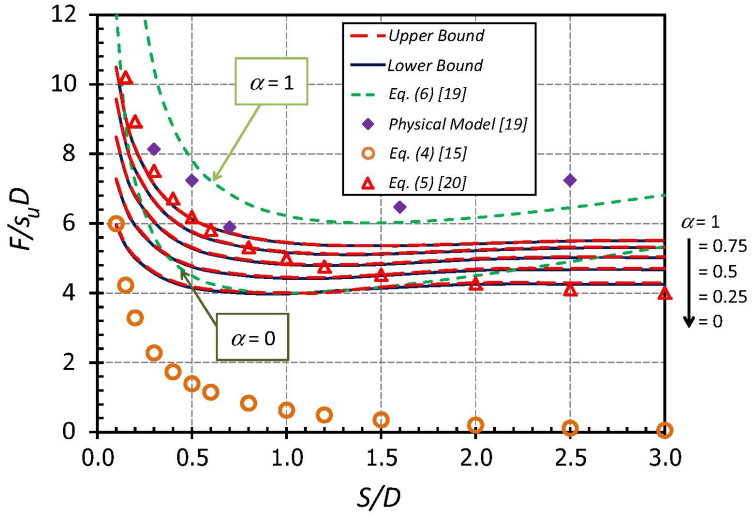

Figure 3.1.5: Undrained limiting lateral pile force factor $\frac{F}{s_u D}$ as a function of soil gap ratio $\frac{S}{D}$, the upper and lower bound solutions from this study compared to other solutions. Taken from [1]

The result comparisons do not fit very well and there are limitations of the methods mentioned above. The different methods gave both safe and unsafe predictions of the solutions. The FELA simulations and the other solutions had the same trend and proved that both the soil gap ratio and adhesion factor had a significant effect on the dimensionless solutions of the limiting pressure behind soil gaps and the lateral force acting on the pile per unit length.

3.2 Landslide stabilizing piles

Slope stabilizing piles has proven to be effective against excessive slope movement. The general practice for this solution is to install the piles at a sufficient depth preferable into a firm layer underneath a potential sliding surface [15]. Bosscher and Gray did laboratory tests on soil arching in sandy slopes, where the piles were simulated by a swing gate with varying width. Their results show that closer pile spacing increases the arching effect. Both engineering practices and laboratory experiments have shown that discrete piles installed in a slope into a firm layer will significantly increase the soil stability if the conditions for soil arching are met (Bosscher et al., 1986). Liang and Zeng (2002) [15] did a 2D FEM analysis on a horizontal soil-pile slice subjected to in-plane soil movements. They did a parametric study of the effect of several soil parameters and the soil gap ratio for both cohesive and cohesionless soils. This was done to study the soil arching mechanisms associated with the drilled shaft stabilized soil slopes [15]. The soil gap ratio, $\frac{S}{D}$, was found to have the greatest influence on both the development and intensity of soil arching. For the cohesionless soils, a higher friction angle was central to transfer more soil stress to the piles, but the cohesive soils had a greater tendency for soil arching. Only a small cohesion value was needed to fully develop soil arching, although it might be that the tendency of cohesive soils to creep may cancel out the arching to some extent. The long-term creep effect should therefore be taken into account for global stability of stabilized slopes.

Chen and Martin (2002) [8] used a 2D FE plane-strain model to simulate the development of plastic yielding and failure modes for the pile-soil interaction for landslide stabilizing piles for different soil conditions. They linked the arching effect to pile load-displacement curves obtained

from the 2D finite difference analysis, in order to explain how the stresses transfer from the soil to the pile. Various pile and soil parameters were studied for both drained and undrained soil conditions. The effect of interface roughness and soil dilatancy and the comparison between active and passive pile response are notable.

3.2.1 2D and 3D analysis

Using a plane-strain 2D model to study soil arching between piles has been done on several occasions. A 3D model has often been used to verify the applicability of 2D models, like in [8].

3.2.2 Laterally loaded piles

Broms (1964) was the first to treat the failure load of latterly loaded piles in detail. The key quantity in the results was the limiting pressure, which is the force per unit length on the pile. An empirical value of $9s_u$ for the limiting pressure was assumed for cohesive soil. Randolph and Houlsby (1984) [26] presented an exact calculation of the ultimate lateral resistance at depth to horizontal movement. Classical plasticity theory was used to derive the exact solutions with theoretical justification. The non-dimensionalized load factor $\frac{p}{cd}$ was found to vary between 9.142 for a smooth pile and 11.94 for a rough pile, shown in Figure 3.2.1.

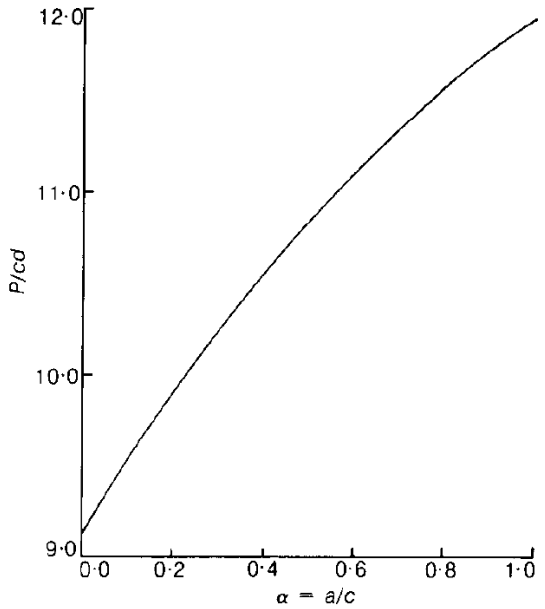

Figure 3.2.1: Shows the variation of the limiting pressure $\frac{P}{cd}$ with the adhesion ratio $\alpha = \frac{a}{c}$. Taken from [26]

The solutions are based on a rigid, perfectly plastic response of the soil with a shear strength independent of the total stress level. The soil is assumed to deform at constant volume, in agreement with the associated flow rule, see Section 2.3.1. A pile moved horizontally through the soil by a lateral load will have an area of high mean stress in front of the pile and a low stress behind. The soil will flow around the pile from the front to the back. When the pile is not smooth, a triangular

region in front of the pile will be produced. This region remains rigidly attached to the pile, and full adhesion is not mobilized at the surface. This zone becomes larger for a larger degree of roughness. The deforming zone around the piles is shown in Figure 3.2.2, for the smooth pile it is rather small, and for a perfectly rough pile the deforming area is larger. When studying plastically deforming cohesive soil, it is usual to work in terms of the characteristics of shear bands, which are the planes with the maximum shear stress.

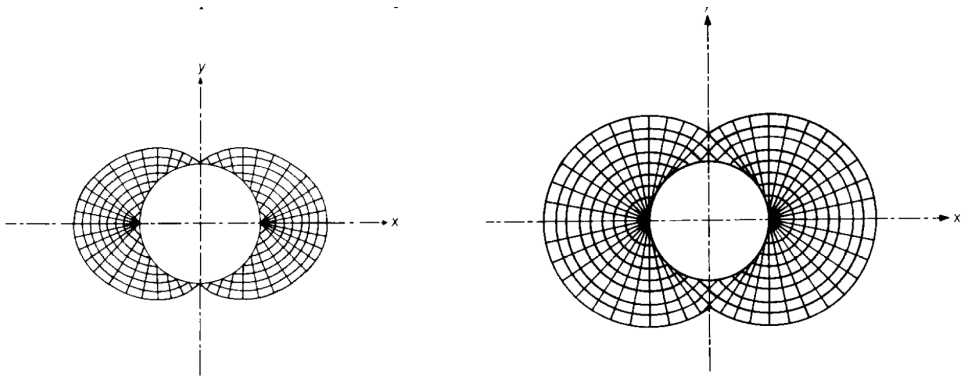

Figure 3.2.2: Examples of characteristic meshes. The mesh to the left is for a perfectly smooth pile with an $\alpha = 0,0$. The characteristic mesh to the right is for a perfectly rough pile. It has a significantly larger deforming region which explains the higher obtained resistance. In front of the rough pile the rigidly attached triangular region can be seen, this region is not present for a perfectly smooth pile. Taken from [26]

3.3 Bored pile wall consisting of tubular steel pipes

The most common piled retaining walls in Norway are bored steel pipes. Internationally concrete piles are frequently used. They are used for deep excavations and do also have a larger axial capacity.

In this thesis, tubular steel pile walls are studied. For projects in Norway, steel pipes have been used, usually with a diameter 168-324 mm, and are defined as micro piles [27].

The piles can be installed with reinforcement and are usually cast with concrete. The steel pipe has a considerable capacity, and reinforcement may therefore potentially be skipped. In Norway, these piles are usually called RD (Ruukki Drilled) for small diameters. The solution is often used in rock-rich masses, where sheet piling is impossible, or in places with limited space or special noise requirements. For rocky ground conditions, drilling pipes is also more gentle to the soil than driving sheet pile walls. This method is therefore a good alternative in urban areas where driving sheet pile walls through hard and rocky top layers without inflicting undesired deformations on nearby structures is challenging [28]. The drilling rig for pipes with a diameter of 168-324 mm is small and is a good solution for places with limited space. The advantage of these piles is that they are thick-walled and are usually bored with a centric drilling system utilizing a ring-bit or alternatively wings. This is a better drilling system when drilling in rock fills and sloping rock surface, compared to eccentric drill bits (Odex). Both internally and externally, bracing is suitable for contiguous pile walls, as will be discussed later in Section 3.4.

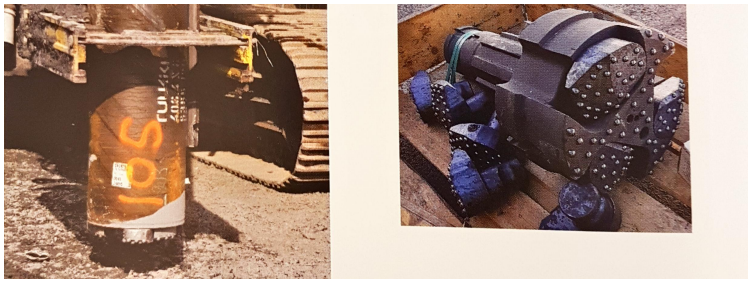

Figure 3.3.1: Shows the connection between the permanent "ring-bit" and the releasable "pilot-bit", taken from Statens vegvesen.

3.3.1 Pipe wall

The bored pile wall solution is rather expensive, but for smaller projects, the rigging costs can be minimized by utilizing light drilling equipment. The design of the wall is performed according to NS-EN 1993-5 "Design of steel structures - Part 5: Piling. Requirements and guidelines for sheet piling work are given in NS-EN 12063 "Utførelse av spesielle geotekniske arbeider - Spuntvegger", according to (Byggegropveiledningen, 2019) [28]. Other aspects regarding the design and execution of the wall, such as the shotcrete and reinforcement mesh, must be done in accordance with regulations of the Norwegian Public Road Administration as described in Handbook R762.

In the Norwegian construction community, the terms "boret rørspunt" and "boret rørvegg" are frequently mixed. "Boret rørspunt" is a type of tangent pile wall made of steel pipes with similar dimensions as the pipes in contiguous steel pile walls (RD pipes). The steel pipes used in the tangent pile wall have two interlocking sections welded along the pile, which connects and locks adjacent piles together, making it a closed watertight wall [29]. "Boret rørvegg" is a contiguous pile wall where the steel pipes are installed with a soil gap between the adjacent piles. The resulting arching effect in the soil behind the soil gaps is utilized. After installation of the piles and excavation of the pit, a shotcrete layer is added and often a reinforcement mesh between the shotcrete and the wall is added as well. The shotcrete seals the soil gaps, which prevents that the soil mass falls through the gaps. This helps to make the arching properly develop, as well as ensuring that the arching effect is not reduced and thus improves the long-term stability.

For the most common projects in Norway, the contiguous bored pile wall has been used as a retaining wall for excavation depth up to 7-8 m. The ground conditions have been good with relatively firm soil and with no particular challenges regarding groundwater. A large axial and bending capacity can be obtained for the retaining wall. The suppliers offer pipes of good steel quality, and they are usually cast out [29].

Additionally, the pipes can be reinforced before casting. If H-profiles are used as reinforcement and not circular steel cores, any rotation of the profile should be taken into account when calculating stiffness and strength. If the bored piles are not straight, the H-profile will make contact at one side of the pipe when installed and follow the direction of the pipe locally. The pipe has different directions further down, which will make the H-profile turn and finally rotate. This rotation can not be adjusted during the installation or after it has reached its final depth because the rotation is a result of the profile's own weight, and therefore the rotational movement goes with great force. The straightness of the pipe depends on the deviations in inclination during drilling, change of angle when welding the subsequent steel pipe, and deviation and curvature of the pipe from the resistance during drilling [30].

During the construction of a 180 meter long and 18 meter high bored pipe wall at Avløs station in Oslo, it was discovered that the reinforcing H-beams inside the pipes wad rotated, as explained above. And it was concluded that quality of the structural cross-section did not meet the design requirements. The tolerance of placement for the beams was limited to 1° rotation, and some of the beams had rotated 45°, in addition it was located against the inner side of the pipe leaving no concrete [30]. The performance of materials, products, and structural components were investigated by forensic engineering, and resulted in the following guidelines from [30]:

- Design of a pipe wall with plastic behaviour instead of elastic. This should be done as a corrective tool in case of deviation from original design.
- Calculation of the section modulus in accordance with the achievable structural properties and dimensions. A reduced moment capacity should be used as a preventive tool in case profile rotates.

These guidelines should be considered in early design stages. For the wall at Avløs it was demonstrated that given the unplanned rotation of the reinforcement it still complied with the current design standards.

The distance of the soil gap is dependant on the soil behind the wall and the pipe geometry. It can vary from $5 - 10$ cm up to $100 - 150$ cm [28]. The soil behind the gaps is held back by the arching effect. The soil gap stability obtained from this effect may change over time, this is further discussed in Chapter 4 and Chapter 6.

Excavation under groundwater level is not recommended since the arching effect will only work in firm clay or in course masses without fine-grained elements. For other materials, the soil will be squeezed out through the soil gaps [28]. The water will erode the fine-grained particles and reduce arching. In order to close the gaps and improve the stability over time, the soil gaps can be sealed with fiber-reinforced shotcrete, possibly with reinforcement mesh between the pipes and the shotcrete. After some time, problems with erosion and squeezing of soil through the gaps may occur. For cases where there is a risk of erosion, the gaps must be sealed; fiber-reinforced shotcrete is the most common way to seal the gaps. Alternatively, steel plates can be welded onto the pipes in order to close the gaps, as done on the Nordenga bridge project, see Figure 4.2.2.

3.3.2 Groundwater

The contiguous pile wall sealed with shotcrete is not a watertight structure. This solution is therefore not suitable for projects where there is a risk of damage due to groundwater lowering, nor cases where construction in coarse masses involves handling large amounts of water. Groundwater flow towards the wall can lead to erosion of the fine-grained material such as sand and gravel, which may weaken the arching effect.

The arching effect can also be reduced in dry sand and gravel if the masses fall out between the pipes. For such cases, it is important to close the soil gaps, either by shotcrete, steel plates or concrete/wood lagging. Sealing the wall with shotcrete gives significantly fewer deformations than a soldier pile wall with timber lagging [28].

The excavation of the pit and subsequently bracing of the wall is done in phases, and for each of these excavation phases, the wall should be sealed with shotcrete. To ensure that the stresses are mainly transferred in the soil behind the gaps through the arching effect, it is important to avoid

high levels of pre-stressing in the bracing. Due to practical considerations, the shotcrete is applied after the tensioning.

(a)

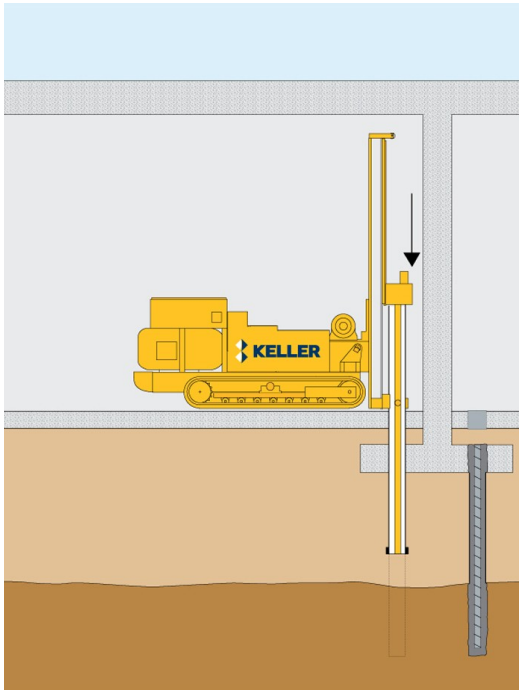

(b)

Figure 3.3.2: **(a)** Drilling rig for installation of bored steel piles [31]. **(b)** A rig for installation of micro-piles / steel core piles, they are drilled down and can be used as a deep foundation element. They consist of small-diameter steel casing, and can be reinforced by bars. Taken from Keller

(a)

(b)

Figure 3.3.3: **(a)** Installation of micro-piles inside of a building, taken from [31]. **(b)** Installation of steel core piles with a small drilling rig, taken from [31]

The bored steel pipe differs from other bored piles. The drill rig is different with full profile drilling of the pile hole through hard fill, loose materials and into rock. The steel pipe remains in the ground after the casting. The picture below is from a highway project at Hunstadmoen in Bodø, Norway, and shows a pipe wall made of steel pipes, they are drilled down to the bedrock. The soil is excavated on one side, and the pipes are joined with reinforced concrete and horizontal steel beams. This is a temporary retaining between highway 80 and the excavation pit. The steel pipes are rather stiff and provide sound reinforcement against displacements. There is a railway on top of the slope behind the pipes, and because of this, the requirements against displacements become stricter.

Figure 3.3.4: Steel pipe retaining system against the railway situated on the left side. On the other side, it is excavated and ready for bracing with steel beams and reinforced concrete

3.4 Bracing systems

The pile wall can be supported both externally and internally, as shown in figure 3.4.1. For internal support, struts can be used as bracing. This can be done as long as the structure providing the support is sufficiently close. In a small construction pit, the opposite pile wall can be used. For trenches and smaller pits with limited width, internal bracing is the natural choice. It may also be a suitable solution for larger construction pits where conditions outside the retaining walls are such that external bracing with anchors is impossible or has undesirable consequences. As a permanent support, a base slab and the intermediate floors of a building may serve as horizontal bracing. Issues concerning installation of anchors underneath neighboring structures are avoided. Another advantage is the re-usability of the internal bracing.

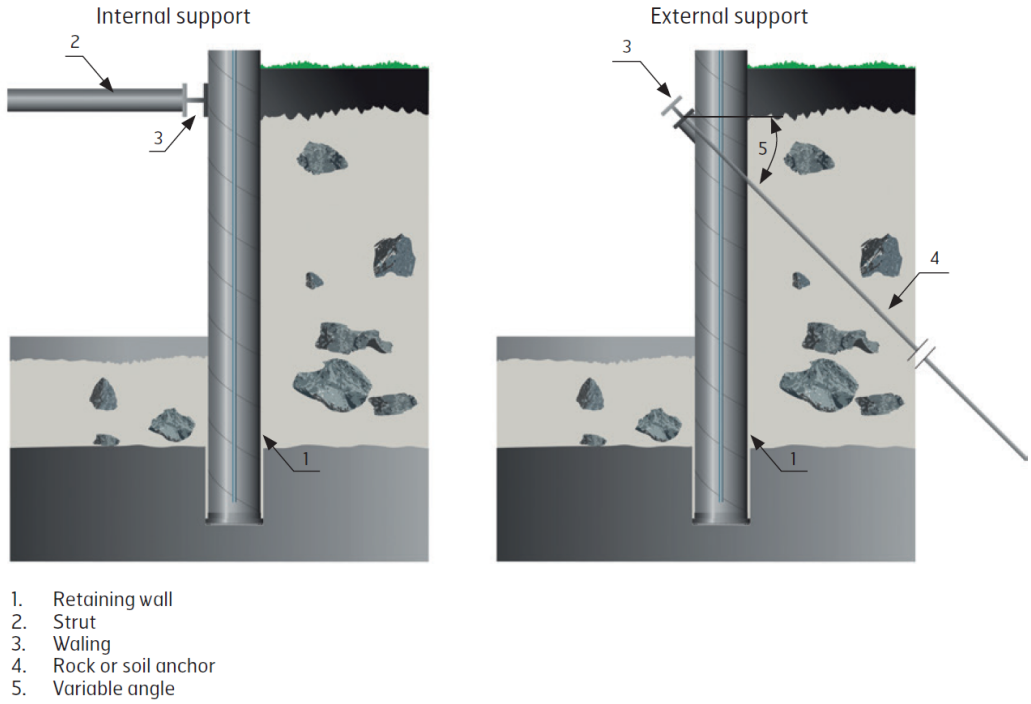

Figure 3.4.1: Internal and external support of an RD pile wall, taken from [29]

A walling is a horizontal beam, usually of steel, fixed to the pile wall. Both anchors and struts are connected to this beam. This beam is necessary to distribute the forces equally over the pile wall. When bracing is needed for short distances, it is most common to use steel beams with a HEB profile. The steel beams are installed along the retaining wall and used to connect the bracing and distribute the load. For increased bracing distances, tubular steel pipes are optimal.

One obvious disadvantage with internal bracing is the influence it has on the construction work in the pit. The excavation work needs to be planned to avoid conflict with the bracing. Traditional construction work becomes more challenging with the obstacles, as well as the transportation of equipment and materials. Although the system is redundant and is designed for loss of a strut, one must be careful and plan in order to minimize the risk of damage to the internal bracing. There are several other details to consider during the design of the bracing, such as the deflection of the compression struts due to dead load, the concentration of loads in bracing joints and deformations of non-pretensioned supports during loading.

For the external bracing both soil and rock anchors can be used, depending on the ground conditions. Tension rods attached to anchor plates can also be used.

Figure 3.4.2: Bored pile wall at Avløs station. There are a total of three girders with rock anchors at different levels, from Geovita AS

When anchoring in rock through soil, it is most common to use steel cable anchors, in Norwegian also called "steel laces". Alternatively, steel rods can be used. To satisfy the regulations for construction of anchors in NS-EN 1537, the anchors must be able to be tensioned after assembly [28]. A hydraulic jack is used to tension anchors with steel laces, and for the anchors with steel rods, a torque wrench is used. To install a rock anchor, the first step is to drill a casing through the soil and into the bedrock. Further drilling into the rock to extend the anchoring zone is done without the casing, using rock drill bits. Then the anchor needs to be assembled, and a steel cable or rod is attached to the anchor. To secure adherence, the anchor is grouted to the rock. After seven days, the mortar has hardened and the anchor can be tightened and locked. The anchor's design load is based on pile wall calculations in the serviceability limit state, ultimate limit state and the accidental limit state. The largest calculated load in one of the limit states gives the design load [28].

The anchor's capacity is determined from the calculation of the external and internal capacity. The calculation that gives the lowest capacity determines the anchor's capacity. The internal capacity depends on the anchor's structure/composition of the components and the capacity of the steel. The external capacity depends on the capacity of the anchoring zone in the rock.

Soil anchors are used when there is a large distance to bedrock, and rock anchoring becomes impossible. The anchors are installed with a smaller angle than the rock anchors, which helps to utilize the load capacity in the horizontal direction. It is also favorable that large vertical forces are avoided. They are usually installed with an angle of $20° \pm 5°$ [28].

There are some disadvantages with soil anchors regarding damage on neighboring structures. Consolidation could affect neighboring properties and structures, caused by either collapse, or erosion and stirring around the borehole. A continuous injection with cement suspension while drilling can avoid collapse and minimize the effects of the erosion.

3.5 Shotcrete in practice

Shotcrete is one of the most important elements in construction of underground facilities, and is used for heavy rock protection. For use in such underground projects it is essential that it satisfies the requirements for toughness and strength, as well as being long-lasting shotcrete. Adherence is one of the most important properties for a good shotcrete protection, and is very important for pipe walls. Cleaning the surface is therefore very important to achieve good adhesion [32]. In some cases, application of water in order to clean can lead to instability and further rock fallout, this is further discussed in Chapter 4.

In the event of significant water leaks, it is difficult to get the shotcrete to "hang" in the tunnel. A solution can then be to drill drainage holes (relief holes) around the profile[32]. This is the case for the pile wall as well, built-up water pressure behind the wall is not good, and neither is water that erodes the soil and weakens the arching. Drainage wholes is a good solution to avoid built-up water pressure. The poorest adhesion is obtained in clay zones and similar ground conditions. With such conditions in a tunnel, alternative methods must be considered. In pipe wall the shotcrete can stick to the steel pipes and the bracing, therefore shotcrete protection may work for clayey soil conditions for pipe walls. For such conditions it should have other structural elements to bind with, so that one can ensure it becomes an integrated element of the braced retaining structure. It is dangerous if the concrete behaves like a concrete shell that is only weakly glued on a retaining wall with soil gaps, further discussed in Chapter 4. The bond between shotcrete and steel is discussed in Chapter 4.

When applying shotcrete there are two properties that are important at the start:

- The ability of concrete to hang onto the surface, and stay there
- Curing should start as soon as possible after application to obtain high early strength

To achieve this, an accelerator is added in the spray nozzle where it is mixed with the concrete. This helps to start the solidification immediately after the concrete hits the rock [32].

The shotcrete is fiber-reinforced, and steel fibers are standard in almost all shotcrete used for rock protection [32]. The normal dosage of steel fiber for rock protection is 20-40 $\frac{kg}{m^3}$ with fiber lengths 30-40 mm. There is a significant quality difference between different types of available fiber. Using a fiber type with poorer properties requires a higher dosage of fiber in the mix to satisfy the functional requirements of the shotcrete. Macroplastic fiber is a more modern type of fiber, and is an alternative in situations where larger deformations are expected.

3.5.1 Reinforcement of the bored steel pipes

Normal procedure is to fill the pipes with concrete with a strength equivalent to B30. They need to be filled from the bottom with a hose [33].

To reinforce the pipes steel profiles or cores are led down into the pipes, as done with the wall at Avløs station [30]. At Avløs HEB160 profiles was used. The guidelines requires the profiles to be mounted with the strong axis perpendicular to the wall, and then a concrete cast around the steel profiles, utilizing a hose from the bottom of the borehole as done in the normal procedure.

3.5.2 Reinforcement mesh

For tunnels, a reinforcing mesh can be an alternative where shotcrete is used to secure clay zones. The mesh is well anchored with bolts on each side of the fragile zone before injecting. The standard reinforcement mesh for shotcrete is K-131 [32]. This is because it has a favorable geometry in order for the shotcrete to penetrate the mesh and gain adhesion with the underlying soil/rock. If the mesh has too small openings, the concrete will easily get stuck in the net and it becomes difficult to get full contact between the concrete and the surface. The K-131 mesh has squares of 150 x 150 mm and steel thickness 5 mm [32]. The usual steel quality used in Norway is B500NA, but a better result is obtained by using a steel quality that is more ductile (B500NB). There are several projects in Norway where reinforced mesh has been welded to the pipe wall. To evaluate the effect of the mesh, the number of welds over a distance, and the length of the welds may be used to calculate the tensile strength provided by the mesh. It is standard to assemble the mesh with few attachment point as explained below, therefore it is nothing to count on when it comes to tensile force.

The design requirements for the reinforced mesh is given in Prosesskode 2, Statens vegvesen håndbok R762 [33]. Section 83.6225 gives the guidelines and standard description for the application of pipe walls:

- The reinforcement mesh needs to be in accordance with NS 3576-4.
- The mesh must be fixed with sufficient points so that the concrete is not damaged by vibrations. There must be at least one attachment point per m^2. The mesh need to be laid with two square overlaps in both directions when a new section is assembled.
- The mesh must be installed successively when excavating the pipe wall.

This is the standard description and depending on the project the adequate mesh needs to be specified by the engineer. On project E18 Vestkorridoren reinforcement mesh K131 is used, with quality B500NA according to NS 3576-1.

With at least one attachment point per m^2 the net is rather mounted on the pipe wall and is not structural integrated to the main retaining structure. With the shotcrete applied on top this could become a steel/concrete shell if the shotcrete do not achieve good bonding with the pipes, which is unfavorable because it could fall out.

According to the guidelines in section 83.6226 in [33], the recommended fiber-reinforced shotcrete is B35 M45 E700 with accordance to NS-EN 14487-1+NA. It is expected that the pipes receive necessary cleaning in order to obtain the best adhesion possible. Other guidelines include filling the gaps behind the mesh, removal of bounce losses, keeping records, necessary curing measures, testing and inspection.

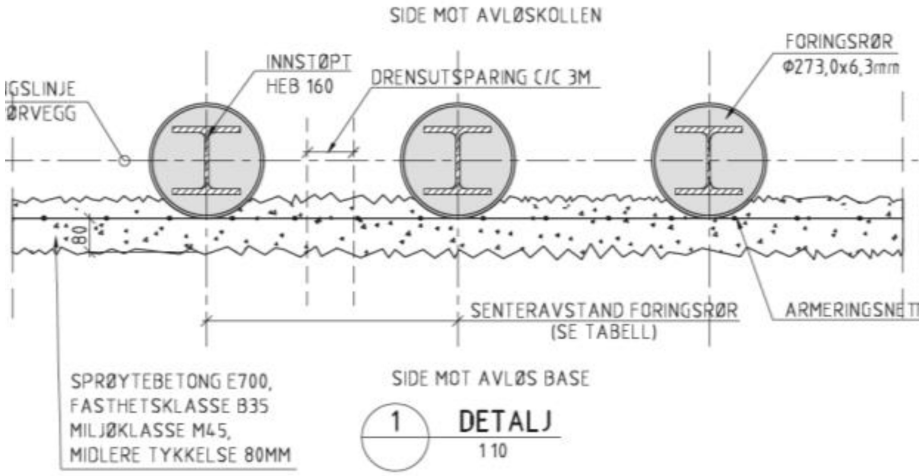

Figure 3.5.1: Cross section of the pile wall at Avløs station, taken from [30]

Chapter 4

Construction and model discussion

In this chapter, the construction of the wall and construction stages used in the FE model are discussed. Special challenges and concerns are reviewed. Experiences and discussions with the geotechnical community in Norway are included. Knowledge about the construction steps and stages, and experiences from the community are important to obtain realistic models and simulations, as well as choosing appropriate and logical boundary conditions. This information helps determine which simulations should be performed, how to model and create boundary conditions, and how to simulate construction stages. This chapter is partly based on literature from piling, construction pits, anchorage systems and tunneling (tunnel safety), and partly on interviews, discussions and experiences from geotechnical consultants from Geovita, construction managers from Hallingdal Bergboring, and Steinar Nordal, professor in geotechnical engineering at NTNU.

4.1 Practical considerations

Spacing between the pipes

The center distance is chosen based on how deep the pipes are installed. A larger center distance is selected for deeper piles to avoid collision. If the soil consists of fine-grained material, the pipes are drilled closer to each other to make it more difficult for the masses to penetrate the gap. With coarser masses such as coarse rocks, it is common to use a larger center distance. The distance varies a lot from case to case since the ground conditions also vary considerably. Ground investigations are often carried out to find out how close the pipes will be installed. There have been cases where pipes are installed with a center distance of 1 meter, but also with a distance between the pipes of 10-15 cm.

The pipe wall solution is expensive, and there are therefore good possibilities to save money by optimizing the distance between the pipes. When installing the pipes, a deviation of 2% may be assumed, and if the pipes are 18 meters long, the obtained deviation can dictate the center distance. Due to this tolerance consideration, the distance between the pipes can get larger than first desired. Engineering judgment and experiences often dictate the dimensions of the pipes and the center distance.

There are weaker zones due to variable masses where the soil can locally be squeezed through

the wall. This may be alleviated by closing these zones with steel plates. The reason for local fallout of soil is usually water, and the water drags the soil with it. Another reason could be that areas has very fine-grained material. From experience, this does not become a problem for the whole wall, but for a limited area called a weakness zone. The construction manager from Hallingdal Bergboring has not heard about or witnessed extensive squeezing. Since this usually is a local problem, that particular zone can be sealed by welding steel plates onto the pipes. The reason why steel plates are used is that the weak area may be sealed faster than with shotcrete, which is not available at all times. When applying shotcrete, it is preferred to apply it for a large area at once and reduce the number of times shotcrete is applied. Therefore, there exist both structural and economic reasons for choosing steel plates instead of shotcrete to close local weakness zones.

4.1.1 Excavation stages

It is very normal to divide the excavation into several stages and to apply shotcrete for each stage. It is very rare that the whole pit is excavated and then the shotcrete is applied at the very end. The pipe wall needs to be stable without the stabilizing shotcrete, because the shotcrete is usually not applied the same day as the excavation is performed. There is no answer or standard procedure for how many days it takes before the shotcrete is applied. It depends on an assessment on how long the wall may stay unsupported whiteout shotcrete, the evaluation of ground conditions and safety is central factors in the evaluation. The contractor wants as few intervals as possible with shotcrete due to economic aspects, and at least no more than originally planned. How long the excavated wall is left unsupported is a decision that the consultant and contractor make together. To ensure safety both during the project and after, the information flow towards the contractor is essential.

Since there are periods where the wall is without any concrete support, it is important to calculate the stability of the wall and soil gaps without concrete. The simulations need to be stable without the concrete before simulating the cases with concrete. The reason is that the shotcrete is not added simultaneously as the wall is excavated, and when the shotcrete is sprayed onto the wall, it usually sprays a significant volume at once. The wall is excavated in different phases, where supports such as anchors or struts are installed, as well as girders along the wall. When excavating a phase, it is normal to excavate several meters and then install the girder and the anchors. Retaining walls can have several levels with bracing. This leaves several meters of the wall without shotcrete sealing for a considerable time. The distance between the support levels is determined according to the acting earth pressure and the stiffness of the pile wall. Therefore, the stability of the freely exposed soil gaps has to be controlled.

4.1.2 Preparations before applying shotcrete

The shotcrete is sprayed in between the pipes and, in some cases, behind the pipes. If there is a large stone stuck between the pipes, it is removed to enable the shotcrete to come all the way to the back of the pipes. The shotcrete is then hanging onto the pipes, which is very favorable for the integration of the shotcrete with the rest of the structure. It is even more common to have the concrete come past the midpoint of the pipes, which will make the concrete wedge between the pipes. This is favorable because it gets stuck, and the concrete takes up stresses by being subjected to pressure instead of letting the interface adherence take up the tensile stresses. It is a goal that the concrete becomes an integrated part of the wall, so that when the concrete is wedged between the pipes, it becomes less dependent on the adhesion to become integrated.

This method is often used where the ground consists of sand and gravel, and from pictures of

different projects one can observe that the piles clearly emerge and a small pit will appear between each pipe. If the ground consists of fine-grained material such as sand and gravel and with a small center distance, the pipes will emerge by themselves. For ground conditions consisting partially of fine-grained material such as sand and gravel some common experience dimensions are pipes with a diameter of 273 or 324 mm with a center distance of 0,5 m or 0,6 m.

For coarse masses such as rocks or moraine, thorough excavation is needed to make the pipes properly emerge. Sometimes the pipes penetrate a large rock, so the whole rock has to be removed, then there will be space behind pipe for the shotcrete to fill. It is important to excavate in such a way that the piles become visible, so that the concrete has sufficient pile surface to attach to. Pictures of pile walls from projects in Norway show that the piles emerge from the ground. If the piles do not emerge naturally when excavating close to the wall, which could be the case for clay as well, a shovel can be used to dig down along the piles to expose more of the pile surface.

In order to achieve good adhesion, it is desired to avoid a poorly cleaned "earth wall" with pipes inside. This is done by excavating enough in front and between the pipes so that they sufficiently emerge. To guarantee enough pipe surface for coarse masses, such as rocks and moraine, it is an advantage with a suitable shovel to dig along and between the pipes. The shovel is often stroked along the pipes to ensure that the pipes clearly emerge.

Clean pipes are essential to guarantee optimal adhesion. Compressed air can be used to clean the pipes a little, but the most important thing to check is that the pipes are not covered with dirt or other substances that can affect the adhesion. It is not favorable with any surface treatment or lining; paint and corrosion protection must be avoided. It is not unusual that the pipes are covered in some type of oil, this is something the producer applies so that they can be stored for period of time without corroding. Contractors have in a few projects received requirements to wash the pipes before applying shotcrete. The pipes have then been washed, degreased and rinsed clean. This has been done after the wall is excavated and before the concrete is applied in order to increase steel-concrete adhesion. When the pipes are washed this way, a pressure washer is used to rinse the pipes, which could lead to some challenges because water may remove stabilizing soil in the gaps. For unstable or fine-grained masses, water might make the overall situation worse. One way to avoid this problem may be to wash the pipes before drilling and use compressed air to rinse them afterwards. Thus, dirt and dust are blown away, and uncontrolled removal of soil between the pipes is avoided.

The contractor has not experienced that the shotcrete comes loose from the wall. An essential risk with the shotcrete is if the only thing that keeps it attached to the rest of the wall is the adherence, and this becomes poor. This can be illustrated like a shell structure that is glued to a badly cleaned soil wall with pipes in it. The uncleaned surface between the steel and concrete will give less adhesion than would be obtained by a clean surface. A concrete shell glued to a greasy and uncleaned pipe wall is not a desired outcome, the desired result is a concrete layer that is properly integrated into the rest of the structure. This concrete shell is 8-10 cm thick and is therefore also heavy. This is not a desired situation, because it may come loose from the wall and would then be a major security risk. The adhesion is therefore essential and is of great interest. A bad adherence could be alleviated by ensuring that the shotcrete becomes integrated with the bracing system of the wall. Excessive excavation between the piles can also have an effect but probably less than the bracing. If anchors, brackets and waling beams are completely covered in shotcrete, they will hold back the concrete. The waling beams have to be pulled out and fall out with the concrete if the two structures are integrated. The waling goes across the wall and keeps the concrete in its place. It will interlock the shotcrete to the rest of the structure.

4.1.3 Walls without bracing

For smaller walls, up to approximately 3 meters of excavation depth, a bracing system is usually not applied. To ensure the structural integrity of the wall itself, the pipes are usually reinforced with beams (H beams or steel cores), and concrete. For these types of walls, the adhesion becomes central. One has to make sure that the shotcrete is well attached and does not become a shell that can fall off.

Important considerations are the adhesion and how far it is necessary to excavate to obtain enough surface between the concrete and the pipes. One may also make sure that the concrete comes behind the center-point of the pipes to take advantage of the concrete's "wedge effect" between the pipes, as mentioned above. For larger walls, it might be necessary to require a bracing system with a waling across the wall, as this will make sure that the shotcrete becomes an integrated part of the wall, as explained above. Some steps that can be taken to achieve better adhesion are mentioned above, like removing the oil coating with a degreaser and rinse them clean with compressed air. A thorough excavation between the pipes also contributes to increasing the integrity of the shotcrete but is not only advantageous, taking into account that stabilizing soil is removed. Another factor that strengthens the adhesion is that the surface of the pipes is not completely smooth like they are when delivered straight from the factory. Since the solution is used where there are hard rocky top layers often consisting of hard rocks or moraine, the surface will get slightly rough when these layers are drilled through. The contractor has not heard about any projects where adhesion is lost or problems related to this have occurred, but the shotcrete layer can get some minor cracks.

4.1.4 Steel-concrete adhesion

The steel-concrete adhesion is a crucial factor for walls without a bracing system. A parametric study of the steel-concrete adhesion was therefore conducted in Section 6.2.1 to study the significance of the adhesion. By placing the shotcrete on the unfavorable outer side of the pipes, the stability depends essentially on the concrete-steel adhesion. A parametric study of this adhesion will give an impression of how the stability varies with different values of adhesion. The strength of the adhesion may realistically vary from some hundreds of kPa up to the strength of concrete in the order of several MPa. The strength of the interface has a considerable influence on the safety, see results in Section 6.2.1. To carry out parametric studies on other parameters such as concrete arc geometry and soil gap ratio, a very conservative adhesion of 500 kPa was chosen.

4.1.5 Reinforcement mesh

In the descriptions and drawings a reinforcement mesh is often prescribed. The requirements for the welding given in Norwegian Public Roads Administration handbook R762 [33], indicate that it is just an assembly of the mesh and no significant tensile strength. This means that the shotcrete is responsible for the bonding with the pipe wall. Although, it has a very good effect, it becomes a wall element that is very load-distributing and favorable. something that wants to fallout will hook on to the mesh. If there is a small area with lack of adhesion, the load from this will be transferred to an area with better adhesion through the concrete layer. The mesh helps to achieve this and makes it a more holistic construction. The mesh may also help to reduce cracking as it does in a concrete floor. It is not sure it is always necessary because the fiber-reinforced shotcrete could do this by itself, and it is not certain that it is used on all projects.

4.2 Shotcrete in Plaxis model

In the horizontal plane strain model of the pipe wall above excavation floor presented in Section 5.1.1, a classic B20 concrete is used. There are also other options with higher compression strength like B30 or B40. With a B20 concrete, the diameter of the Mohr circle is 20 MPa and therefore the cohesion becomes $c = 10$ MPa, as explained in Section 2.3.3. When simulating shotcrete, the tensile strength is essential for the stability of the concrete sealing in the soil gap. Setting this value to zero or considering a low value is not realistic considering that a fiber-reinforced concrete is used. This could result in unrealistic failure. When using a compressive strength of 20 MPa, a tensile strength of 5-10 MPa is reasonable. For most of the simulations, a tensile strength of 5 MPa has been used to obtain a safe design.

For the simulations where the concrete comes behind the center line of the pipes, the concrete will take up stresses by being compressed and pushed between the pipes. This is a favorable positioning of the shotcrete, and from simulations, larger safety factors are obtained see results and comments Section 6.2. These results shows that a large capacity is obtained when a pressure arc is formed in the concrete. Depending on how much stresses the soil takes up with soil arching, the concrete receives the rest of the stresses. When the concrete layer is below the center of the pipes, it will essentially depend on the adhesion between steel and concrete.

4.2.1 The need for shotcrete sealing

Even though the stability of the wall needs to be calculated without the shotcrete, it does not mean that shotcrete is unnecessary. The excavation is executed in stages, and shotcrete is normally applied for each stage, which means that the soil gaps need to be stable for that particular excavation depth and not for the whole depth of the wall. The shotcrete sealing is also necessary since the gap between the piles is exposed for erosion, and when the fine particles are eroded, the arching effect is reduced. A loss of particles because of time and gravity may also reduce the arching effect. The value of the cohesion parameter is therefore potentially reduced over time. This retaining wall method works best when the water table is underneath the excavation floor, so that groundwater does not pose any particular problem. However, erosion from rainwater and loss of cohesion due to any material that falls out during and after the construction, is a problem that shotcrete will reduce.

To prevent collection of water behind the shotcrete which produces an unfavorable ground water pressure, small cavities in the concrete can be made to let the water escape.

4.2.2 Health, Safety and Environment

In order to ensure safety when working in the construction pit, good cleaning of the wall must be ensured during excavation. The distance between the pipes must be adapted to the quality of the soil, so that fallout of stone between the pipes is avoided. The choice of center distance is of great importance for the safety of the pipe wall. The distance that provides an acceptable level of safety must therefore be determined separately for each individual project [28]. Shotcrete must be applied at the right time, which means that the wall should not stay unprotected without shotcrete for a long time if there is a risk that material can hit workers. One must make sure that the concrete becomes an integrated part of the structure. This is especially important for cases of deeper excavations of 2,5 meters or more, where the use of bracing may be a good idea to ensure

that the concrete layer does not become a shell structure glued to the pipe wall. As mentioned before, with clearly emerged and clean pipes, one can assume a significant adhesion.

4.2.3 Plaxis model and reality

There is no guarantee that the shotcrete will come past the midpoint of the pipe piles (the favorable side), so that it becomes a pressure arc in the concrete. Therefore, it becomes more relevant to model the concrete layer from the center of the pipes and towards the construction pit (the unfavorable side). The issue is when the shotcrete does not come on the favorable side, then it would just depend on the adherence between the shotcrete and the steel. Therefore, it is interesting to find what extent will it will work when the shotcrete only rests on the adherence to the steel pipes (interface). This may be studied by doing a parametric study of the adhesion, by varying the strength of the interface.

4.2.4 Steel-concrete adherence

The utilized concrete is fiber-reinforced and it therefore has a tensile strength. The evaluation of the bond between shotcrete and steel, further referred to as adhesion, is essential for this problem.

The bond between the steel pipes and the shotcrete is developed by adhesion, friction and mechanical means [34]. Adhesion is the adhesive effect between the two materials primarily created by the chemical interaction between the concrete and the steel, and micro irregularities in the steel surface. Friction bond is the resistance created by the concrete surface pressing against the pipes. Mechanical bond occurs when there is a physical interlocking between the steel and the concrete, because of larger irregularities on the steel surface. The bracing system is integrated with the wall and has a favorable surface for adhering to the shotcrete, and creates a physical interlocking of the pipes and shotcrete.

The support from the shotcrete has a considerable effect in friction materials, it is not a large initial stress (p') that is required to obtain stability. The initial stress p' propagates inwards in the stress field through the log-spiral and significantly increases the capacity. This is illustrated with Equation (2.6.2), and is described in Section 2.6. One starts off with some initial support, in this case from the adherence between the concrete and the steel, and when multiplied with the N_q factor, Equation (2.6.3), it builds up a considerable bearing capacity as shown in Equation (2.6.2). Therefore, not much support is needed to make it work, just an initial stress to help initiate the arching, and this initial stress will increase by itself inwards in the stress field.

When the adhesion is studied it is relevant to study this effect alone, and for those simulations the concrete is modelled so that it do not take compression on the favorable side. In reality, the concrete could reach the favorable side, but it is not guaranteed that it will reach this position every time.

Figure 4.2.1: Construction pit for a railway foundation at Dokknes. The pipes were drilled through a railway embankment and finished in hard clay, from Geovita AS.

Figure 4.2.2: Pile wall for construction of Nordenga bridge, from Geovita AS.

4.3 Squeezing under excavation floor

Squeezing of soil mass through soil gaps under the excavation floor may be a potential problem. This is a problem because the assumptions of passive-active earth pressure or earth pressure at

rest against a closed sheet pile wall may disappear. The pipes which transfers the passive pressure to the soil could be pushed through the soil, this problem is from now called squeezing. This is especially an issue for soft clay. The pile wall solution is not recommended for soft and sensitive clay, and especially not for quick clay where there is a large possibility for failure and extensive squeezing through the wall. The pipe wall solution is not a solution to retain very soft clay and is not recommended for soft clay's either, soft clay should not be retained by freely exposed soil gaps. If the pipes are drilled through hard top layers such as an embankment or moraine, the lower parts of the pipe could end in soft clay. This was the case at Nordenga, see Section 4.3.1. For such cases the squeezing under the excavation floor might be a problem. For situations where there are hard top layers and sensitive clay under, a pipe wall with interlocking pipes may be used. This interlocking secant wall is called "rørspunt" in Norwegian and is described in Section 3.3.1.

For ground conditions with soft or medium clay where squeezing may become an issue, sheet piling is the preferred choice. There are various cases of successful construction in medium to firm clay, like the project in Doknesevja and Nordenga bridge, but sheet pile walls are standard for such conditions. Although in urban areas, hard top layers may be found, from railway embankments to big rocks in the clay. For hard crusts, stones and other difficult conditions, pre-drilling or excavation of the hard top layer is done in order to continue the sheet piling. In some cases, this is not possible or insufficient, and the pile wall becomes a good solution. Preparatory excavation for sheet piling becomes less favorable when hard layers are deep, which was the case for Nordenga bridge. For this case, excavation was also challenging because of large stones belonging to an old stone wall. Deep layers of hard railway embankments was the reason for choosing a bored pile wall solution, even though there were softer clay masses under the embankments.

At Doknesevja there was built two retaining structures for two foundations that was going to be the foundation for a new railway bridge. This was built right next to an existing railway bridge, and similar to the retaining wall at Nordenga, a railway embankment had to be retained.

4.3.1 Nordenga bridge

Nordenga bridge was a project where these issues were found. Nordenga bridge span over several railway tracks and is situated right besides Oslo central station. A sheet pile wall was first designed, but thick railway embankments and old stone walls at the bottom of the filling made it practically impossible. Therefore, a bored pile wall became the solution. The wall is built in axis 8, which is in the middle of a slope, and the filling is thicker in this location. The ground under the embankment was not so sensitive medium-firm silty clay with the following interpreted parameters: $a = 5$, $\phi = 30$, undrained shear strength $s_{uA} = 0,3p'_0$ and with a module number in the order of 15. In axis 8 the excavation was approximately 4,7 meters and the silty clay layer is found at a depth of roughly 5,6 meters. The undrained shear strength of the silty clay was estimated to be $s_u = 24Pa + 4kPa/m$. The top layer of the filling consists of good quality rock, further down the fill material is of lower quality mainly consisting of sandy material. Right under the filling, a stone wall made of large stones. The pile wall is anchored and has a soil anchor at a depth of 1,5 m and a strut bracing system at a depth of approximately 4,6 m.

Shields were established around the foundations, as these were to be built between train tracks under partly very narrow conditions. For one of the foundations, three of the walls were sheet pile walls and one was a pile wall. The ground under the pile wall consisted of an old stone wall and bigger rocks than under the other walls. The pile wall consists of 12 m long pipes with diameter Ø323x7,1mm, with a center distance of 0,6 m. The pipe wall was braced with 30 m long soil anchors. The soil gap was sealed with welded steel plates, see Figure 4.2.2.

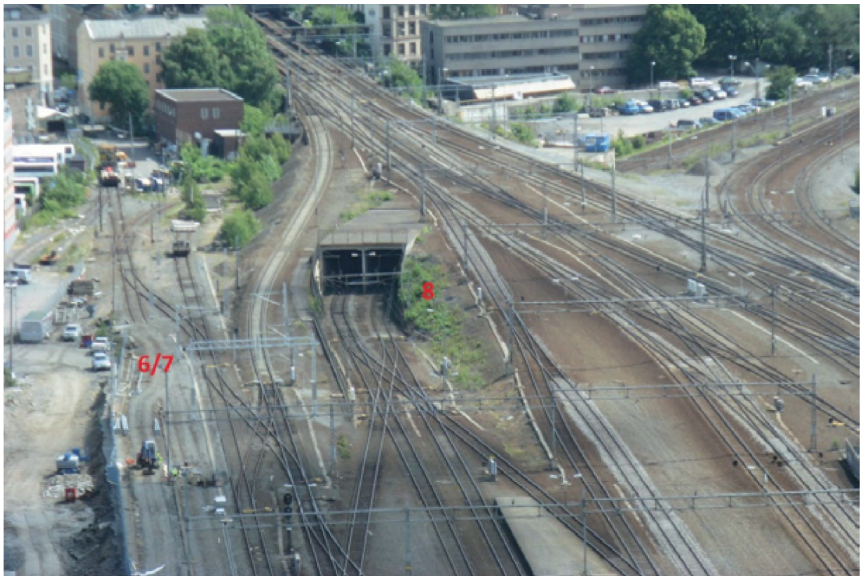

(a)

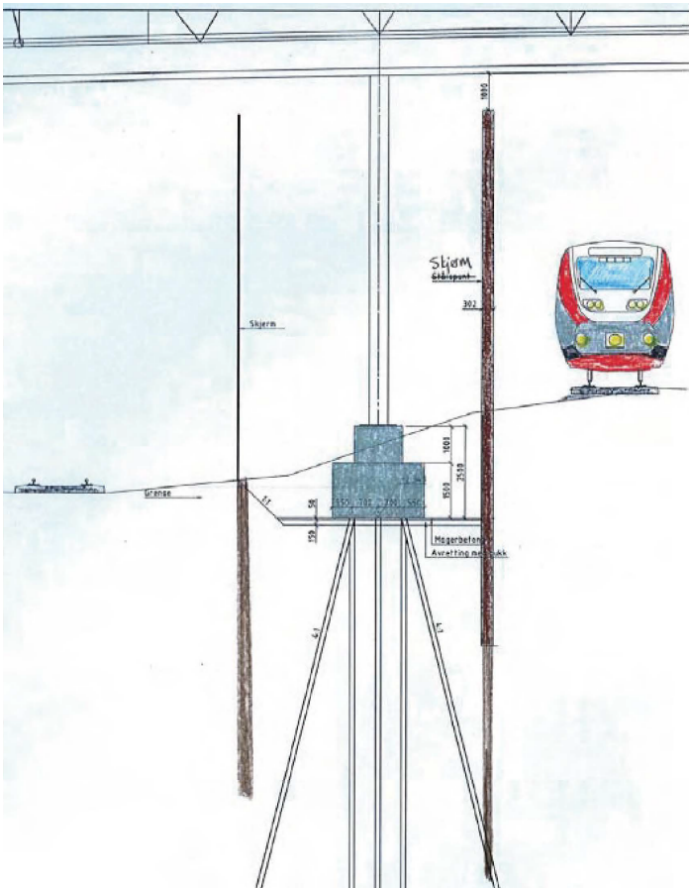

(b)

Figure 4.3.1: **(a)** Overview picture of the track area at Axes 6, 7 and 8 [35]. **(b)** Illustration of the problem for Axis 8, taken from [35].

A stability calculation was done to evaluate the squeezing problem between the pipes under the excavation floor, and tolerance requirements for drilling was checked with regards to pile depth to avoid collision further down. The performed stability calculation was equivalent to that for soil slipping between lime cement ribs, according to the Norwegian Administration's handbook V221 [36], see Figure 4.3.2

For the calculation of slipping between two stabilizing lime cement discs, a standard stability calculation is done, where the effect of the shear forces on the slice surfaces are included as stabilizing forces. It is the shear strength τ_k in the unstabilized soil volume between the ribs that is used in the calculations [36]. For a pile wall, this effect is not included.

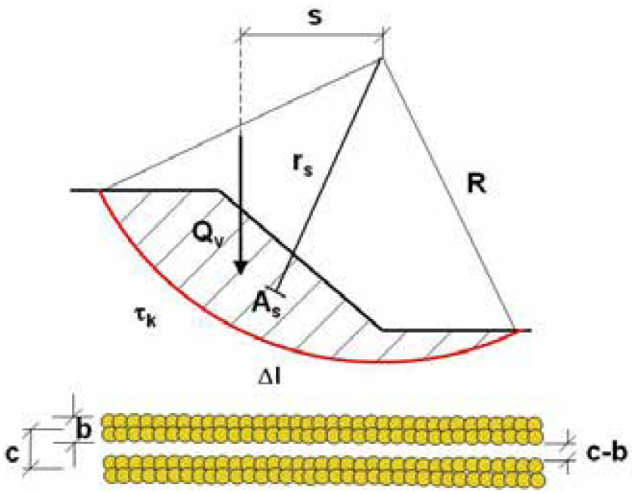

Figure 4.3.2: Stability control for soil mass between stabilizing discs, taken from [36].

The equation for the factor of safety between two stabilizing discs of lime cement piles is:

$$SF = \gamma_M = \frac{M_{stab}}{M_{driv}} = \frac{R \cdot \sum \tau_k \cdot \Delta l \cdot (c-b)}{Q_v \cdot s \cdot (c-b)} \tag{4.3.1}$$

where γ_M is the material safety factor, τ_k is the shear strength of the soil, Δl is the length of the sliding surface, c is the center distance between the piles, and b is the width of the disc. Q_v is the driving forces per meter of the resultant, s is the torque arm of the load resultant, and R is the radius of the sliding circle.

The distance c between the discs can be determined from a consideration of the equilibrium between M_{stab} which consist of the total shear strength along the sliding surface in the width of the disc b, times the radius of the circle, and M_{driv} which constitutes the weight of the soil mass and external load over a width c, see Figure 4.3.2.

4.3.2 Squeezing

Squeezing has to be prevented and the ultimate lateral resistance to horizontal movements is an essential factor. Randolph and Houlsby (1984) [26] wrote a paper on the limiting pressure on latterly loaded piles. The soil was modeled as a perfectly plastic cohesive material, so that the capacity calculation was reduced to a plane strain problem in plasticity theory, where the pile moves laterally

through an infinite medium. The N_c factor which is non-dimensionalized with respect to the soil strength (S_u) and the diameter (D) was found to vary between 9,142 for perfectly smooth piles ($\alpha = 0$) and 11,940 for perfectly rough piles ($\alpha = 1$), see Table 1 in [26]. They also calculated the load factor (N_c) for other friction values between 0-1, see graph in Fig. 5 and Table 1 in [26].

Randolph and Houlsby found the ultimate lateral resistance for a single pile submitted to a displacement. This capacity increases if the pipes are placed with a sufficient small center distance. In the pipe wall case, the pipes may be located so close to each other making the pipes failure mechanism interfere with the adjacent pipes, and therefore the lateral capacity increases. When the pipes are placed close together, there will be a squeezing of soil mass through the pipes, unlike the failure for single piles where the failure goes around the pile. If the distance between the pipes approaches zero, the N_c factor would approach infinity since it would be impossible to squeeze the soil through. If the space between the pipes is between half a diameter and two diameters, the necessary force to squeeze the soil is close to $10 \cdot S_u$.

If there was no excavation, σ_v would be the same on both sides of the wall. If the pile was moved and σ_v on both sides of the wall was the same, the difference between the passive pressure (P_P) and active pressure (P_A) for undrained condition would be $4 \cdot S_u$ for a smooth pile and $5,14 \cdot S_u$ for a fully rough pile. For an excavation, the σ_v would not be equal on both sides.

The capacity is calculated with the bearing capacity formula in Equation (2.5.1) explained in Section 2.6. The force needed to move a pile through the soil per unit length is given by:

$$P = D \cdot N_c \cdot S_u \tag{4.3.2}$$

The following hand-calculation could be used to find a sufficient center distance S when the difference between the active and passive earth pressure is known. It can also be used to find the needed earth pressure for a chosen center distance. This is an equilibrium calculation of a section of the pipe wall, see Figure 4.3.3.

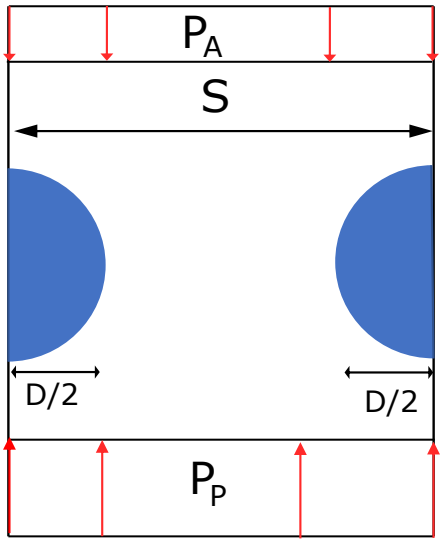

Figure 4.3.3: Section of the pipe wall, with active and passive pressure.

The resistance from Equation (4.3.2) is equal to the difference between active and passive earth pressure times the distance:

$$D \cdot N_c \cdot S_u = (P_P - P_A) \cdot S \tag{4.3.3}$$

S_u is the undrained shear strength for the specific horizontal plane that is examined, and N_c is the bearing capacity factor for undrained S_u-analysis. The following equation gives the maximum limit for the passive pressure when the active pressure is known as a function of the center distance S.

$$P_P = P_A + \frac{D}{S} \cdot N_c \cdot S_u \tag{4.3.4}$$

If the passive pressure is larger than the calculated value from the Equation (4.3.4) above, the piles would be pushed through the soil. Increasing the ratio between the diameter and center distance makes the soil squeeze through for a lower passive pressure.

From a standard sheet pile calculation in Plaxis 2D, the active and passive pressure can be found, the allowable center distance for that situation can then be calculated:

$$S = \frac{D \cdot N_c \cdot S_u}{P_P - P_A} \tag{4.3.5}$$

The center distance can be quite big since the N_c factor times S_u is quite large; it can transfer a significant amount for a relative large center distance. The situation above the excavation level therefore becomes the critical area and dictates how close the pipes need to be installed. The situation under the excavation floor will only be a problem if the bottom part of the pipes is installed with a very little depth underneath the excavation floor, unless the pipes are drilled into bedrock.

For the Nordenga bridge project, the pipes where installed with a relative large depth, and the anchors less passive pressure is mobilized. For an undrained situation the difference in pressure is $\pm S_u$, which is close to $4 \cdot S_u$ as mentioned above. For an excavation, there will be a smaller σ_v plus s_u, and a slightly larger σ_v minus s_u. Therefore, the difference in pressure is quite small and squeezing may not be the critical factor.

For a hypothetical case where the difference between P_P and P_A is 30 kPa and with a S_u of 35 kPa, the S has to be less than:

$$S = \frac{D \cdot N_c \cdot S_u}{P_P - P_A} = \frac{0,323 \cdot 10 \cdot 35}{30} < 3,7m \tag{4.3.6}$$

The plane-strain Plaxis simulation of the squeeze problem confirms the factor of $10 \cdot S_u$ as found in the paper from Randolph and Houlsby [26]. It is useful to be able to calculate the necessary center distance S, and the earth pressure can be found using a Plaxis simulation where interface stresses are used to find the difference, see Figure B.4.4. But it could also be calculated theoretically, calculating σ_v on both sides and add and subtract $\kappa \cdot s_u$:

$$P_P - P_A = \sigma_{v,inside} + \kappa \cdot s_u - (\sigma_{v,outside} - \kappa \cdot s_u) \tag{4.3.7}$$

The Plaxis squeeze model can also be used to calculate N_c when this is larger due to small spacing between the piles. For the case with a center distance of 0,6 meter, N_c was approximately 14. The model in Figure 5.5.1 can be used to verify the N_c factor and study the failure mechanism. For the simulation with cc 0,6 m, $P_P = 75$ kPa and $P_A = 43$ kPa, with an assumed $S_u = 25$ kPa, the obtained safety factor was 6,06, which gives a τ_c of:

$$\tau_c = \frac{25}{6,06} = 4,13 \tag{4.3.8}$$

The N_c for this center distance is found by the equation:

$$N_c = \frac{(P_P - P_A) \cdot S}{S \cdot s_u} = \frac{(75 - 43) \cdot 0,6}{0,323 \cdot 4,13} = 14,3 \tag{4.3.9}$$

The resistance of the piles increases when there is no space for the failure mechanism of a single pile due to interaction from the adjacent piles. This is shown in Figure 6.3.1 and explained in Section 6.3. This agrees well with the results from [1] where the undrained limiting pressure behind soil gaps was studied. In this study, there was only clay on one side of the piles, which means that the failure that occurs on the other side of the piles is not included. Since there is a bearing capacity failure on both sides of the piles, the double pressure given by the results in Figure 3.1.4 and Figure 3.2.1 may be used to find the maximum difference between the pressure on active and passive side of the wall.

For a single pile, a resistance of $10 \cdot S_u$ is obtained because there is failure on each side with a factor $N_c = 5,14$. In a pile wall, the adjacent piles will interfere with the piles failure mechanism, and the resistance will increase due to the arching effect, $N_c = 5,14$ is therefore not relevant to find the pressure that produces squeezing between piles. N_c is relevant for the pressure against the piles when the distance between the piles is more than $2 \cdot D$.

Chapter 5

Plaxis simulations

In order to study the stability in the soil gaps, various Plaxis simulations have been done and in this chapter. The model for the case above the excavation floor is reviewed and explained in Section 5.1. To examine the stability in the freely exposed soil gaps, an idealized model was made with a fundamental geometry, see Figure 5.1.1. The model is a section of the wall, with the soil gap in the center and with half of each pipe at the sides, see Figure 5.1.1. The width of the model is the same as the center distance of the pipes (cc). The excavation geometry and concrete geometry between the pipes have been varied.

A standard "sheet pile" model was made in Plaxis 2D to find the pressure acting on the wall, see Section 5.4. The earth pressure acting on the wall can be found in the results for interface normal stresses, see Figure B.4.4. These values may be used for the simulations above and below the excavation floor.

To study the problem with squeezing under the excavation floor, a model similar to the model of the freely exposed soil gap was made, see Figure 4.3.3. This model has soil on both sides of the pipes with a lateral pressure on on both sides representing active and passive pressure against the wall. The squeez model is reviewed in Section 5.5.

5.1 Plaxis model

First, the project properties were defined, 15-noded elements is used for the plane strain model, strains that extend perpendicular to the model plane are not considered. Then the contour of the model was designed. The model for the simulation is 2 meters deep (measured horizontally inward from the wall) and 1 meter for the widest models, with a varying width. When the geometry modeling is complete, the next step is to generate the mesh and finally define the construction stages. In engineering practice, a project is divided into construction phases, and similar to this the Plaxis calculation is also divided into phases [17]. The calculation of a safety factor is also an individual calculation phase, as explained in Section 2.8.1.

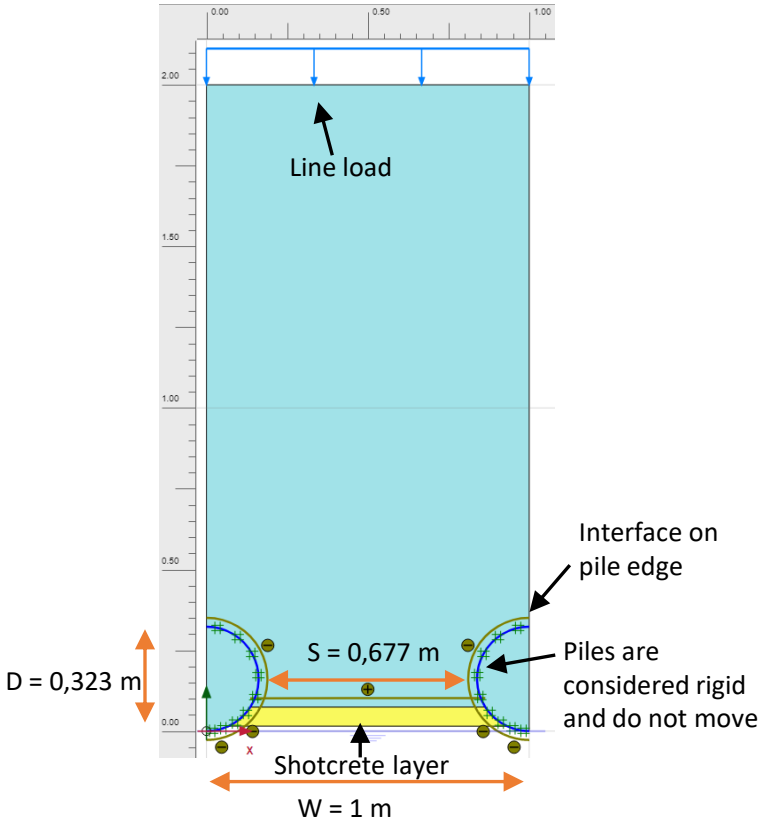

Figure 5.1.1: Problem definition from Plaxis, the line load produces a lateral pressure behind the soil gap in a contiguous pile wall. This lateral pressure causes a general failure in the soil mass.

5.1.1 Interesting parameters

There are several parameters that are interesting to investigate considering the stability and optimizing the design:

- Cohesion (c)
- Soil gap ratio ($\frac{S}{D}$)
- Dilatancy (ψ)
- Geometry of the shotcrete
- Geometry of the excavation
- Adhesion between steel pipe and shotcrete (R_i)

Cohesion is very interesting because it contributes to initiate the arching effect and makes the soil stable even at zero effective stress (as at the surface), and even when there is no shotcrete to help stabilizing the sand in the soil gap. The significance of the cohesion is shown through the equation for bearing capacity, see Equation (2.6.2).

For the simulations, a friction angle of 35° was used, which has a considerable effect on the stability but is not unreasonable to use considering what is realistic for sand, see Table 2.3.1. The dilatancy is an interesting soil property. It is a kinematic volume expansion as the sand is sheared due to the load, see explanation in Section 2.2. This could result in a favorable locking of the problem, which results in a rather large safety factor. However, there is no guarantee that the dilatancy will have the same effect in practice due to inhomogeneities and localized failures. Therefore, it is interesting to compare the results from varying the dilatancy parameter. A dilatancy of 5 degrees was tested since it seems reasonable when having a friction angle of 35°. The effect of the dilatancy was tested by setting the value to zero, since this could be a more conservative estimate.

5.1.2 Material definition

The soil parameters for the sandy fill material are inserted in the Material sets window, with an interface value of $R_i = 0,65$ for the soil-structure interface. A drained MC material model is utilized, with the following input parameters:

Table 5.1.1: Soil parameters for the sandy material.

Sandy fill material		
Soil parameter	Value	Unit
Cohesion (c)	1 - 5	kPa
Dilatancy (ψ)	$\psi = 0°and\ 5°$	Degrees
Friction angle (ψ)	35°	Degrees
Elastic modulus (E)	25	MPa
Poisson's ratio (ν)	0,3	-

A uniform lateral load produces the pressure behind the soil gap and the pipes, this is modeled as a line load of 50 kPa, as illustrated in Figure 5.1.1. Because of the assumption of plane strain condition, the soil is defined as weightless. Therefore, the only driving force is the line load.

The steel pipes in the model are made with the tunnel designer function in Plaxis. First the cross section is made by defining the shape as circular and defining half of the circle. Then it needs to be positioned right, and the geometry and properties need to be selected. An interface is applied to the pipes and they are given prescribed displacement of zero in both x- and y-direction. The steel pipes are modeled as elastic plates with the material parameters given in Table 5.1.3. The input parameters are normal stiffness (EA), bending stiffness (EI), weight (w) and Poisson's ratio (ν), with the following values:

Table 5.1.2: Material parameters for the steel pipes

Steel pipe material		
Parameter	Value	Unit
EA	2,0E6	kN/m
EI	8000	kN m^2/m
w	2,0	$\frac{kN}{m}/m$
ν	0,2	-

The piles modeled are assumed equally spaced rigid circular piles with diameter D and that each pile has a continuous bracing such that it behaves as a rigid structure whose movements are restrained.

The shotcrete is modeled using the Tresca material model,and has a compressive strength of 20 MPa and a tensile strength of 5 MPa. These values are on the conservative side. The tensile strength is obtained by setting the tension cut-off to 5000 kPa. It is essential that the factor between the stiffness of the sand and concrete is large, about 1000, ($E_{sand} = 25$ MPa and $E_{concrete} = 20GPa$). To simulate the correct behavior the concrete needs to be much stiffer than the sand. The following concrete parameters are used:

Table 5.1.3: Material parameters for B20 reinforced shotcrete.

Parameters for the reinforced shotcrete		
Parameter	Value	Unit
E	20	GPa
c	10	MPa
ν	0,25	kN -

A separate material is used to model the adhesion between the steel and the concrete. This material is the same as the shotcrete, but with a compressive and tensile strength of 500 kPa.

The piles and the geometry of the excavation and concrete arcs are created using the tunnel designer. It is utilized to generate geometry and add additional features. The tunnel design option is located in the structure tab of the main menu. To create the geometry, the first step is to select the insertion point and design the shape by inserting radius, angle of the arc, start and endpoint, and position it in the center of the model. The radius input is the value of the radius for an arc segment. Segment angle is the value of the arc length expressed in degrees, and start angle is the value of the arc length expressed in degrees, see Figure 5.1.2 [17].

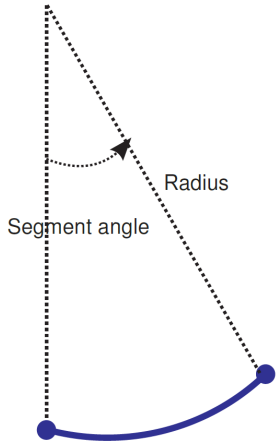

Figure 5.1.2: Properties of Arc segments. Taken from [17].

The construction stages are simulated as close to reality as possible, and the process is divided into different phases. In the initial phase, the initial stresses are generated. In the next phase, the line load is activated. Then the pipes are activated. In the following phase, the excavation takes place, and then a safety calculation is done to check the stability without shotcrete protection, since the wall has to be stable without shotcrete. In the consecutive phase, the shotcrete is activated and the cohesion is reduced, followed by a safety calculation.

5.1.3 Initial stresses

Before excavation, the wall is surrounded on every side by soil. For the specific plane modeled in Plaxis there are horizontal stresses in all directions. This could be $40-100\ kPa$ according to a usual horizontal stress for a given depth. Then the pipes are kept in place while the soil is removed on one side of the wall. A $50kPa$ line load seems like an ordinary load for the excavation depths done in several projects. The excavation is done in phases, where bracing and shotcrete is introduced sequentially.

To obtain the right initial horizontal stresses, the stresses need to be the same in the x- and y-directions with $\gamma = 0$. The stresses in the y-direction are given by the line load, and the stresses in the x-direction depend on the Poisson's ratio of the soil material. In the initial phase, the soil specimen is enclosed with the boundary conditions of a closed box. When a horizontal stress is introduced in the y-direction, the Poisson effect will give stresses in the direction perpendicular to the specific direction of the line load. A perfectly incompressible isotropic material deformed elastically at small strains would have a ratio of exactly $0,5$. The material will then behave similarly to rubber which has a Poisson ratio of nearly $0,5$, which becomes noticeably thinner when stretched. If a Poisson's ratio of $0,5$ is used, the horizontal stresses in the y- and x-direction would be the same.

The horizontal stresses in phase 1 and the initial phase in Plaxis should be isotropic. To do this, the material model and Poisson's ratio need to be changed. The same soil material which is otherwise used in the simulation can be used, but with a linear elastic material model instead of the Mohr-Coulomb. And with a Poisson ratio of $\nu = 0,495$ which gives approximately $K_0 = 1$. The rest of the parameters can stay the same. The ν is set to 0,495 instead of 0,5, to avoid numerical

problems in Plaxis.

The material with $\nu = 0,495$ is introduced in the initial phase and in phase 1 where the line load is activated, and the same correct initial horizontal stresses in x- and y-direction are obtained. In phase 2, where the pipes are activated, the soil material is changed to the original one, with Mohr-Coulomb material model and $\nu = 0,3$. Plots of Cartesian stresses, see Figure 5.1.3, shows something that looks like a large uniaxial compression test, with some disturbance at the bottom. As noted in Figure 5.1.3 the horizontal stress in the y-direction is the largest and the stress in the x-direction is a bit smaller. The lateral pressure is 100 kPa, σ_{yy} is slightly above and close to 100 kPa and σ_{xx} is slightly under 100 kPa.

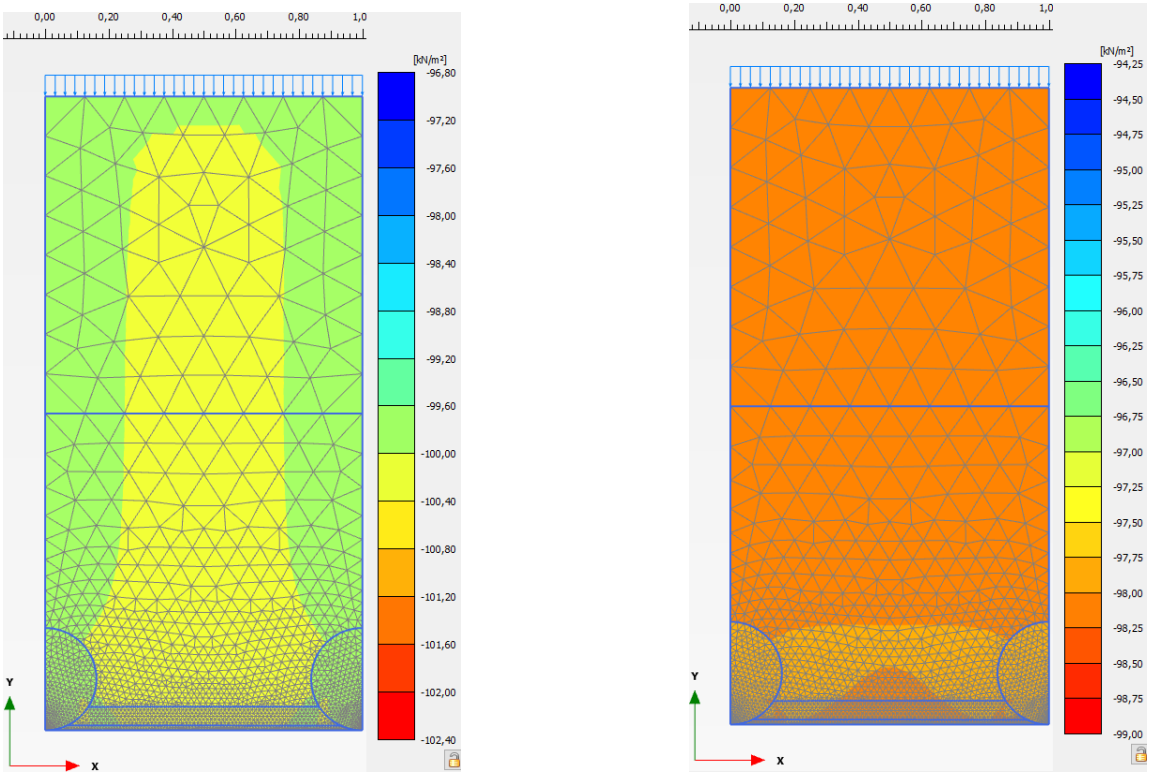

(a) **(b)**

Figure 5.1.3: **a** Cartesian effective stress σ_{yy}, maximum pressure is -102,1 kPa. **(b)** Cartesian effective stress σ_{xx}, maximum pressure is -98,75 kPa.

If the soil used in the initial phase has a $\nu = 0,3$ like the soil in the other phases, instead of $\nu = 0,495$, Equation (2.11.4) would give a $K_0 = \frac{\nu}{1-\nu} = 0,43$. For a simulation with a line-load of 100 kPa the Cartesian σ_{xx} plot gives $\sigma_{xx} = 39,2$ and the σ_{yy} close to 100. For that case the mobilization would be given by Equation (2.3.4):

$$N = \frac{\sigma_1' + a}{\sigma_3' + a} = \frac{100 + 7,14}{39,2 + 7,14} = 2,3 \tag{5.1.1}$$

If the friction angle is more than 30°:

$$N = \frac{1 + sin\phi^\circ}{1 - sin\phi^\circ} = \frac{1 + sin30^\circ}{1 - sin30^\circ} = 3 \tag{5.1.2}$$

the corresponding SF would be greater than 1, see Equation (2.3.4). In this case the plot of plastic points shows that not everything is elastic.

5.1.4 Excavation phase

For the excavation phase, there are also plastic points indicating plastic deformation. In the top part, it has the tendencies of a uniaxial compression, with some disturbances in the bottom where the soil is squeezed out.

In the model, the sides are restrained and keep the soil confined, and for applied stresses in such circumstances the Poisson ratio will be more or less as in an oedometer. That will also be the case for stresses applied under a wide footing [5]. See Section 2.11 for further explanation.

In the excavation phase, the load may be changed to the value obtained from the interface normal stresses in the sheet pile calculation, see Section 5.4. The stresses introduced in the initial stress phase is the lateral earth pressure at rest (K_0), and after excavation the pressure perpendicular to the wall will be the active pressure.

5.1.5 Excavation geometry

The soil is excavated on one side of the wall, and how much soil is removed between the pipes and what geometry should be used can be discussed. Different excavation geometries are simulated, with both concave and convex arcs and straight lines, above, under and in the center of the pipes. To successfully excavate, one must have a certain cohesion, which is responsible for initiating the arching effect and keeps the soil stable at the soil gap surface with zero effective stress as mentioned initially. Since $\gamma = 0$, there is no γ to help the soil fall down and flow out of the gap. It is important to keep this non-conservative effect in mind. The Plaxis model is a horizontal plane with zero vertical gravitation to help the soil particles fall down. For the initial phase all stands in its place just because it's there, so this part is exaggerated. Exceptionally if there is water or anything else that could drive it out, as mentioned in Section 4.1. When excavating, one may encounter local areas with water which make the area weaker, and this can be elevated fast by welding steel plates onto the pipes. If the wall is left exposed, heavy rainfall may erode away the fine-grained material, and therefore reduce the arching effect and make a weakness zone. A more critical challenge is if the groundwater level is above or raises the excavation level, but that should not be the case, or else there would be problems. There is included some cohesion in the calculations and realistically a cohesion of 5 kPa may be expected, which is an experience value often used by consultants for this type of ground conditions. This originates from the cementation that may be between the grains in the soils.

5.1.6 Mesh dependency

As a step to verify the proposed model, a mesh refinement study was done. The study was done with and without the concrete sealing. Since the concrete layer is rather thin, it is reasonable to assume that sufficient elements over the height is essential to simulate realistic response. This assumption was backed up with a mesh refinement study for the concrete. The problem with having a thin concrete layer is that it is essential to have a fine mesh in the arc to see how the arc fails and a more exact location of where the plastic points occur, which can be a problem because of

the small area. The mesh in this region needs to be refined and then controlled. The quality of the results cannot be guaranteed if there are not at least two elements in height.

A mesh dependency test was done both for the case with and without concrete. The test was carried out by doing three different simulations, one with very coarse mesh, medium mesh, and very fine mesh. The concrete layer was modeled with at least two elements over the height. Both displacements and stresses were controlled, and the overall trends were similar. The stress distribution was the same, with similar values for maximum and minimum values. The arching effect with rotation of the principal stress direction from one pipe to the other was prominent in all meshes. It seemed like a finer mesh needed mote calculation steps to converge and approach the results from the coarser meshes.

An area of particular interest regarding the mesh is above the excavation edge. This is important regardless of the concrete arc in order to obtain a detailed failure mechanism. The mesh was optimized by dividing the model into three soil clusters, where the soil cluster at the bottom around the pipes is refined and the rest are coarser.

The soil body consists of three clusters. This is done to optimize the mesh. The upper part of the model may have quite coarse mesh, while the bottom part, the area around the pipes has to be more refined.

5.2 Simulation

5.2.1 Construction phase for the concrete

In practice, the earth pressure induced stresses will first be taken by the soil through the arching effect. After some time, the concrete will take up the load because there will be a reduction in cohesion as well as other varying factors. The reduction of cohesion comes from unloading of the retained soil due to excavation. The unloading may lead to a reduction of the cementation in the soil material. Erosion from weather and water will also reduce the arching effect, the arching is reduced when stabilizing material is removed, the water may erode the fine-grained material which is a component in the stabilizing soil. As explained in Section 5.1.5 gravity will contribute to the movement of soil in the soil gaps as well, and increase the stress acting on the wall. All of these factors make the stability of the freely exposed soil gaps time dependent. As discussed in Section 4.1 the cohesion in the material could be reduced some time into the project and depending on the conditions the geotechnical consultant and the contractor assesses how long it can remain unprotected.

After the first calculation phases where the initial stresses in the soil are introduced and the piles are activated, a calculation phase named excavation is simulated followed by a safety calculation. Here the stability of the unprotected soil gap is examined, it has to be stable since it must be able to stand without shotcrete for at least some days, as explained in Section 4.1. Then the shotcrete is applied, with a separate material as the steel-concrete interface. The interface material is called "adhesion" and has a compression- and tensile strength of 500 kPa. In the same phase the cohesion is reduced to 0 kPa and for some simulations 2 kPa. The soil's ability to hold back the pressure reduces, since the cohesion is necessary to obtain the arching effect, as seen from the results of the parametric study of cohesion. When the cohesion is reduced one want to achieve the real transfer of stresses from the soil to the concrete, which are the stresses that the concrete in practice ends up having to take. That is why shotcrete is used, to secure the long-term structural integrity of

the wall even though the soil stabilizing mechanism is heavily reduced, along with other short- and long-term Health, Safety and Environmental factors mentioned in Section 4.2. A safety calculation is performed in the subsequent phase, and the safety factors for different concrete geometries and center distances are plotted in Figures 6.2.4, 6.2.3, 6.2.2, and 6.2.7.

As mentioned there are several factors which are included in the fact that the concrete takes up more stresses after some time. For example, it is not unusual that there are requirements for the use of the space behind the retaining wall during the excavation of the pit, due to excess loading in a critical phase. Some time into the project the space outside would be needed to the further construction, and the loading from equipment would as well increase the stresses acting on the wall.

These increased stresses due to excess loading or a loss of cohesion need to be accounted for in the simulations. As explained, the cohesion is reduced when the concrete is applied, but there are other methods to simulate this. It could be done by:

- Change the total multiplier giving it a value less than 1 ($\sum Mstage < 1$).
- Utilizing the $\beta - Method$, deciding the percentage of the total stresses that is going to be taken by the concrete, the rest is taken by soil-arching.
- Reducing the cohesion, the soil will take less of the stresses through arching and the concrete will have to take it.
- Increase the lateral loading, by changing the line-load.

Mstage < 1

When changing the $Mstage$ from 1, there will be unbalanced forces that need to be accounted for in another phase in order to successfully finish the simulation. This is explained in Section 2.8.1. With $Mstage < 1$ the actual load is reduced from what it should be in the specific calculation step, and it is possible to estimate the load that has actually been applied with this Equation (2.8.1). A part of the load can therefore be taken by the soil without reinforcement, and another by the concrete. A calculation step where the gap is excavated may have a $Mstage = 0,5$, which approximately gives 50% of the load. In the following step the concrete is activated and the rest of the load is introduced by setting $Mstage = 1$.

β-method

The plot of the effective stress in the output program shows that arching occurs around the soil gap. This arching in the soil reduces the stresses acting on the concrete, the same way that arching reduces the stresses on the lowered section of the support base in Terzaghi's trap-door experiment [20], explained in Section 3.1. One way to make this happen is to emulate the arching effect by using the β-method. This method lets the soil take up a part of the stresses before the support is introduced and the deformation of the soil mass decreases. This is done by taking the stresses p_k behind the retaining wall that comes from the excavation, and divide it into a part $(1 - \beta) \cdot p_k$ that is applied before the shotcrete is activated so that the soil arching can take some of the stresses. Then the other part, βp_k is applied to the shotcrete support.

Reducing the cohesion

As mentioned above in Section 5.2.1, one of the reasons the concrete experiences an increase of stresses after some time is due to a decrease of cohesion. One obvious way of simulating this is by

decreasing the cohesion in the subsequent construction stage after the concrete is inserted. This is a very logical way to simulate it and has therefore been chosen.

Increasing the lateral load

An increase of line load will increase the stresses in the concrete put may not be a realistic behavior in practice. It could be a useful, but it is more logical to reduce the cohesion. In the safety calculation the strength of the shotcrete arc must correspondingly and proportionally be reduced to obtain a realistic safety factor and failure mechanism. This is done as described in Section 2.8.1 The concrete material is therefore modeled as a volume element (soil), and the option to apply strength reduction for the material needs to be selected. The dilatancy angle ψ is not affected by the reduction, unless the friction angle ϕ is reduced so that it is equal to ψ, then the further reduction of ϕ is also applied to the dilatancy ψ. The steel pipes in the model are fixed, and their strength is not reduced in the calculation.

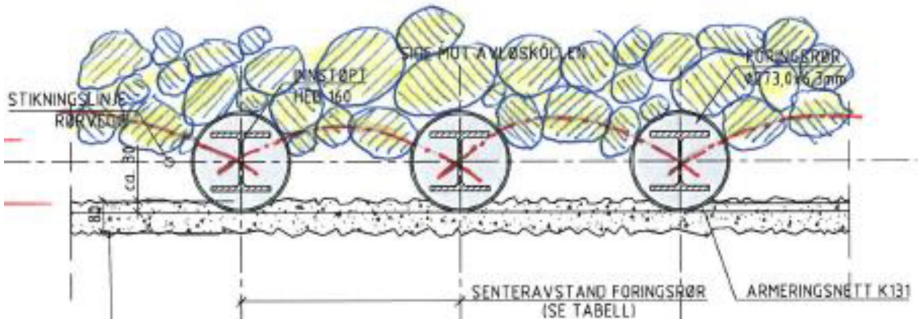

Figure 5.2.1: Arching effect in coarse masses behind the permanent wall at Avløs station, taken from [30]

5.3 Different simulations

The dimensions of the pipe wall i the simulations are the same as the dimensions used in practice. In practice, pipes with diameter 273 or 324 mm are used, with a center distance of 0,5 m or 0,6 m.

Based on information from consultants in Geovita a sheet pile walls in Plaxis 2D was made, and from this, typical forces were obtained.

For the plane strain horizontal model of a pipe wall section, the lateral pressure was obtained from regular sheet pile wall simulations in Plaxis 2D, and from this an overview of the resulting earth pressure was obtained. In the horizontal model, the earth pressure in the x-direction is calculated from earth pressure at rest. In the y-direction, the pressure is obtained from active-passive earth pressure calculations in Plaxis.

5.3.1 Concrete and adherence simulations

In order to make guidelines for construction of the pipe pile wall the adherence between the concrete and steel is interesting. In the design process it is relevant to know what a bad adherence can lead to. The interface value R_{inter} is therefore changed in order to see how the adherence is influencing the stability. When the interface moves along the pipe surface, the adherence is broken and is

therefore interpreted as a failure.

5.4 Nordenga bridge model

A standard "sheet pile" was model of the pipe wall at Nordenga was made in Plaxis 2D. The wall is roughly 11,5 m deep, with bracing at 1,5 and 4,5 m of depth. There is a distributed load of 66 kPa on the ground floor outside the pit, which is the railway load. A 20 m x 20 m FEM mesh box is used for the simulations. See Figure B.3.9. This figure shows the right hand side sheet pile wall for a 5 m wide and 4,7 m deep, symmetric excavation in sandy fill, with a layer of medium firm silty clay under the excavation floor. The undrained shear strength at the beginning of the layer is $s_u = 25kPa$ and increases with 4 kPa/m.

The top layer is a sandy fill material and is the same material used in the horizontal model. The sandy fill material is defined in Table 5.1.1, with a unit weight of 20 $\frac{kN}{m^3}$. The soil parameters for silty clay are defined in Table 5.4.1

Table 5.4.1: Soil parameters for the silty clay material

Silty clay	
Soil parameter	Value
Undrained shear strength s_u	25 kPa increasing with 4 kPa/m
Elastic modulus (E_u)	15 MPa
Poisson's ratio (ν)	0,495

Elastic beam elements are used for the wall with interface elements on both sides. An $R_{inter} = 0,65$ is applied for these interfaces. For numerical reasons the interface has been extended below the tip of the wall, and a horizontal interface is applied at the bottom due to possible horizontal movements at failure. For the extensions an $R_{inter} = 1,0$ has been applied.

The bracing consists of an internal strut bracing made of H-beams at the bottom and a self-drilling soil anchor called MAI anchors. Both the strut and the anchor are elastic, the strut and the soil anchor is modelled as a fixed end anchor. Soil anchor properties are defined in Table 5.4.2, and strut properties are found in Table 5.4.3.

Table 5.4.2: Soil parameters for the silty clay material

Soil anchor	
Properties	Value
Axial rigidity (EA)	219 MN
Spacing between the anchors ($L_{spacing}$)	1,8 m

Table 5.4.3: Soil parameters for the silty clay material

Strut	
Properties	Value
Axial rigidity (EA)	500 MN
Spacing between the anchors ($L_{spacing}$)	1,0 m

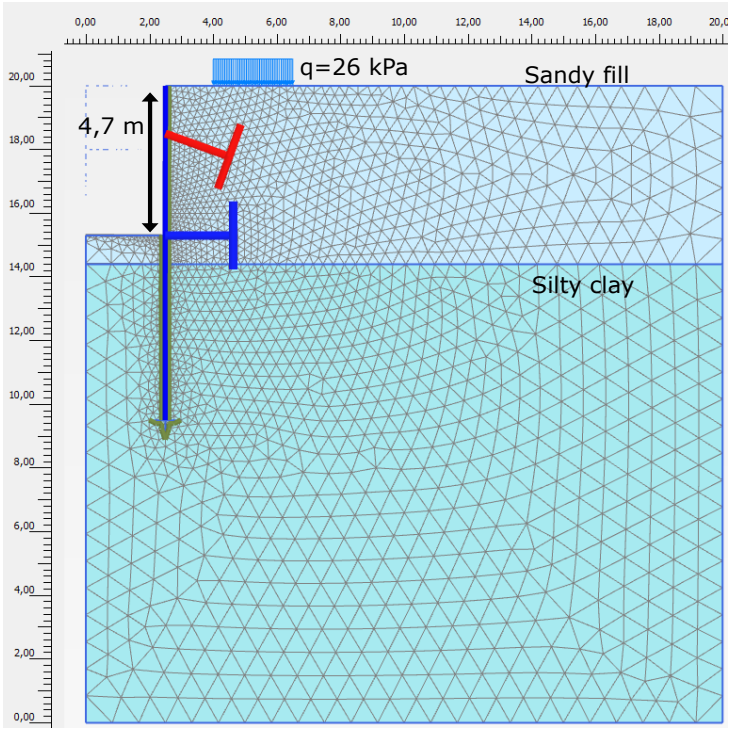

Figure 5.4.1: Plaxis model of the pipe wall at Nordenga bridge

5.5 Squeezing under excavation floor

To study the failure mechanism and find the N_c factor for a particular situation as explained in Section 6.3, a horizontal plains strain model of the wall under excavation floor can be made, see Figure 5.5.1. The inputs for this model is the material parameters and the undrained shear strength for that specific depth, and both the active and passive pressure. The passive and active earth pressure may be calculated in Plaxis, by performing a sheet pile simulation. The inputs to the model shown in Figure 5.5.1 are from the the wall at Nordenga, explained in Section 5.4. The values for the earth pressure are found in the plot of interface normal stresses, shown in Figure B.4.4. The values from the plot of interface normal stresses are exported to excel, and there the active and passive pressure acting on the same point is found.

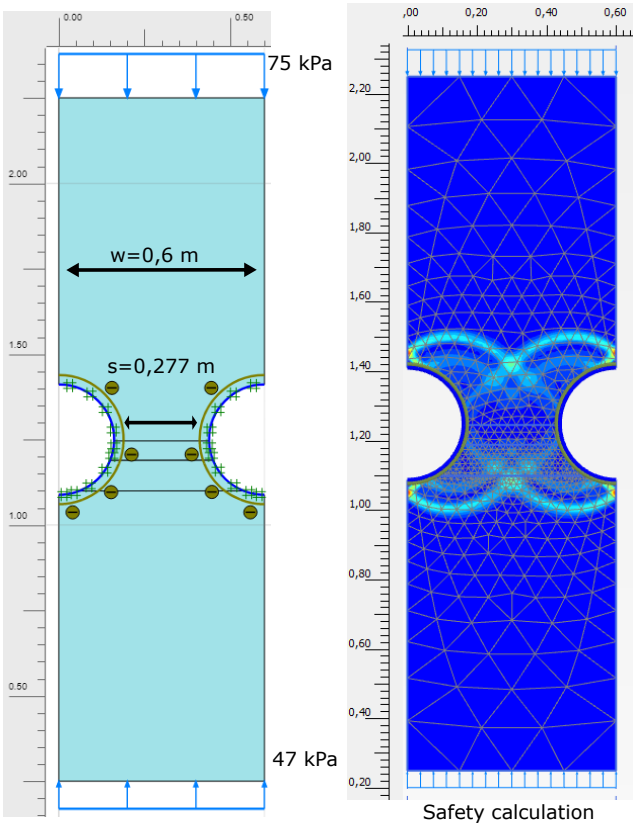

Figure 5.5.1: To the left: Plaxis model of the squeeze problem with cc 0,6 m, $P_P = 75$ kPa and $P_A = 47$ kPa. To the right: a incremental deviatoric strain plot showing the failure mechanism. Note that a double reversed bearing capacity failure can be seen. Obtained SF=6,06

Chapter 6

Results

In this chapter, Plaxis results are presented with comments and brief discussions. In the following Chapter 7, the entire system with relationships is discussed. What happens during the different construction stages and the behaviour of the soil-structure interaction is explained. The behavior of the soil is studied through plots of incremental strain, principal stresses and plots with plastic and tension cut-off points. The groundwater level is underneath the area of interest, so the effective stresses and the total stresses are the same.

Principal stress plots show how the applied stresses are transferred to the pipes through arching, and in the following phase they show the stresses in the concrete. Principal stresses are also used to illustrate the arching effect in the soil, the rotation of principal stresses show how stresses are transferred through from the yielding soil to the stationary pipes.

Simulations of the horizontal model of the pile wall above the excavation floor have been done. Both the unsupported and shotcrete supported soil gaps have been simulated. The center distance between the pipes can not be too small since there is a risk of collision between the pipes further down. This consideration is especially important for long pipes. The most common pipe dimensions are pipes with a diameter of 273 or 324 mm, with a center distance of 0,5 or 0,6 m. For the simulations pipes with a diameter of 324 mm are used, with a center distance of 0,6 m, 0,8 m and 1,0 m.

6.1 Simulations without shotcrete

For the simulations without shotcrete, the excavation geometry has been varied along with soil parameters such as cohesion and dilatancy. A reduction of cohesion has been simulated, this represents the decrease of cohesion over time due to erosion from weather and unloading of the retained soil due to excavation. In Section A.1, plots showing principal stresses for different values of cohesion are found, and in Figure 6.1.1, a graph showing the cohesion vs safety factors (SF) for different excavation geometries is presented.

The variation of geometry has included straight lines in different levels, in the middle of the pipe, above and under. Convex pressure arcs (bridge arc) over the midpoint, and concave arcs under the midpoint. For the geometries where more soil is removed between the pipes, lover safety

factors are obtained.

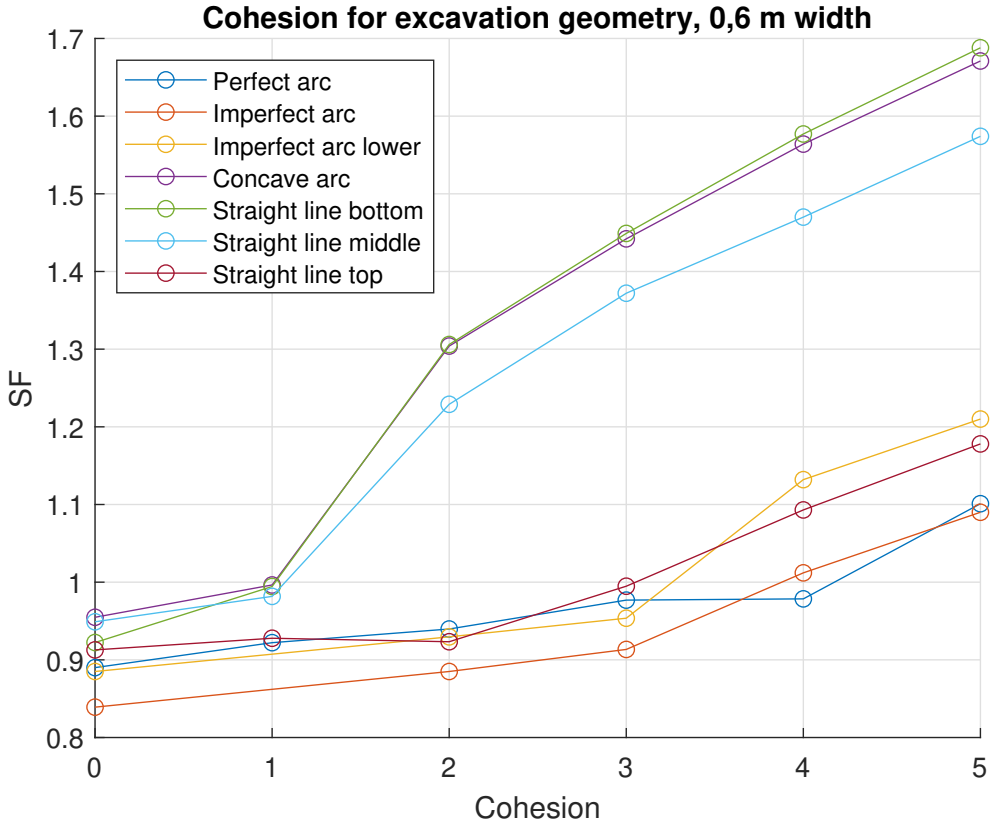

Figure 6.1.1: SF vs cohesion for different excavation geometries.

In the plots of deviatoric strain, the failure shape for the different excavation geometries is shown, see Figures 3.1.3, A.2.5, **??** and A.2.9. The failure shapes show shear bands which resembles the characteristic shape of bearing capacity failure from stress field theory. For a small center distance, the active Rankine zone becomes more visible. The failure shapes are presented in both deviatoric strain and plastic point plots.

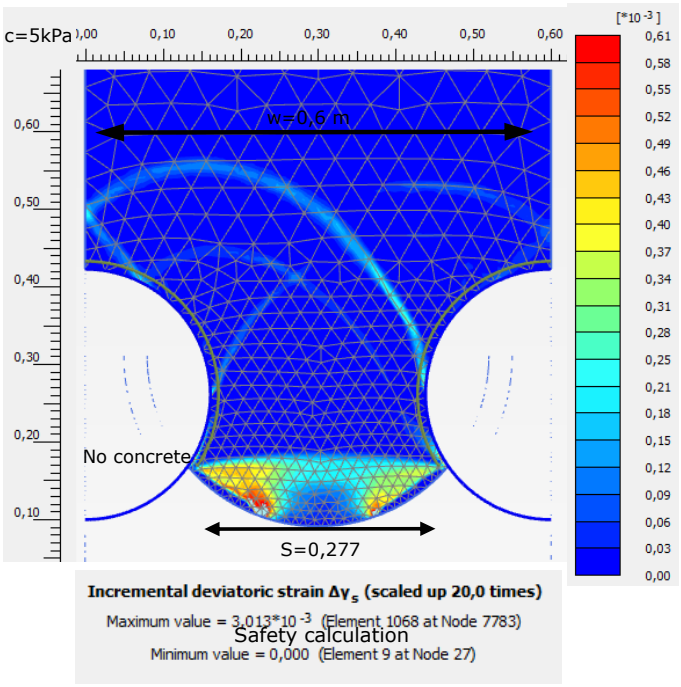

Figure 6.1.2: Failure mechanism for concave excavation geometry cc 0,6 m

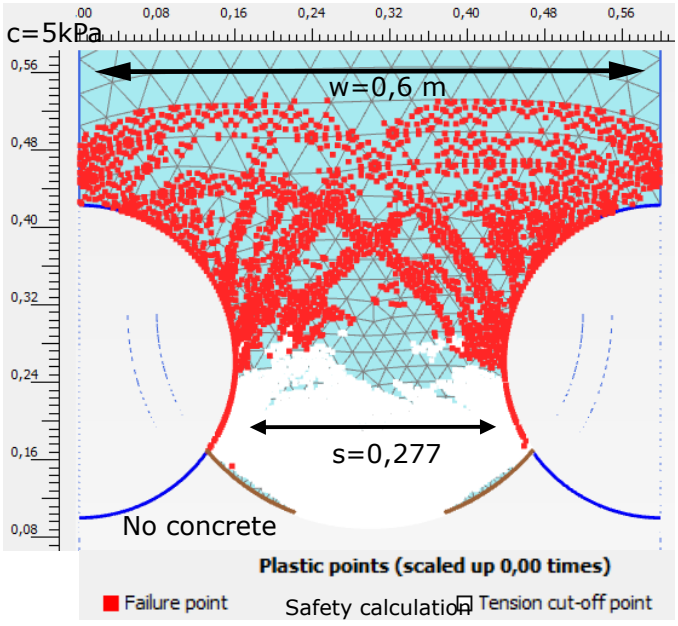

Figure 6.1.3: Plastic points plot for concave excavation geometry cc 0,6 m. A lot of tension cut-off points in the bottom part of the soil. This is hanging onto the rest of the soil because of the cohesion and friction between pipe and soil.

6.1.1 Principal stresses and arching

The principal stress plots show that the stresses are divided and transferred to the two piles, there is a rotation in the principal stresses which forms an arc from one pipe to the other.

6.1.2 Excavation area

When excavating behind the pipes, the safety factor is reduced. From simulations there has been found a clear link between the extent of excavation behind the pipes and a reduced safety factor. This is not unreasonable, considering that soil is taken away so that there is less soil to support and distribute the load. More load on a smaller area will increase the deformations and further reduce the stability.

This becomes a dilemma when discussing the benefits of excavating more thoroughly and further in between the pipes to get the concrete on the favorable side so that it can be wedged between the pipes. Like these results are indicating, lower safety for excavation over the middle line, the short-term stability is decreased when more soil is excavated. The soil itself is stabilizing, and as discussed in Section 2.4, less soil reduces the arching effect. This means that one can not depend on the large effect of wedged concrete behind the pipes, since the short-term stability is important. The concrete is introduced after excavation, and the wall needs to be able to stand without this support.

The wall needs to be excavated so that the pipes emerge, which is important because the shotcrete needs a pile surface to stick. Due to the short-term stability, it may not seem like a good idea to remove too much of the stabilizing soil in the area behind the center-line of the pipe. Like discussed earlier, what gives the concrete tensile strength, which is used to make it stick to the wall and take the earth pressure induced by a decreasing cohesion, is the concrete-steel adhesion to the pipes and the integration of the concrete with the bracing. The bracing with its anchors and girder keeps the concrete in its place, and may contribute considerably to the stability of the soil gaps. This is because that in order for the shotcrete to fall off the wall, it needs to brake the bracing loose, which most likely requires a very large load.

6.1.3 Dilatancy

As seen in Table 6.1.1 the stability increases when the dilatancy angle is changed from ° to 5°. It has an positive effect, because it is a kinematic volume expansion as the sand is sheared due to the load, see explanation in Section 2.2. This will probably make the sand dilate in the area above the pipes and makes it more difficult for the sand to be squeezed through, thus the safety factor increases.

Safety factors	Perfetct arc	Imperfect arc	Concave arc	Bottom line	Middle line	Top line
Without concrete						
c=5	1.101	1.09	1.671	1.688	1.574	1.178
c=5 & ψ=5	1.123	1.124	1.697	1.717	1.595	1.199

Table 6.1.1: SF vs dilatancy (ψ) for different excavation geometries.

6.2 Simulations with shotcrete

For the arcs on the favorable side, high safety factors are obtained, see Figure 6.2.1 and Section 6.2. When the cohesion is reduced, the concrete will take all the resulting stresses and it can take a lot because of the favorable location of the concrete where it is subjected to pressure. The strength parameters in the soil and the concrete can therefore be reduced a lot before failure and a high SF is obtained. For the concave arc on the bottom side and the straight lines in the middle and at the bottom, lower safety factors are obtained. The concrete can not take the same stresses when it is not on the favorable upper side. For concrete located under the center point failure occurs when the concrete-pipe interface slip, which means the adhesion is the critical factor. When the concrete is on the favorable side, the adhesion becomes of less importance since the concrete is pushed against the pipe, and does not hang on the pipes by adhesion like for the other cases.

There is a large difference between the straight concrete layer on the upper part of the pipe and the other arcs located at the same place. It is clear that the arc geometry helps distribute the stresses so that the concrete is subjected to compression. The straight concrete layer fails in the interface, and the arc geometry is less dependent on the interface adhesion and friction since it is pushed directly into the pipes. For the concrete arc with perfect circular geometry the highest SF is obtained see Section 6.2, this is not realistic. It is not realistic because it is impossible to make a similar perfect arc in practice, but nevertheless a concrete arc with imperfect but similar geometry will give high safety factors as showed in the results for the imperfect arc, see Section 6.2.

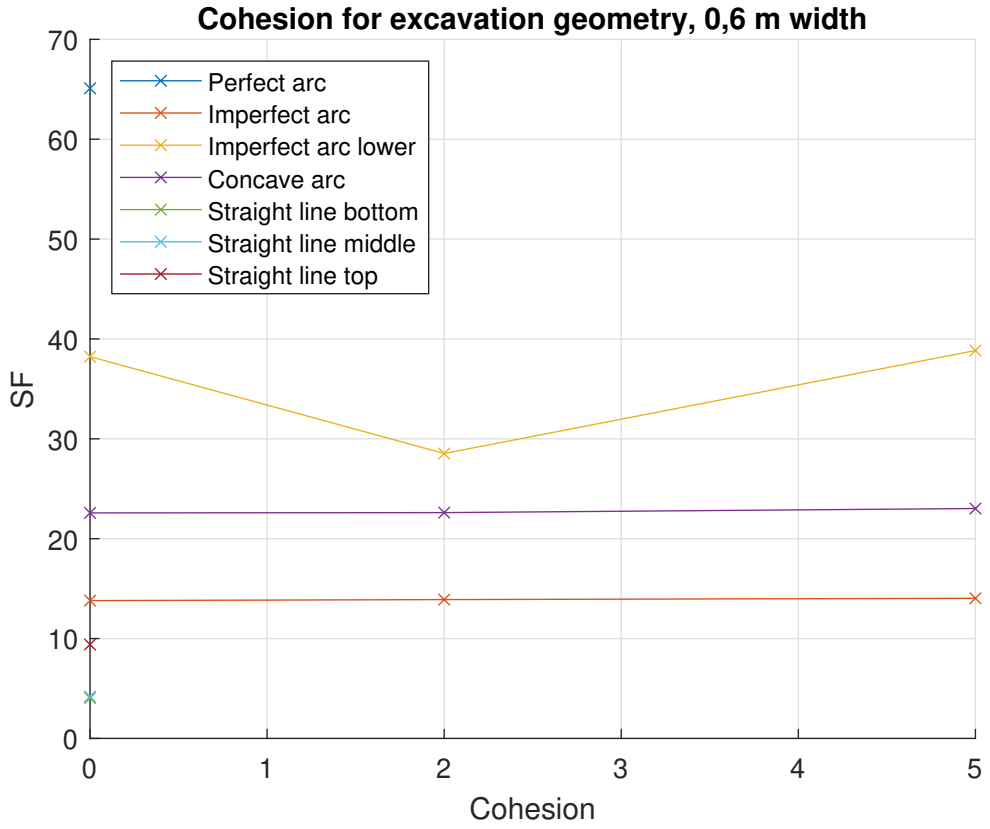

Figure 6.2.1: SF vs cohesion for different excavation geometries.

With shotcrete	Perfetct arc	Imperfect arc	Imperfect arc low	Concave arc	Bottom line	Middle line	Top line
c=0	65,1	21,83	38,23	22,58	4,044	4,197	9,409
c=2		22,04	38,53	22,61			
c=5		22,32	38,84	23,02			

Table 6.2.1: Safety factors for different shotcrete geometries. For a center distance of 0,6 m.

In Section 6.2, one can clearly see that it is more favorable with an arc geometry in comparison to a straight layer. The concrete arcs that are closer to the mid point, for example, the imperfect arc which is placed lower than the other has a higher safety factor. The same tendency can also be seen from the results of the straight concrete layers, the bottom layer has a SF=4 and when it is applied at the top, it has a SF=9,4.

The perfect arc has a very high safety factor, as expected, and when it is made imperfect, the safety factor is reduced with $\frac{2}{3}$. The concave arc has a relatively large safety factor.

For the simulations with concrete, the adherence to the pipes has been varied, along with the geometry. The adherence is an interesting parameter since it is important for safety reasons, and contributes to the concrete's tensile strength which helps the concrete stick to the wall and not

fall off. Professor Steinar Nordal has recommended an interface with a strength equal to 500 kPa, this value can be discussed and recommended as a potential good and safe value. It is not too big, and this is what it may be for a sandy, rusty and a bit rough surface. The assumption can also be strengthened with a cleaning requirement for the pipes before they are installed, in order to not reduce the arching by washing away soil. Following, compressed air can be used in order to remove sand and other soil remains.

6.2.1 Significance of adhesion

Figure 6.2.7 shows that the safety factor is reduced when the adhesion is reduced. Adhesion has a great influence on the SF. The adhesion is essential for the safety, especially when bracing is not used. Dirty pipes will reduce adhesion significantly, properly cleaning of the pipes may help to secure a good adhesion and therefore increase safety significantly. The shotcrete must not loosen from the wall, because this will lead to a high risk of injuries. The safety is significantly increased even with a small adhesion value, which is explained by the initial stress p' produced in the soil gap. This value depends in this case on the adhesion, the p' is multiplied inwards in the soil's stress field and helps to initiate the arching effect as explained in Section 2.6. This has a huge effect for the ultimate bearing capacity and since it is soil with friction, a great effect is obtained from the log-spiral in the stress field, illustrated in Equation (2.6.2) and Figure 2.6.2.

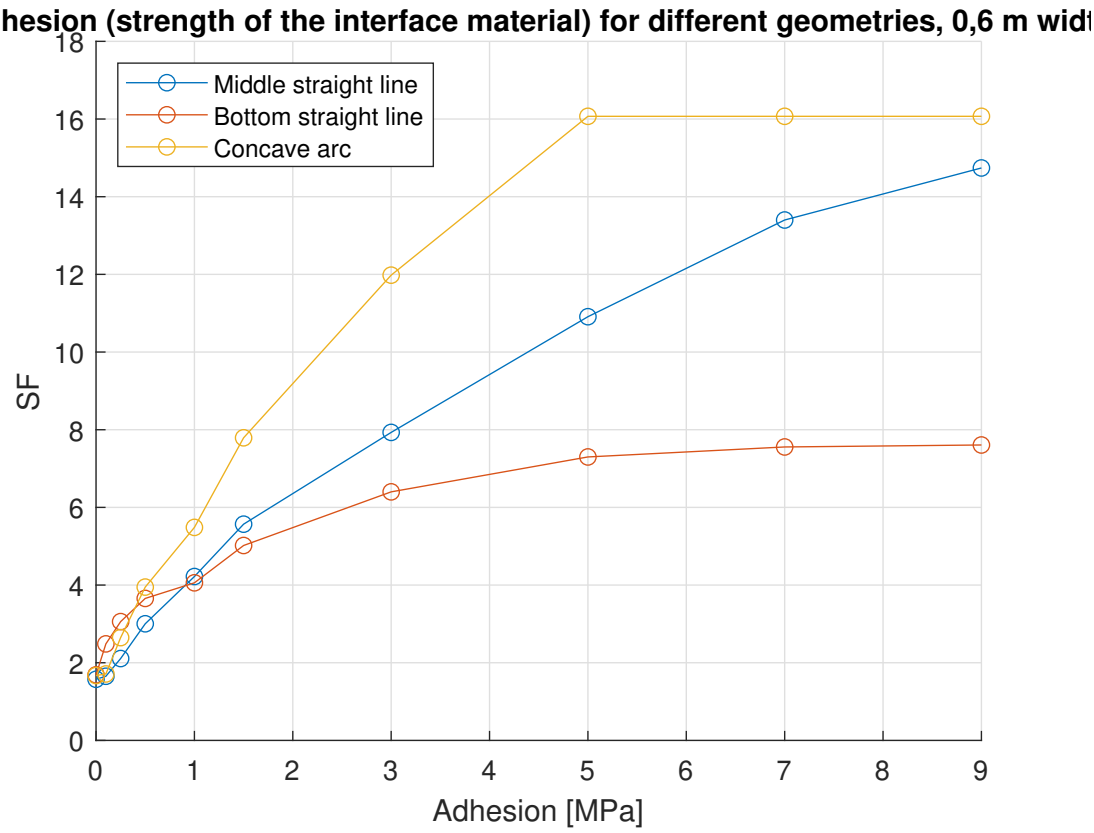

Figure 6.2.2: cc 0,6m. The adhesion is calculated by assigning a concrete material with a reduced strength that represents the adhesion. The adhesion is the strength of the interface material. The significance of the adhesion is examined for three different shotcrete geometries; a concrete layer slightly below the center of the pipes, a layer at the bottom and a concave arc below the center point of the pipes.

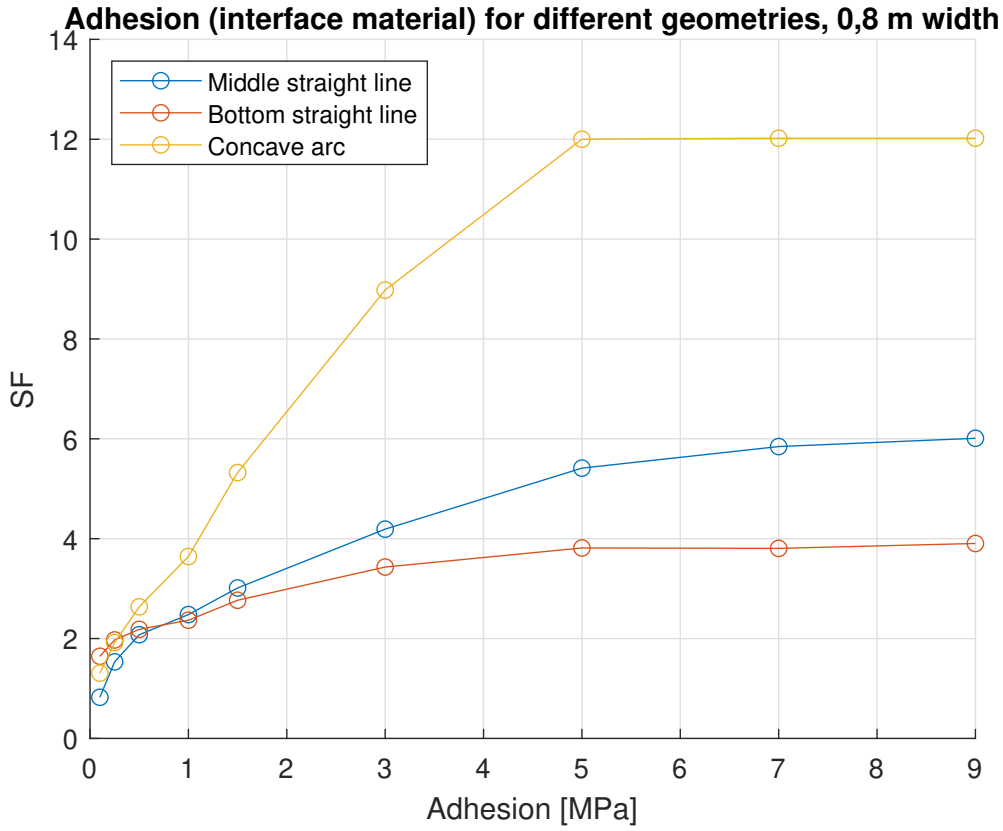

Figure 6.2.3: cc 0,8 m. The adhesion is calculated by assigning a concrete material with a reduced strength that represents the adhesion. The adhesion is the strength of the interface material. The significance of the adhesion is examined for three different shotcrete geometries; a concrete layer slightly below the center of the pipes, a layer at the bottom and a concave arc below the center point of the pipes.

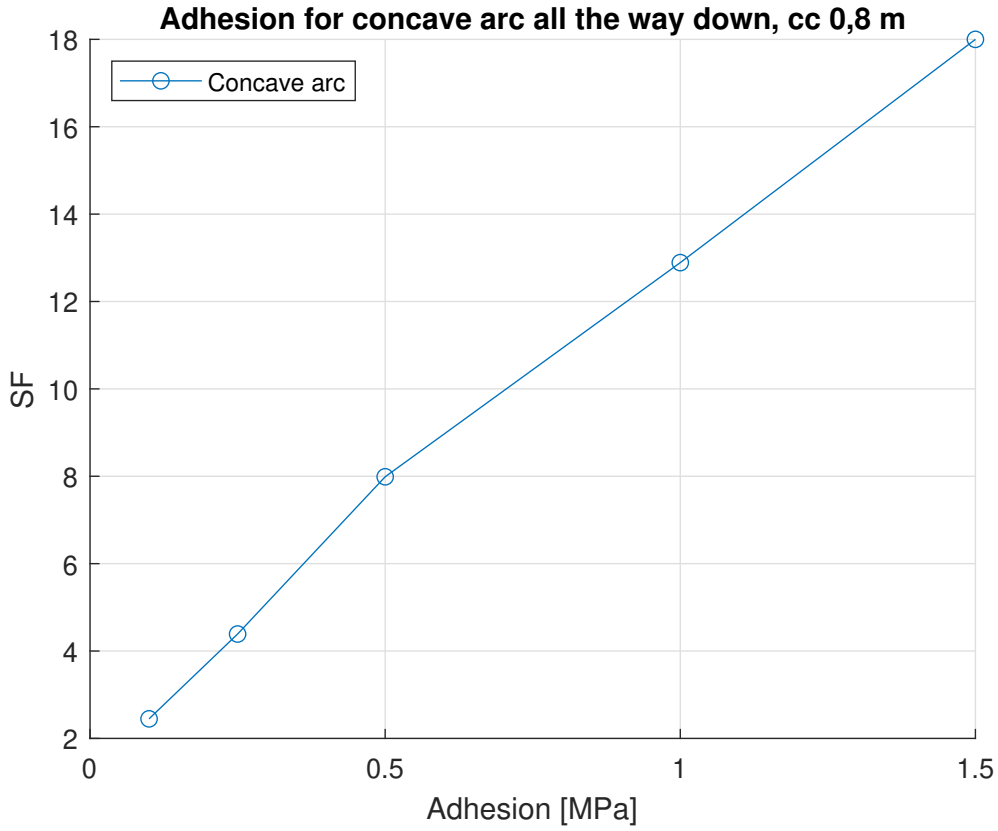

Figure 6.2.4: cc 0,8 m. The graph shows the obtained SF when varying the adhesion for a concave concrete arc going all the way down, as shown in Figure 6.2.5.

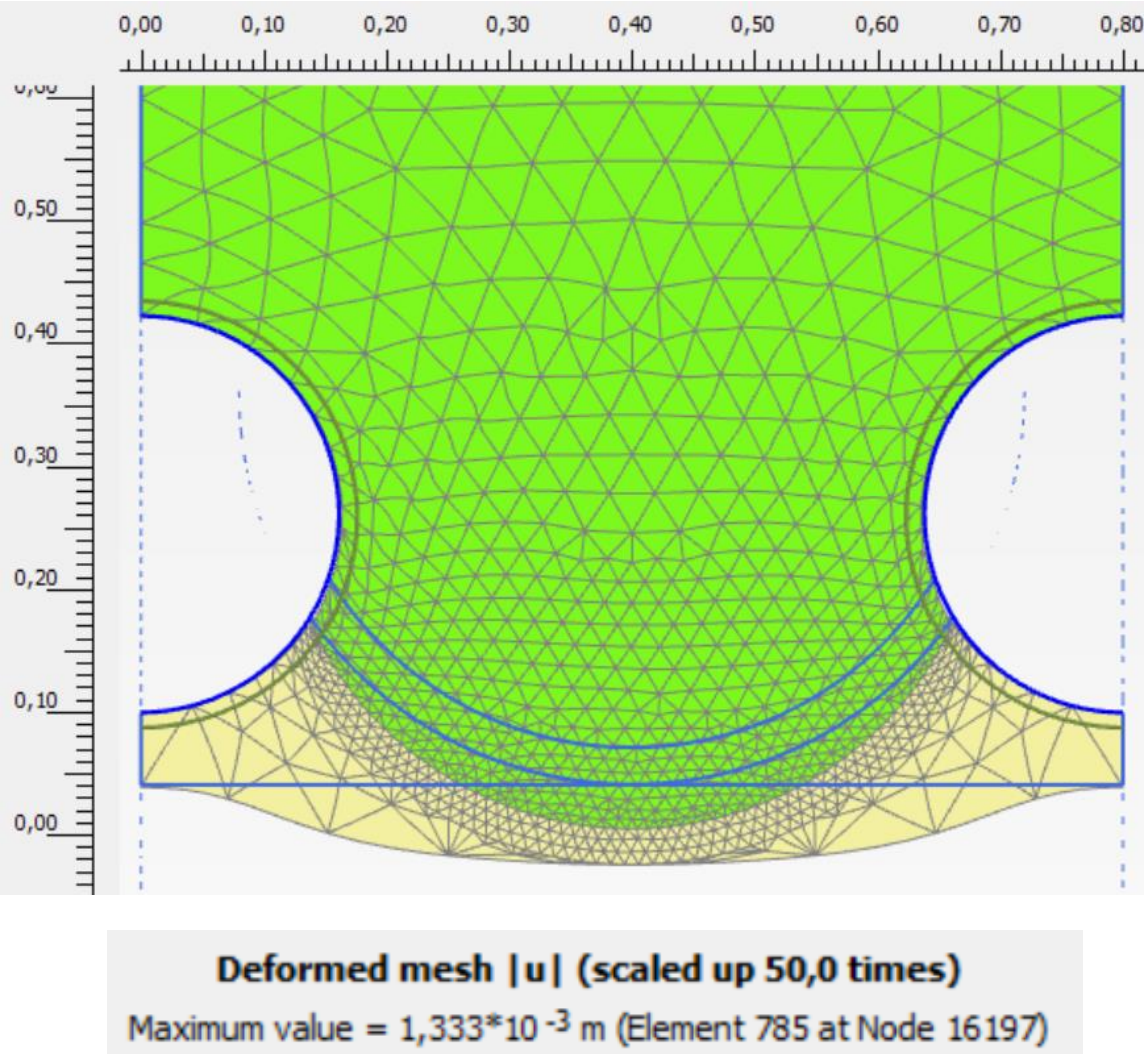

Figure 6.2.5: cc 0,8 m. Failure mechanism for concave arc with concrete all the way down.

Cc=0,8m Concave concrete arc all the way down

Adhesion 500 kPa, c=0 kPa. D=0,323 m

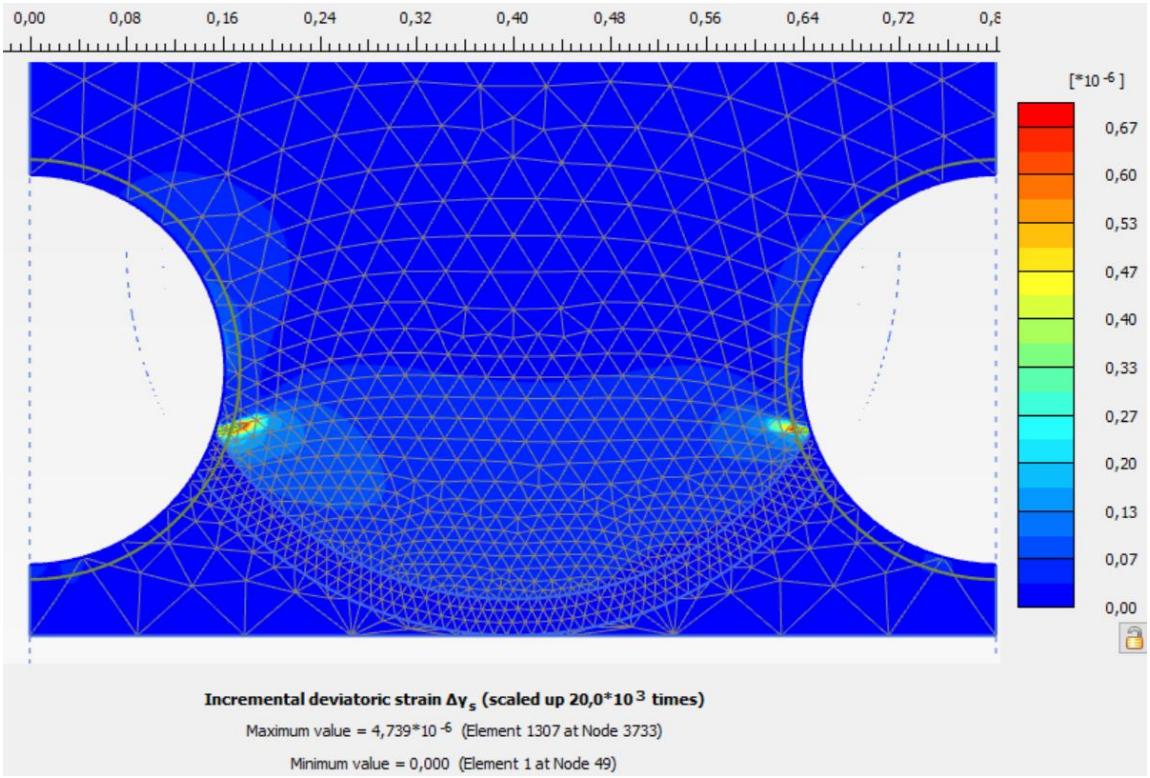

Figure 6.2.6: cc 0,8 m. Failure mechanism for concave arc with concrete all the way down, see Figure 6.2.5 for geometry and Figure 6.2.4 for simulation results.

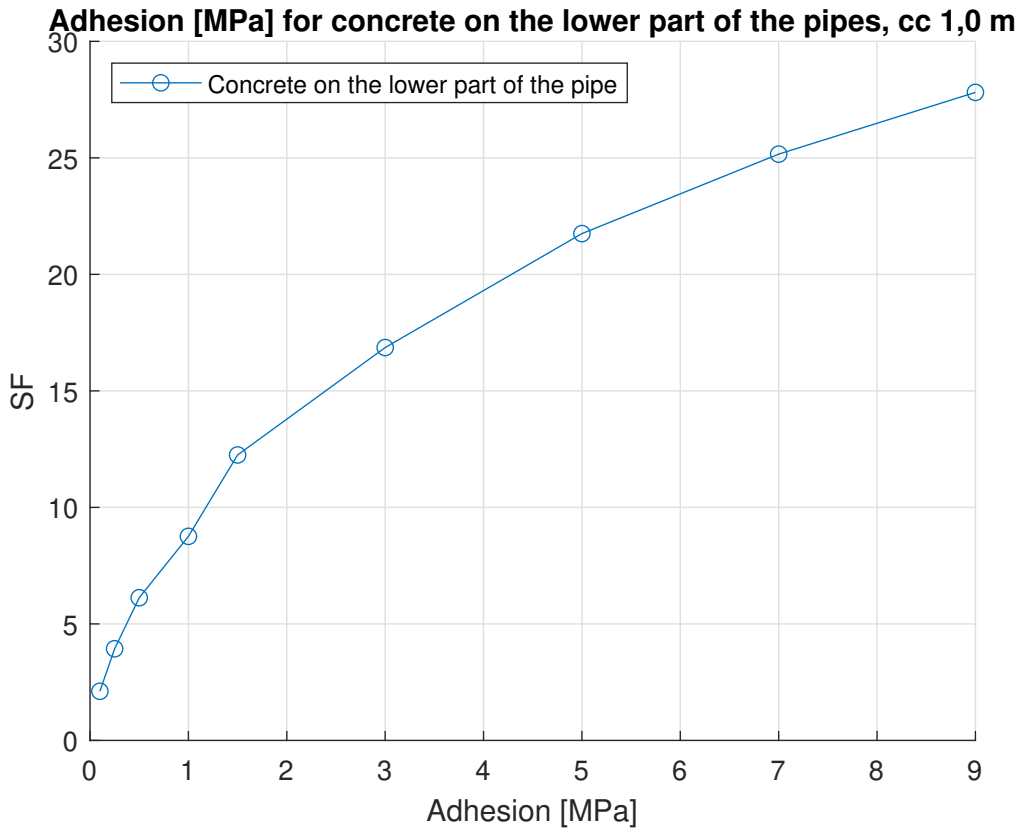

Figure 6.2.7: cc 1,0 m. Straight line and concrete on the lower part of the pipe.

6.2.2 Imperfect concrete arc

The imperfect arc's geometry is similar to the perfect arc. It is on the favorable side of the pipes and behaves like a bridge where the two pipes are the abutments. The arc starts off like a convex arc but changes to a concave geometry at the top of the arc, see Figure B.2.1 and Figure B.2.3. An arc with perfect circular geometry on the favorable side, supported by the pipes as abutments, may be able to carry a lot of load as seen from the results showing the stress distribution in the arc and the magnitude of the stress, see Figure B.2.2. The results from the imperfect arc show that the stability is significantly reduced when the geometry is imperfect, even though it is located in the same favorable area with a similar shape as the perfect arc.

The incremental deviatoric strain plot in the appendix shows the failure mechanism for the imperfect concrete arc, see Figure B.2.4. The shear bands have the shape of a fan and has similarities to the mechanism without shotcrete. The plastic point plot, see Figure B.2.2, shows a large concentration of plastic points and tension cut-off points in the center of the arc.

6.2.3 Perfect concrete arc

When the concrete arc is modeled as a circle and placed in a position where a pressure arc is formed, the arc has proven to withstand significant loads. The high safety factors occur when there are perfect arcs subjected to pressure. In reality, the probable cause of failure is imperfections in the concrete arc, it is impossible to construct perfect shotcrete arcs in practice. The arc was made imperfect with an imperfection on the top of the arc, see Figure B.2.3. This was further explained in Section 6.2.

6.3 Soil squeezing under excavation floor

Figure 6.3.1 shows the obtained failure mechanism from Plaxis utilizing the model explained in Section 5.5. The resistance against squeezing increases when the pipes are so close that there is no room for the failure mechanism for a single pile. The red circle number 1 shows half of the triangular section which remains rigidly attached to the pile. Within this zone, the full adhesion is not mobilized at the pile surface. This deformation mechanism is similar to the deformation mechanism presented in Figure 3.2.2 for a perfectly rough pile. The geometry seen in circle 1 comes from the fact that it is not a smooth pile. Because of this area, the deforming region increases significantly which leads to higher resistance for rough piles.

Circle 2 shows that the adjacent pile interferes with the failure mechanism to the pile and thus the resistance increases.

Circle 1 and 2 show the same mechanism that happens between the pipes above the excavation floor. In incremental strain plots of situations above excavation level, the triangular rigid zone in front of the pipe is present and the shear bands always collide with the adjacent pipe.

6.3.1 Arching

The soil behind the soil gap is mobilized by the horizontal stress, and plastic deformation will occur. From the plots without concrete shown in Chapter A, the failure mechanism can be noted, as well as plastic plots showing plastic deformation in the area of the failure mechanism. There is an evident arching in the mobilized soil, and from the principal stress plots in the same Chapter A, a rotation of the principal stresses shows how the stresses are transferred in the soil from one pipe to the other. The plots show that the stresses are distributed to piles through the soil.

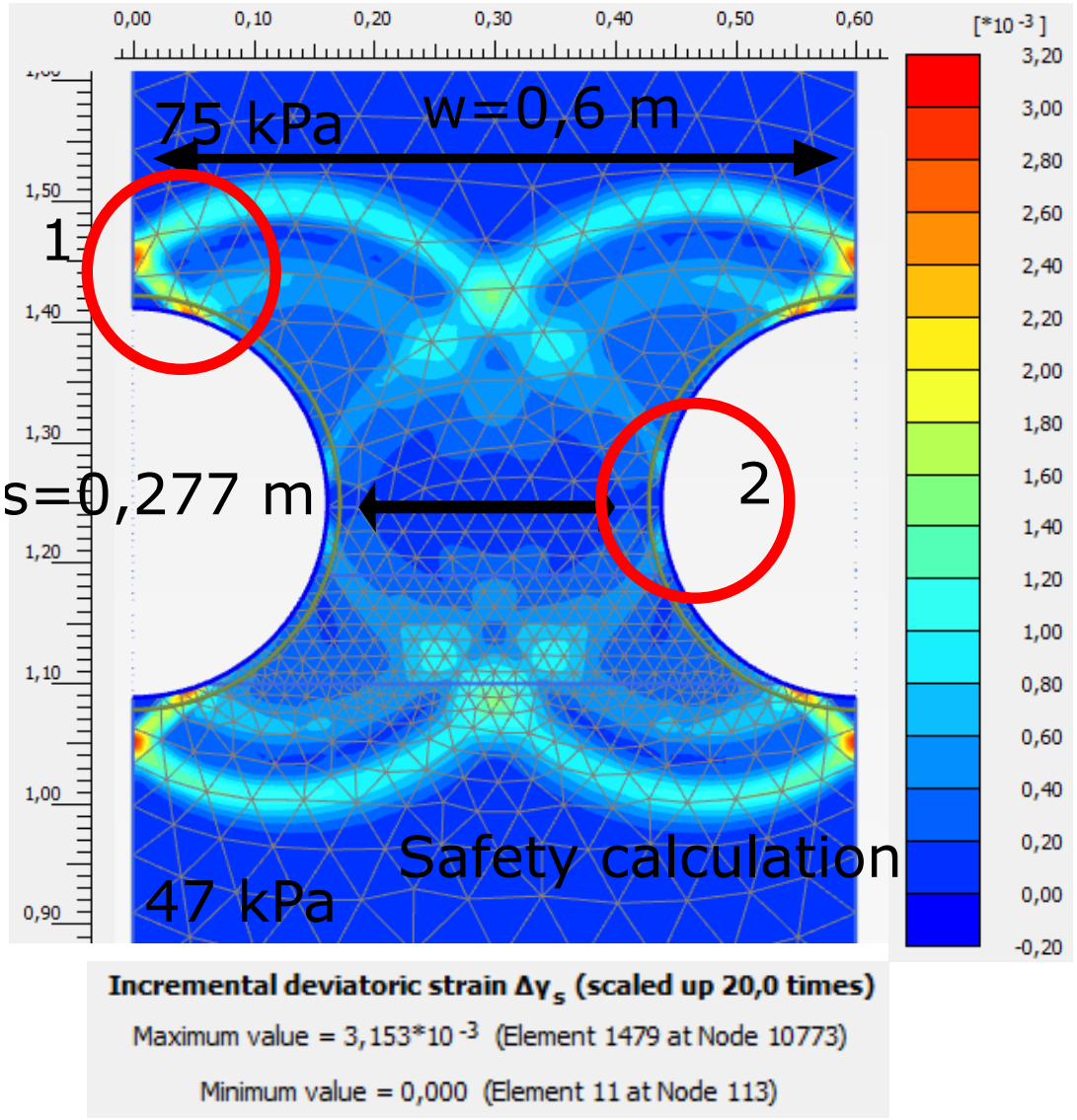

Figure 6.3.1: A close-up illustration of the failure mechanism obtain in the Plaxis squeeze model for an active pressure of 47 kPa and a passive pressure of 75 kPa.

Chapter 7

Discussion

In this chapter, the results are discussed and linked to existing theory, and observation and experiences on the construction site.

7.1 Cases without concrete

7.1.1 Concave geometry and tension cut-off points

For the concave excavation geometry, higher safety factors are obtained than for the cases where the soil was excavated further in between the pipes. In practice, it may seem like this could possibly be a more unfavorable excavation geometry, since the soil that is on the unfavorable side is not squeezed behind the pipes. The soil behind and in between the pipes is retained by the pipes. The gravity, which will affect the soil, is not included in the model. The gravity will drag the soil down and make it fall out which especially will affect the soil that is not behind the pipes, as explained in Section 5.1.5. As can be seen from the plastic point plots, see Figure A.2.8 and Figure 6.1.3, almost the whole part of the soil located a little below the center point of the pipes, has tension cut-off points. The stresses at these points are zero, so the stability over time when the cohesion is reduced is most likely not certain.

The principal stress plots without concrete in Chapter A, show a rotation of principal stresses. Large stresses can be observed on the pipes, as well as in the arc where the arching takes place. There are smaller stresses further down in the soil gap and along the pipe surface. Arching between the pipes is evident and comes from the friction between the piles, as explained in Section 2.4.2. The soil furthest down with almost 0 stresses is barely supported by the piles. Soil arching is developed even for very small values of cohesion as seen in Section A.1, which also was found in [15].

7.2 Cases with concrete

Results from simulations of the shotcrete protection show high safety factors when the concrete is behind the center of the pipe. The concrete takes up the load by compression and is pushed against

pipes, it is hanging onto the pipes and gets wedged between. As informed in Section 4.1, this might be the case for coarse masses where a shovel excavates alongside the pipes and if it encounters big rocks they are taken out and leave a space behind which can be filled. If there is clay material, a shovel is used to excavate alongside the wall, and it is possible to excavate past the midpoint. For sand and gravel, where the center distance is not that large, the piles will emerge naturally with a gap between as seen in various pictures of pipe walls. This might not be too far past the mid point but there is a possibility to use pressurized air to make some more room between the pipes. It is therefore very favorable to come past the midpoint and should be aimed for.

A safety risk with the shotcrete protection is associated with poor integration between the shotcrete and the wall. For such a situation, the shotcrete will behave like a concrete shell attached to the wall and would become two separate structures, where there is a risk of them loosing connection. This is not an unlikely behaviour when taking into account that poorly cleaned pipes lead to bad adhesion and that the shotcrete layer is very heavy considering it can be more than 8-10 cm thick. This heavy concrete shell can inflict serious damage on workers and others if just a part of it falls off. For larger walls, bracing is almost always applied, which is needed to make the wall meet serviceability requirements, but it may be just as important for securing the shotcrete. The whole bracing system, consisting of walling and anchors, becomes covered in shotcrete and for the "concrete shell" to come loose from the wall, the bracing system will have to loosen as well which is unlikely to happen. Anchoring in several levels will give a very good integration.

For smaller walls where bracing is not used, adhesion is very important since the integration of the pipe wall and shotcrete essentially depends on it. This is not recommended for excavation deeper than 3 meters, which from practice seems like the limit. For larger walls, bracing is recommended since this will give a superior integration with the rest of the wall when the anchors and walling are covered in shotcrete. Some useful guidelines for walls without bracing are presented below.

Since the adhesion becomes so important and has shown to have a significant influence of the stability of concrete, they need to be clean before applying concrete. They should therefore be sprayed with a degreaser, washed and rinsed clean before installation. When the wall is excavated, the pipes need to be inspected again, since water in the soil gaps is disadvantageous. Pressurized air may be used to remove soil rests and dust. If there is soil with elements of clay or something that makes the soil stick to pipes, a broom or something similar can be used to scrub away difficult parts. The pressurized air may also be used to remove some soil if it seems necessary, since a larger surface area is favorable when depending on adhesion. A reinforcement mesh is probably even more favorable when there is no bracing, since the stability without bracing depends essentially on adhesion and the mesh will help distribute the loads from an area without adhesion. The loads will be transferred to other parts of the wall and the reinforcement mesh helps with this transfer. The mesh has a good load distributing effect that will also be advantageous for a braced wall.

Chapter 8

Conclusion

A profound literature study of the arching effect between piles, both for slope stabilizing piles and for piles used in contiguous pile walls where the soil has been excavated on one side, has been done. The situation for the slope stabilizing piles is being addressed as a squeezing problem in the thesis. This is because the situation under the excavation level is similar to the situation for slope stabilizing piles. The lateral resistance to purely horizontal movement for single piles has been reviewed, and this capacity is a lower limit for resistance against squeezing of soil through the pipe wall. The lower limit is still a considerable capacity and therefore the stability of the freely exposed soil gaps supported by the self-supporting mechanism produced by the arching effect, is the deciding factor when designing the center distance of the pipes. In order for the assumption of the squeezing capacity to be valid, the pipes can not have a very small depth under the excavation floor. Bracing also helps reduce the passive pressure that the pipes introduce to the soil, which helps to minimize the risk for squeezing. In Section 4.3.2, the squeezing problem is presented, along with equations to predict maximum center distance between the pipes when the pressure difference between active and passive pressure is known, as well as a formula to calculate either the minimum allowed active pressure or the maximum allowed passive pressure.

The stability for the freely exposed soil gaps can be calculated in Plaxis. For the calculation, a realistic and not too conservative cohesion has to be chosen to initiate the arching effect and obtain a realistic capacity. The guidelines given and discussed in Chapter 3 and Section 4.1 have to be accounted for when making the model, and included in the evaluation of the global stability. The contractor excavates approximately to the center point of the pipes and does sometimes excavate further behind the pipes often in coarser masses. For coarser masses, the center distance is larger than for more fine-grained material like gravel and sand. For coarser masses, the soil in front and between the pipes is thoroughly excavated, and for more fine-grained soils with a smaller center distance, the soil in front of the pipes and partly between will fall out by itself. For both coarse and fine-grained soils, it is conservative to assume that the concrete does not pass the center point of the pipes, which means that the shotcrete stability essentially depends on the adhesion between the steel and concrete. The results from the adhesion simulations show that it has a significant effect.

For smaller walls up to almost 3 meters, it is unusual to use a bracing system when it is not needed to fulfill other structural requirements such as deformations. As discussed, the bracing will have a very favorable effect because it physically interlocks the shotcrete to the wall, and thus making sure the concrete does not come loose and fall off. For larger walls and especially permanent

walls like the one at Avløs, see Figure 3.5.1, bracing is strongly recommended and usually always included since it is necessary to obtain serviceability. A highly undesirable situation is having the shotcrete behaving like a concrete shell poorly glued to wall, because this has risk of coming loose and fall down. This is really dangerous since it is very heavy and could fall on people. The goal is to properly integrate the shotcrete with the rest of the structure. For larger walls it is therefore recommended that the shotcrete is built in as a part of the bracing system.

For smaller walls, it may not be necessary to use bracing, but there should be requirements regarding degreasing and thoroughly washing the piles before they are installed. When the wall is excavated, before applying shotcrete, the pipes should be blown clean with pressurized air. The pressurized air could also be used to further remove soil between the pipes, aiming to come past the middle point of the pipes. It is important that the pipes emerge from the soil, and one should aim to excavate a little past the middle of the pipes, because the steel surface area is important for the adhesion and the concrete could get wedged between the pipes. Following these guidelines, one can make sure to obtain satisfactory pipe surface and arrange for the best achievable adhesion. Adhesion is the clue for the wall without bracing, and therefore reinforcement mesh may have a very beneficial effect since this has a good load distribution property. If there is an area with reduced adhesion, the shotcrete with the reinforcement mesh will make sure that this load is distributed to the surrounding areas.

8.1 Soil parameters

The center distance was found to have a large influence of the stability as confirmed by Liang et al. [15], Chen and Martin [8], Lei et al. [12] and Keawsawasvong et al. [1]. Adhesion factors for the soil-structure interface were also found to have significant effects [1]. Based on discussions and experience, an R_{int} of 0,65 was chosen for the model to perform the parametric study, the center distance of 0,6 m and 1 m was also chosen as a foundation for the parametric study. These values are experience based values for Norwegian practice.

8.2 Arching effect

The arching effect behind the soil gaps was clearly manifested by the predicted failure mechanism of a pile wall with a narrow gap. In the principal stress plot, the arching effect was clearly illustrated, the direction of the major principal stress formed an arch trajectory between the pipes. All factors being the same, arching is more prominent for larger values of c and ψ.

8.3 Future work

For future work, it would be interesting to study the friction in the pile-soil interaction for the freely exposed soil gaps for drained conditions, before the concrete is applied. In [1], it was found to have a significant effect for clay in undrained conditions.

In [15], drilled shafts for slope stabilization have been studied and the friction angle was found to have a significant effect on soil arching for low values of cohesion and cohesionless soil. As seen in the study and in the results found in this thesis, only a small cohesion value is needed to fully

develop soil arching. For soils with a very low value of cohesion, a higher friction angle will make the soil more likely to develop stronger arching effect and produce greater granular interlocking than soils with a smaller friction angle. This is interesting to study further using the model presented in this thesis.

It would be very interesting to do tests in the laboratory, possibly a centrifuge test like performed in [12], but with more typical soils and situations found in Norway instead of only dry sand which is not very representative for real life conditions.

From the simulation results, a reduction in stability was found when more soil was excavated between the pipes. This is plausible because stabilizing soil is removed, which reduces stabilizing friction against the pipes. As pointed out in [12], if the confinement of the soil between the pipes is lost, it accelerates the failure in the soil gap. Studying this in laboratory tests would be interesting because it may give a better picture of the behavior leading to this effect.

For the simulations done in this thesis, it was assumed that the 2D model was satisfactory for studying the problems with soil gap stability. It would be useful and reassuring to perform 3D simulations of the problem, because a more realistic model could be made with fewer assumptions. Then, other possibly occurring effects could be discovered.

Laboratory tests of steel shotcrete adhesion would be very useful, because it has been difficult to find a realistic value as it varies a lot with the roughness and cleanliness of the surface. Based on academic discussions, a conservative value of 500 kPa was chosen for the simulations in the thesis. Through the parametric study, the adhesion was found to be essential for the stability. A laboratory test could be done with pipes varying the roughness and cleanliness.

Bibliography

[1] S. Keawsawasvong and B. Ukritchon, "Undrained limiting pressure behind soil gaps in contiguous pile walls," *Computers and Geotechnics*, vol. 83, pp. 152–158, 2017. [Online]. Available: http://dx.doi.org/10.1016/j.compgeo.2016.11.007

[2] S. Nordal, G. R. Eiksund, and G. Grimstad, "TBA 5100 Theoretical Soil Mechanics," 2016.

[3] G. Barnes, *Soil mechanics: principles and practice*. Basingstoke: Palgrave Macmillan, 2010.

[4] Geotechnical Division at the department of civil and environmental engineering, "Geoteknikk beregningsmetoder," 2016.

[5] S. Nordal, "Geotechnical engineering advanced course," 2019.

[6] O. Hopperstad and Tore Børvik, "Materials Mechanics 1," -, 2017.

[7] Plaxis, "Material Models Manual," *Plaxis*, p. 202, 2018.

[8] C. Y. Chen and G. R. Martin, "Soil - Structure interaction for landslide stabilizing piles," *Computers and Geotechnics*, vol. 29, no. 5, pp. 363–386, 2002.

[9] P. J. Bosscher and D. H. Gray, "SOIL ARCHING IN SANDY SLOPES," vol. 112, no. 6, pp. 626–645, 1986.

[10] "Stability of a shallow circular tunnel in cohesionless soil: Atkinson, J H; Potts, D M Geotechnique, V27, N2, 1977, P203–215," *International Journal of Rock Mechanics and Mining Sciences & Geomechanics Abstracts*, vol. 14, no. 5, p. A85, 1977. [Online]. Available: https://www.sciencedirect.com/science/article/pii/0148906277908233

[11] "Guide to soil mechanics: Bolton, M London: MacMillan, 1979, 439P," *International Journal of Rock Mechanics and Mining Sciences & Geomechanics Abstracts*, vol. 18, no. 3, p. 43, 1981. [Online]. Available: https://www.sciencedirect.com/science/article/pii/0148906281909852

[12] G. Lei, S. Usai, and W. Wu, "Centrifuge study of soil arching in slope reinforced by piles," *Springer Series in Geomechanics and Geoengineering*, pp. 105–115, 2019.

[13] C. Li, H. Tang, X. Hu, and L. Wang, "Numerical modelling study of the load sharing law of anti-sliding piles based on the soil arching effect for Erliban landslide, China," *KSCE Journal of Civil Engineering*, vol. 17, no. 6, pp. 1251–1262, 2013.

[14] T. Adachi, M. Kimura, and S. Tada, "Analysis on the preventive mechanism of landslide stabilizing piles," in *International symposium on numerical models in geomechanics. 3 (NUMOG III)*, 1989, pp. 691–698.

[15] R. Liang and S. Zeng, "Numerical Study of Soil Arching Mechanism in Drilled Shafts for Slope Stabilization," *Soils and Foundations*, vol. 42, no. 2, pp. 83–92, 2002. [Online]. Available: https://www.sciencedirect.com/science/article/pii/S0038080620308349

[16] Q. Yan, J. Zhao, C. Zhang, and J. Wang, "Ultimate Bearing Capacity of Strip Foundations in Unsaturated Soils considering the Intermediate Principal Stress Effect," *Advances in Civil Engineering*, vol. 2020, 2020.

[17] Plaxis 2D, "PLAXIS 2D Reference Manual 2018," pp. 1–168, 2018. [Online]. Available: https://www.plaxis.com/support/manuals/plaxis-2d-manuals/

[18] PLAXIS, "PLAXIS 2D Scientic Manual 2018," 2018.

[19] M. v. d. Sloot, "Modelling soil-structure interaction: interfaces," 2019. [Online]. Available: https://communities.bentley.com/products/geotech-analysis/w/plaxis-soilvision-wiki/45944/modelling-soil-structure-interaction-interfaces

[20] K. Terzaghi, "Stress distribution in dry and in saturated sand above a yielding trap-door," 1936.

[21] L. Shao, X. Zhou, and H. Zeng, "Comparison of Soil Pressure Calculating Methods Based on Terzaghi Model in Different Standards," 2016.

[22] T. Ito and T. Matsui, "Methods to Estimate Lateral Force Acting on Stabilizing Piles," *Soils and Foundations*, vol. 15, no. 4, pp. 43–59, 1975. [Online]. Available: https://www.sciencedirect.com/science/article/pii/S0038080620335885

[23] C. H. Evans, "An examination of arching in granular soils," Ph.D. dissertation, MIT, 1984.

[24] T. Matsui, W. P. Hong, and T. Ito, "Earth pressures on piles in a row due to lateral soil movements," *Soils and Foundations*, vol. 22, no. 2, pp. 71–81, 1982.

[25] W. Haema, "Influence of Pile Spacing on Lateral Resistance of Contiguous Bored Pile Wall for Deep Excavation," Ph.D. dissertation, Master Thesis, Suranaree University of Technology, Nakhonratchasima, Thailand, 2010.

[26] M. F. Randolph and G. T. Houlsby, "Limiting Pressure on a Cricular Pile Loaded Laterally in Cohesive Soil." *Cambridge University, Engineering Department, (Technical Report) CUED/D-Soils*, no. 4, pp. 613–623, 1984.

[27] Statens vegvesen, "Håndbok V220 Geoteknikk i vegbygging," *SVV Håndbok*, no. Håndbok, pp. 1–624, 2018.

[28] K. f. Byggegropveiledningen, *Byggegropveiledningen 2019*. Norsk Geoteknisk Forening, 2019.

[29] RUUKKI, "RD pile wall," pp. 1–12, 2011.

[30] W. R. D. Bruin, "Forensic engineering of a bored pile wall," pp. 403–410, 2016.

[31] D. N. Pelekomité, *Peleveiledningen 2012*. Norges Geotekniske Forening, 2012.

[32] R. Sve, J. Elvøy, T. Sagen, L. Backer, K. G. Holter, P. Bollingmo, K. Boge, K. B. Pedersen, and A. Aarset, "Tung bergsikring i undergrunnsanlegg – Håndbok nr. 5," *NFF Håndbok*, no. 05, p. 75, 2008.

[33] *Håndbok R762, Prosesskode 2*. Statens vegvesen, 2015.

[34] "Rock anchors-state of the art part 2: Contruction : Littlejohn, GS Bruce, DA Ground Engng., V8, N6, Nov. 1975; P36–45," *International Journal of Rock Mechanics and Mining Sciences & Geomechanics Abstracts*, vol. 13, no. 10, p. 128, 10 1976.

[35] K. Tilrem Ørjavik, "Nordenga Bridge - Challenging foundation across the railway lines at Oslo Central Railway Station," 2012.

[36] Statens vegvesen, "Grunnforsterkning, fyllinger og skråninger – Håndbok V221," *SVV Håndbok - Veiledning*, p. 353, 2014.

Appendices

Appendix A

Plaxis plots without concrete

A.1 Principal stress plots for different values of cohesion

The soil is excavated approximately to the center of the pipes in a straight line.

- cc=0,6 m
- Excavation close to the center point of the pipes
- ϕ=35°

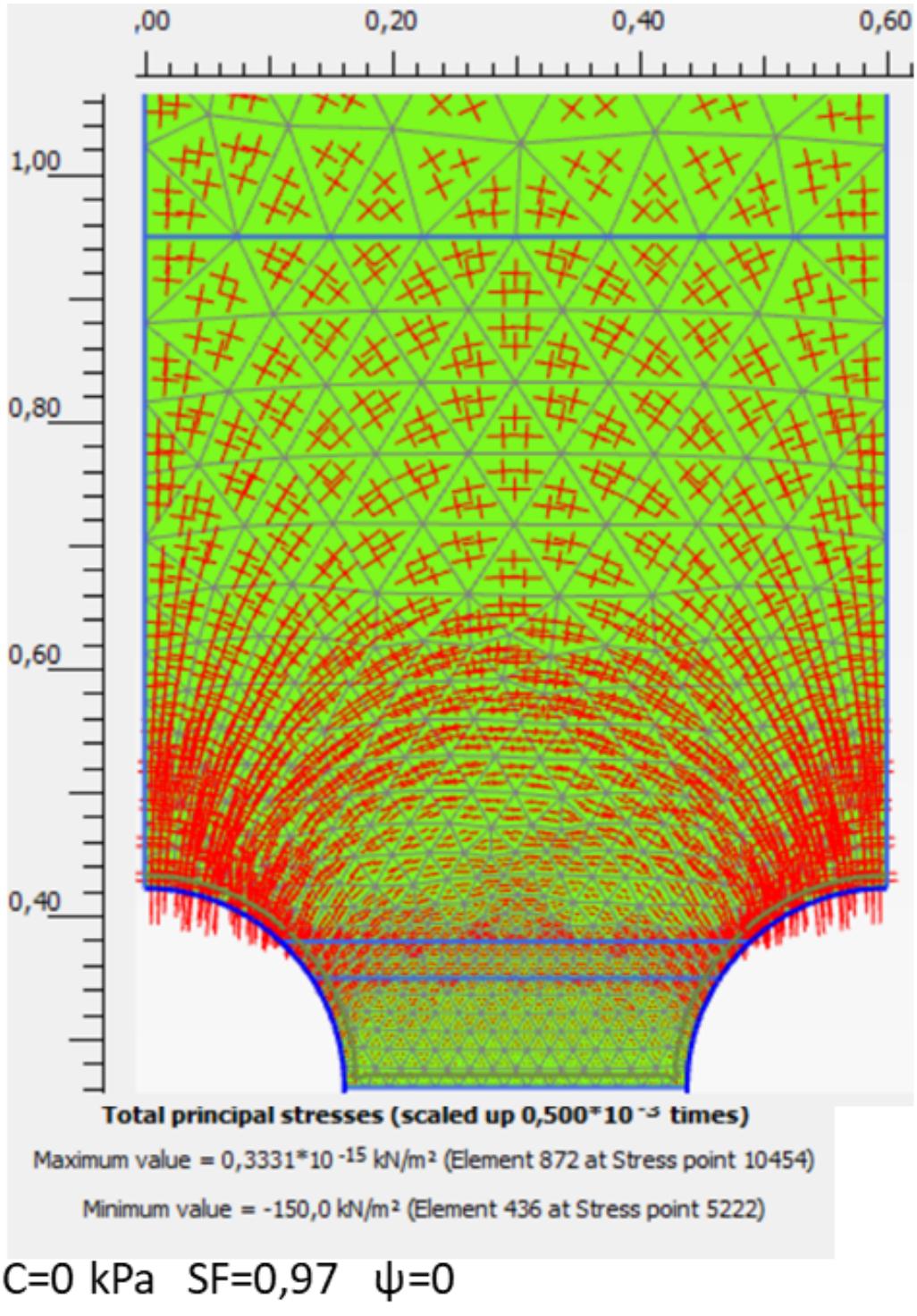

Figure A.1.1: Principal stress plot for center distance 0,6 m with c=0 kPa and $\psi = 0$

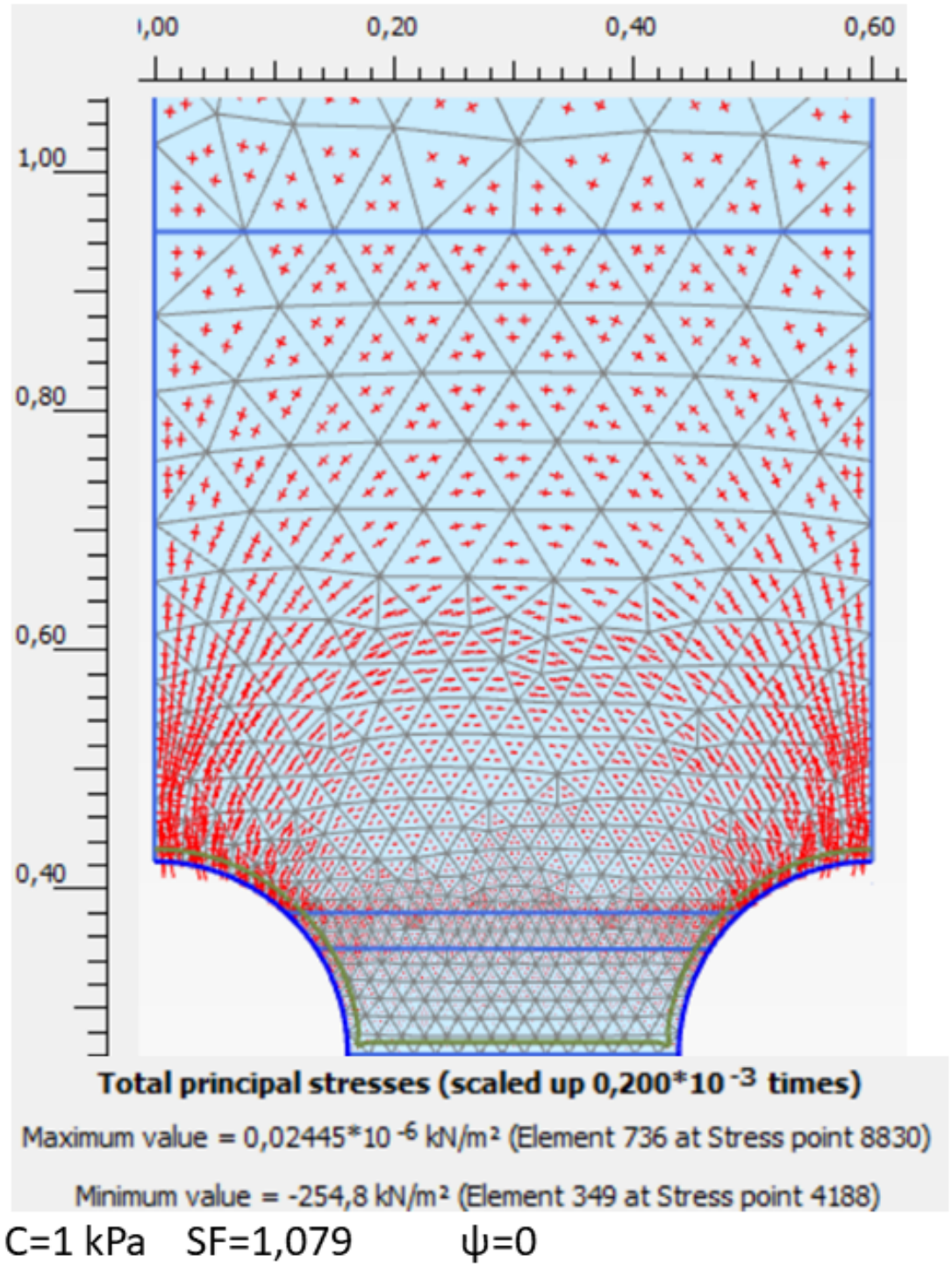

Figure A.1.2: Principal stress plot for center distance 0,6 m with c=1 kPa and $\psi = 0$

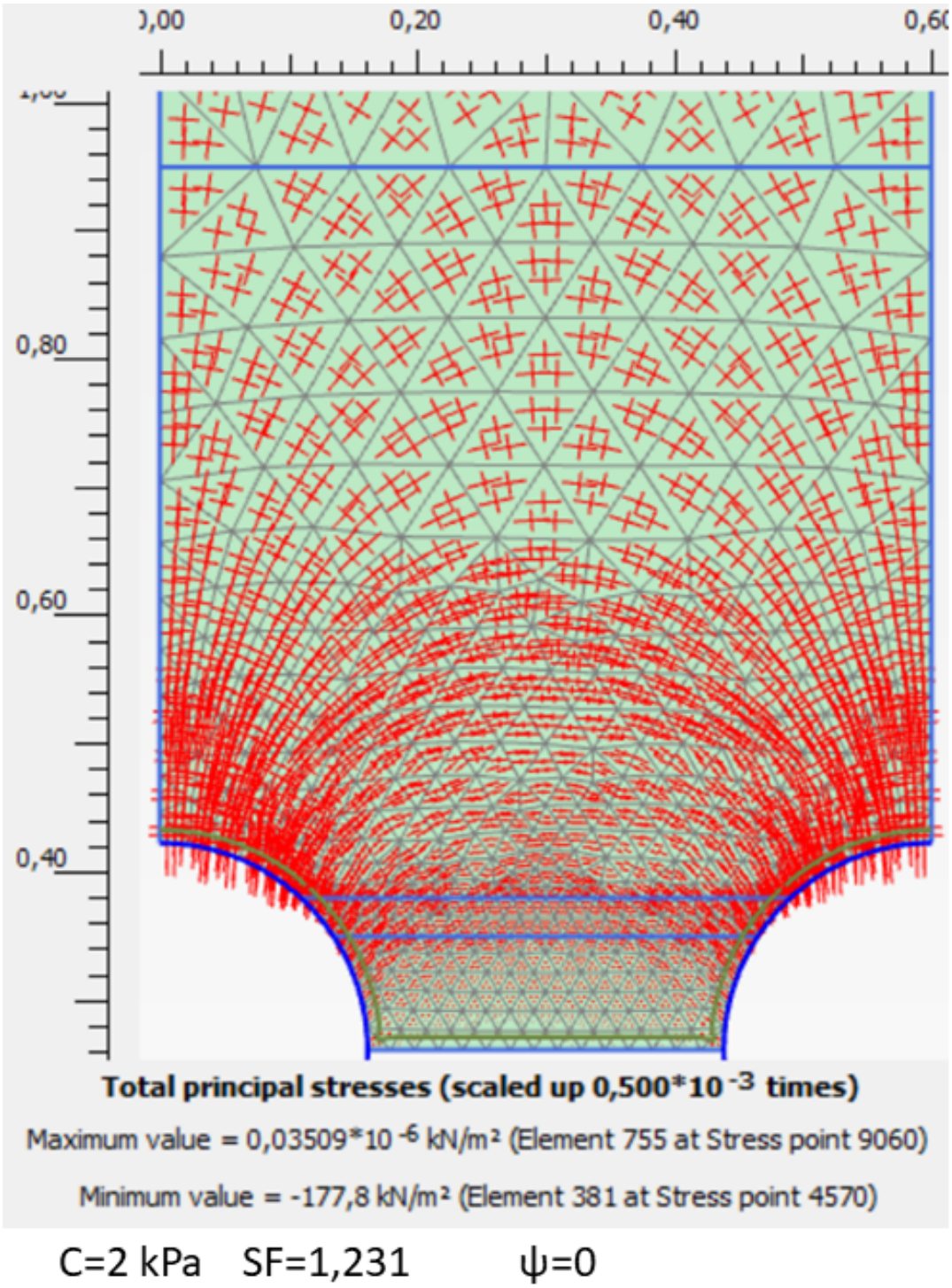

Figure A.1.3: Principal stress plot for center distance 0,6 m with c=2 kPa and $\psi = 0$

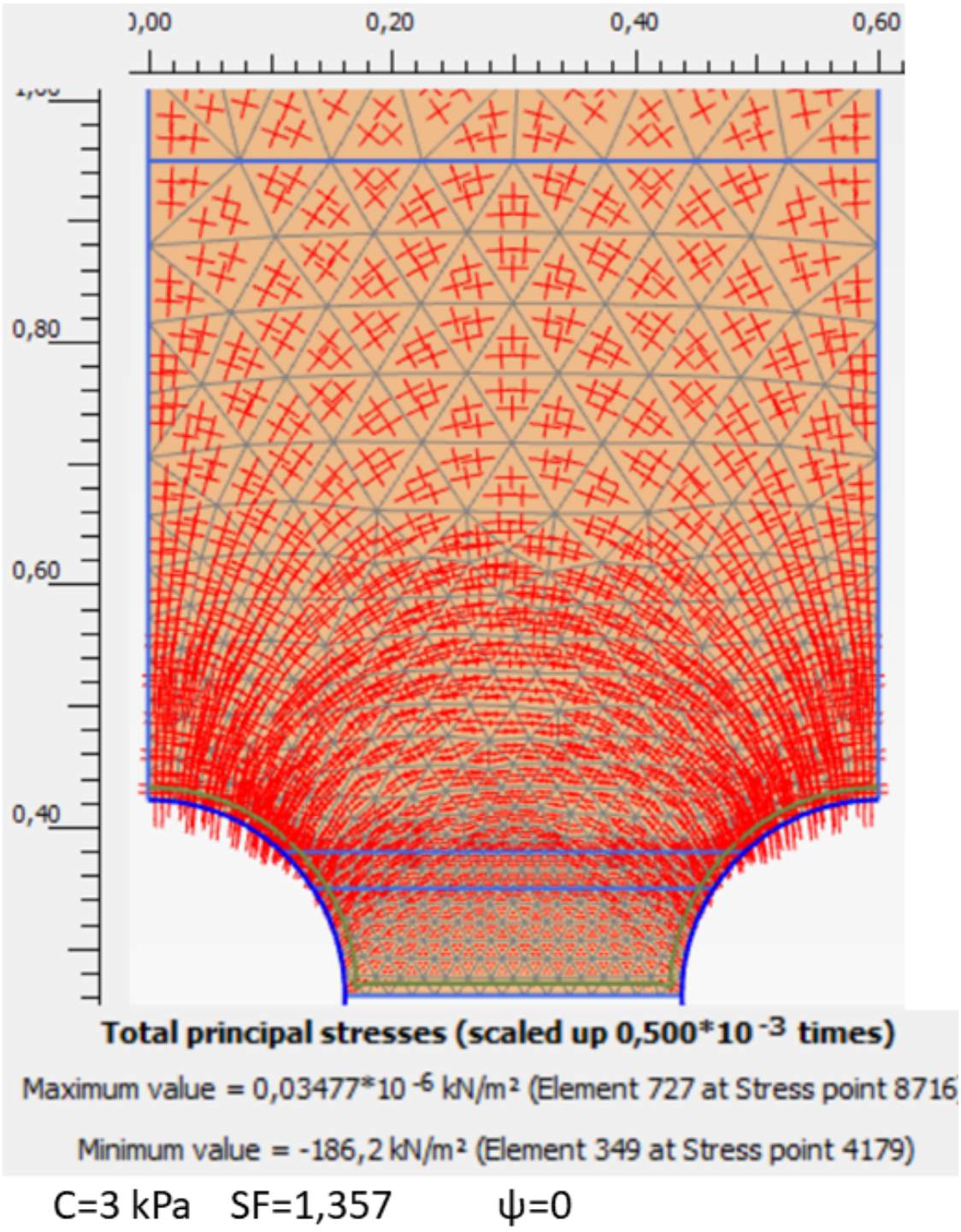

Figure A.1.4: Principal stress plot for center distance 0,6 m with c=3 kPa and $\psi = 0$

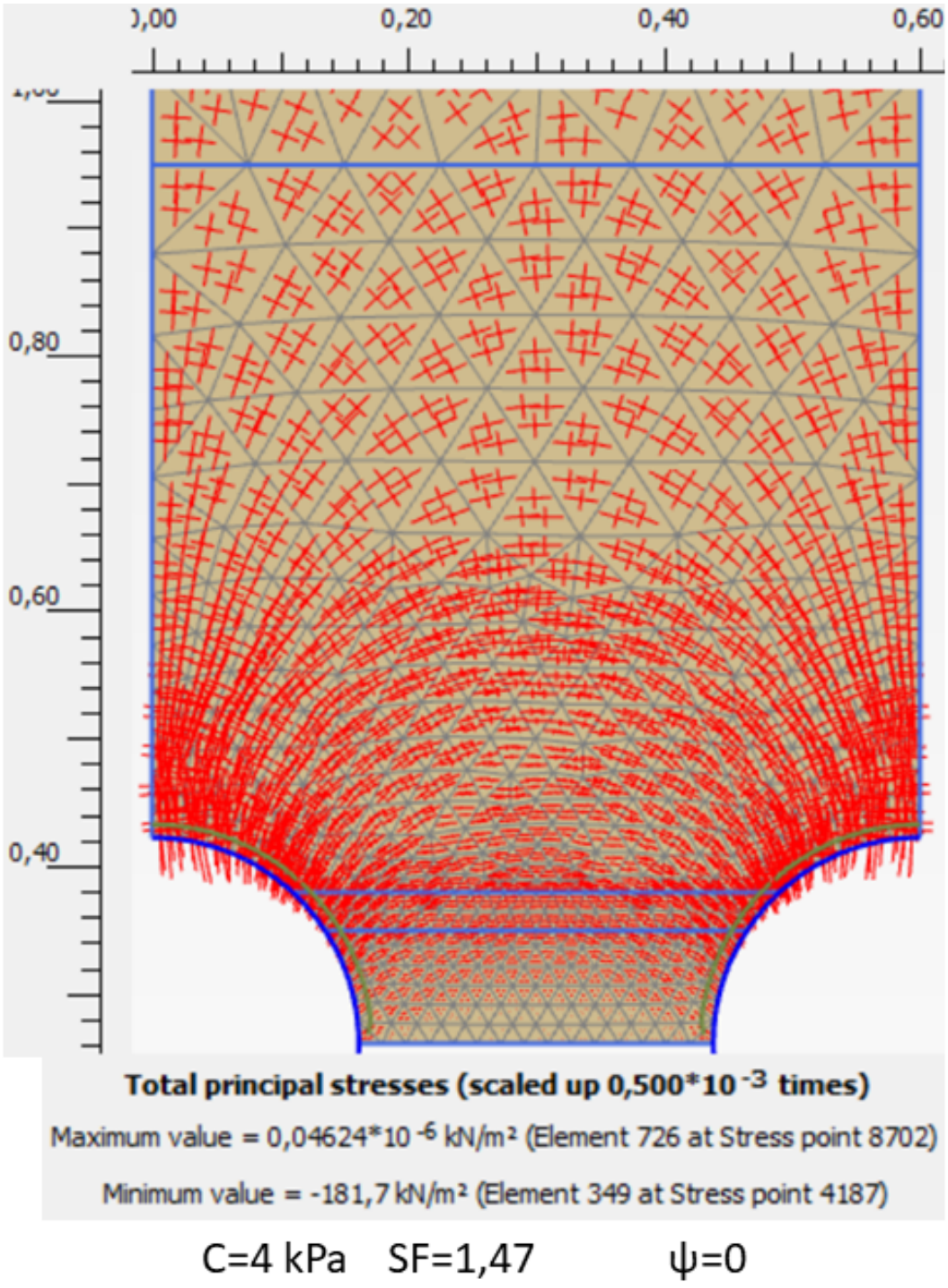

Figure A.1.5: Principal stress plot for center distance 0,6 m with c=4 kPa and $\psi = 0$

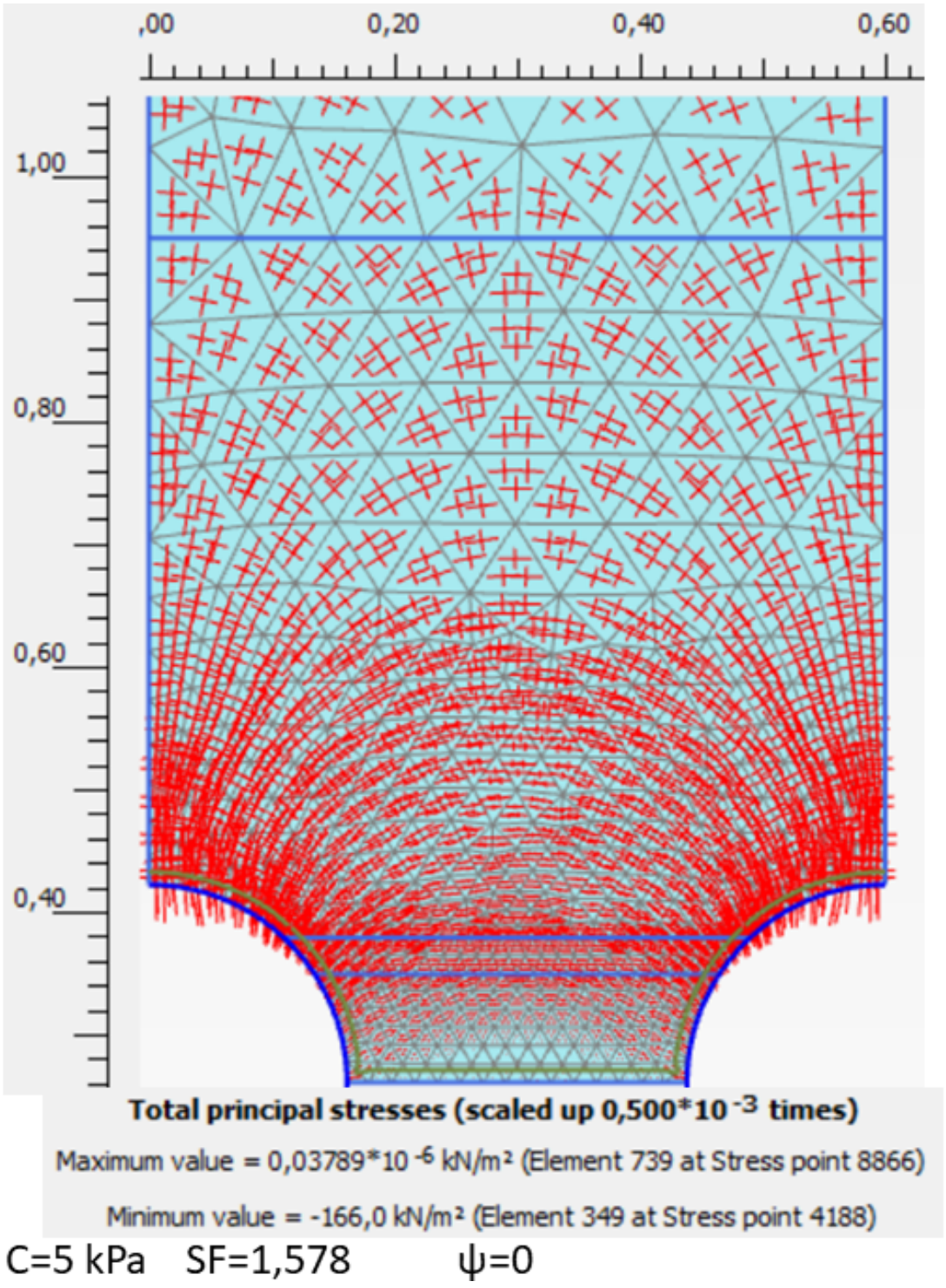

Figure A.1.6: Principal stress plot for center distance 0,6 m with c=5 kPa and $\psi = 0$

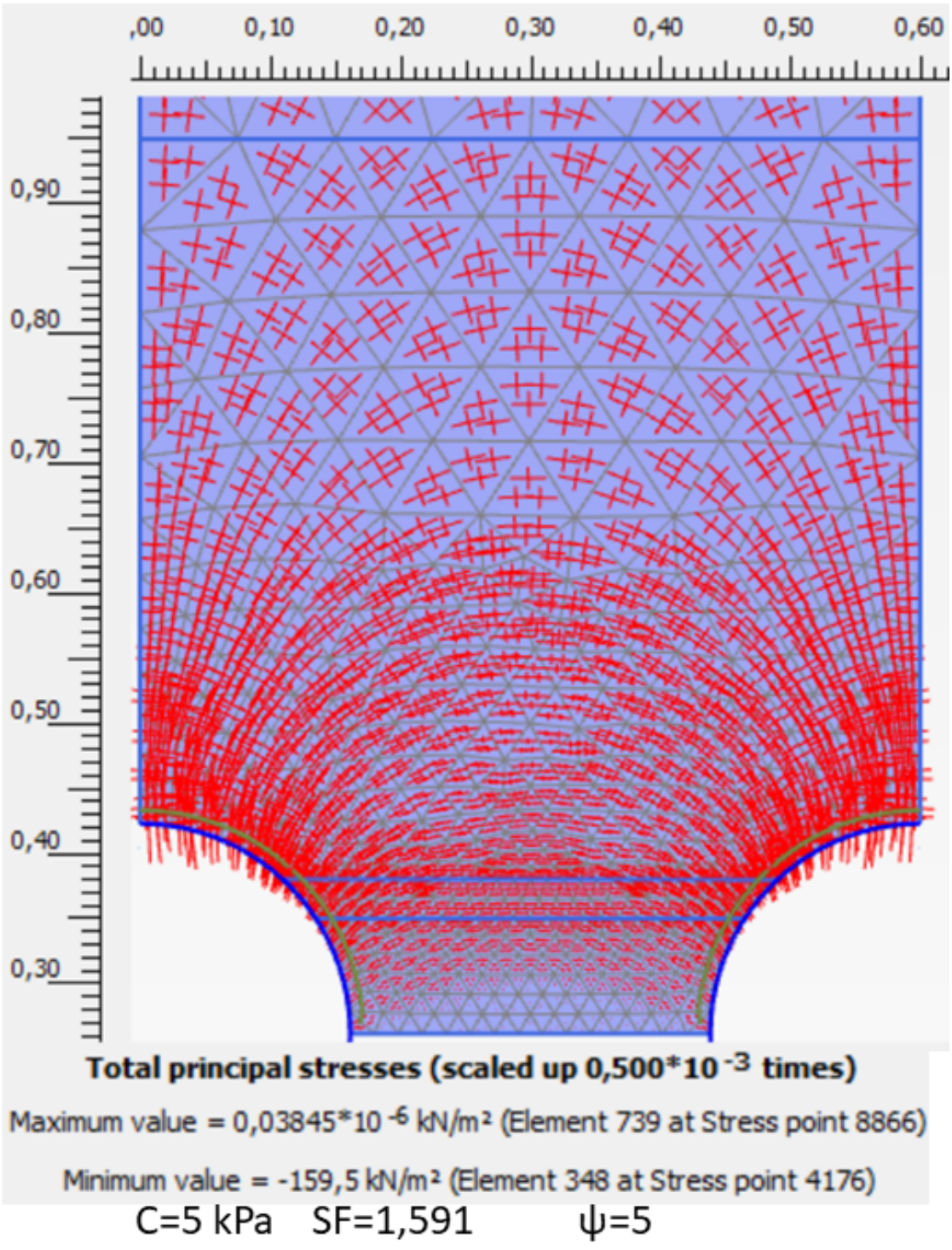

Figure A.1.7: Principal stress plot for center distance 0,6 m with c=5 kPa and $\psi = 5$

A.1.1 Incremental strain and plastic points for straight excavation line to the center of the pipes

Incremental strain and plastic point for the straight excavation geometry to the center of the. Center distance of 0,6 m and c=5 kPa and $\psi = 0°$

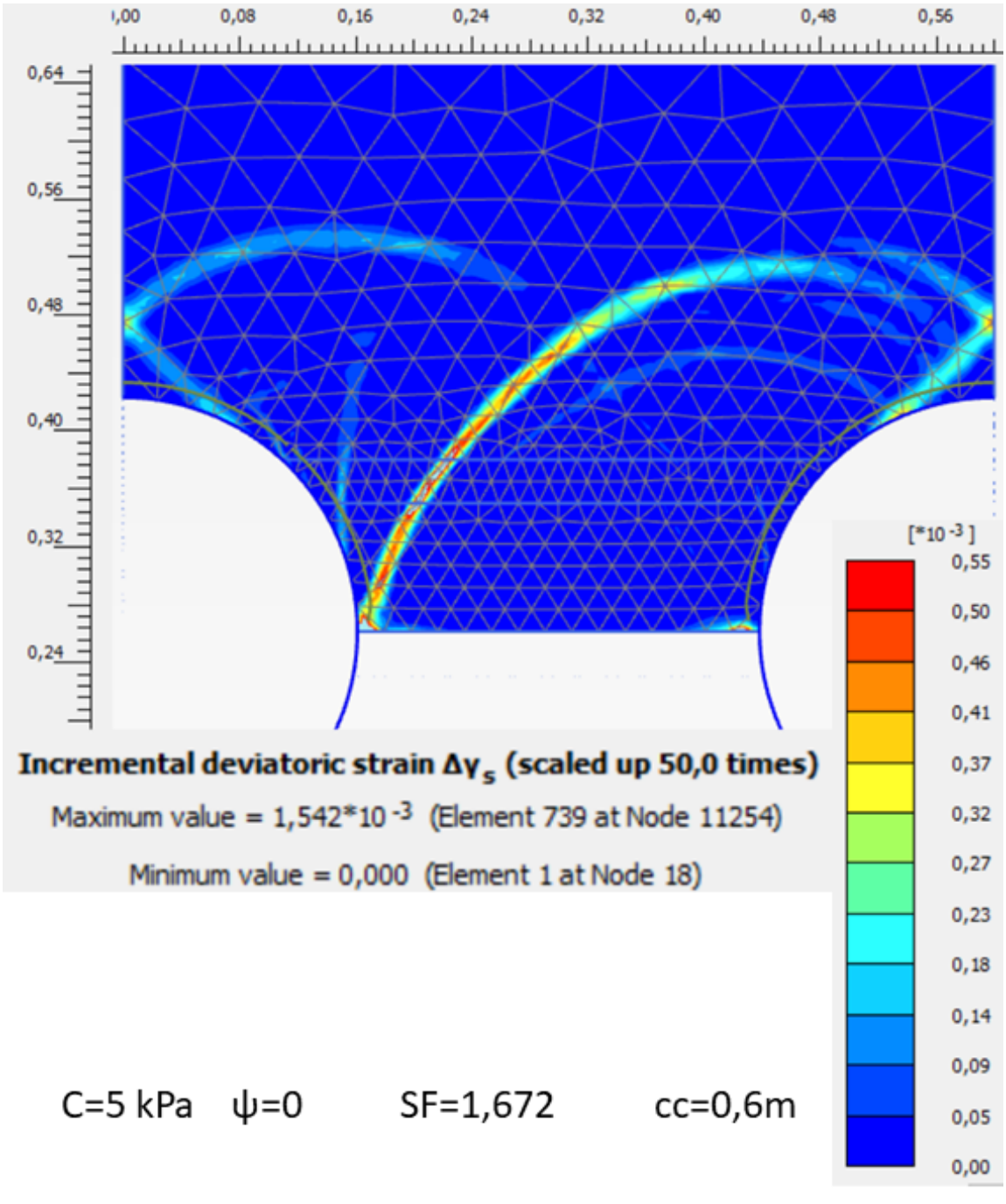

Figure A.1.8: Incremental strain for center distance 0,6 m with c=5 kPa and $\psi = 0$

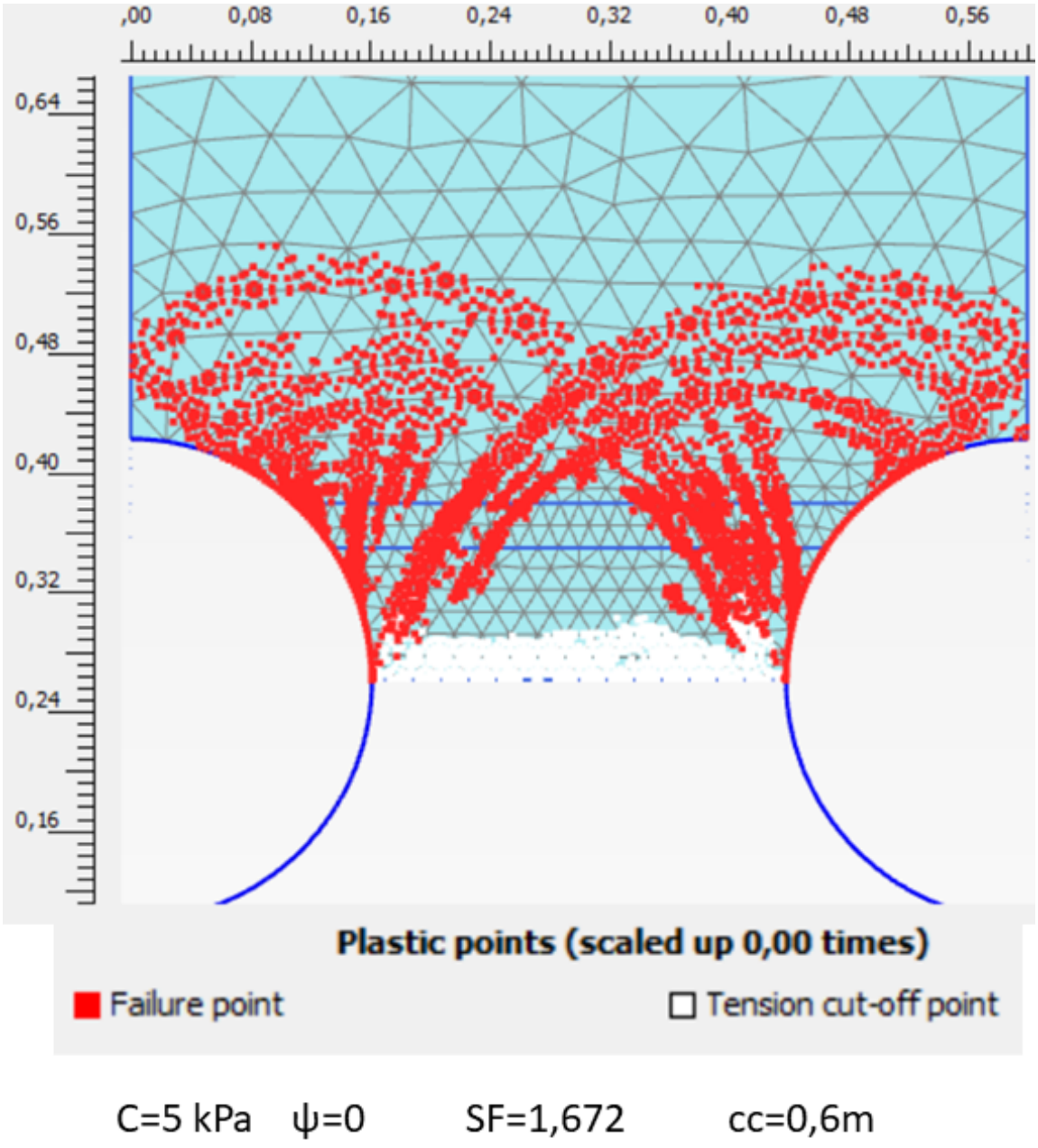

Figure A.1.9: Plastic points for center distance 0,6 m with c=5 kPa and $\psi = 0$

A.2 Simulations with different excavation geometries

A.2.1 Concave geometry

SF=1,672. c=5kPa, S=0,277 m, D=0,323 m, $\psi = 0$. Plastic points are shown in Section 6.1.

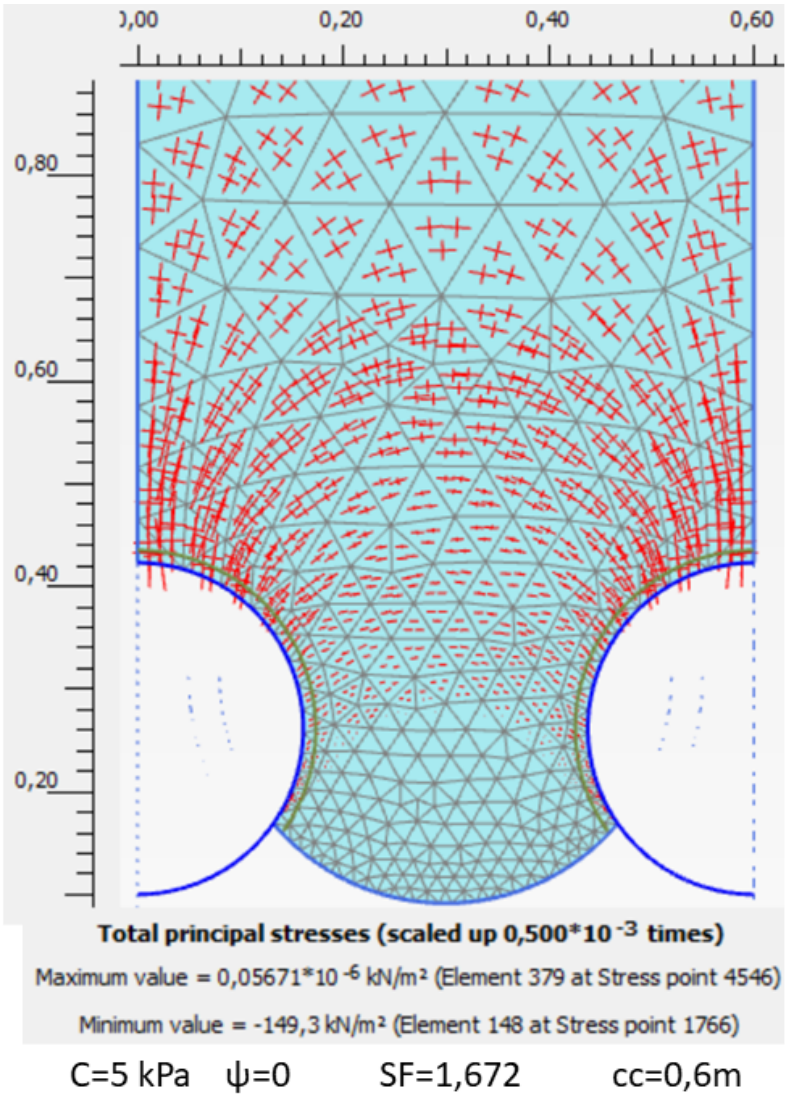

Figure A.2.1: Principal stresses for center distance 0,6 m with c=5 kPa and $\psi = 0$

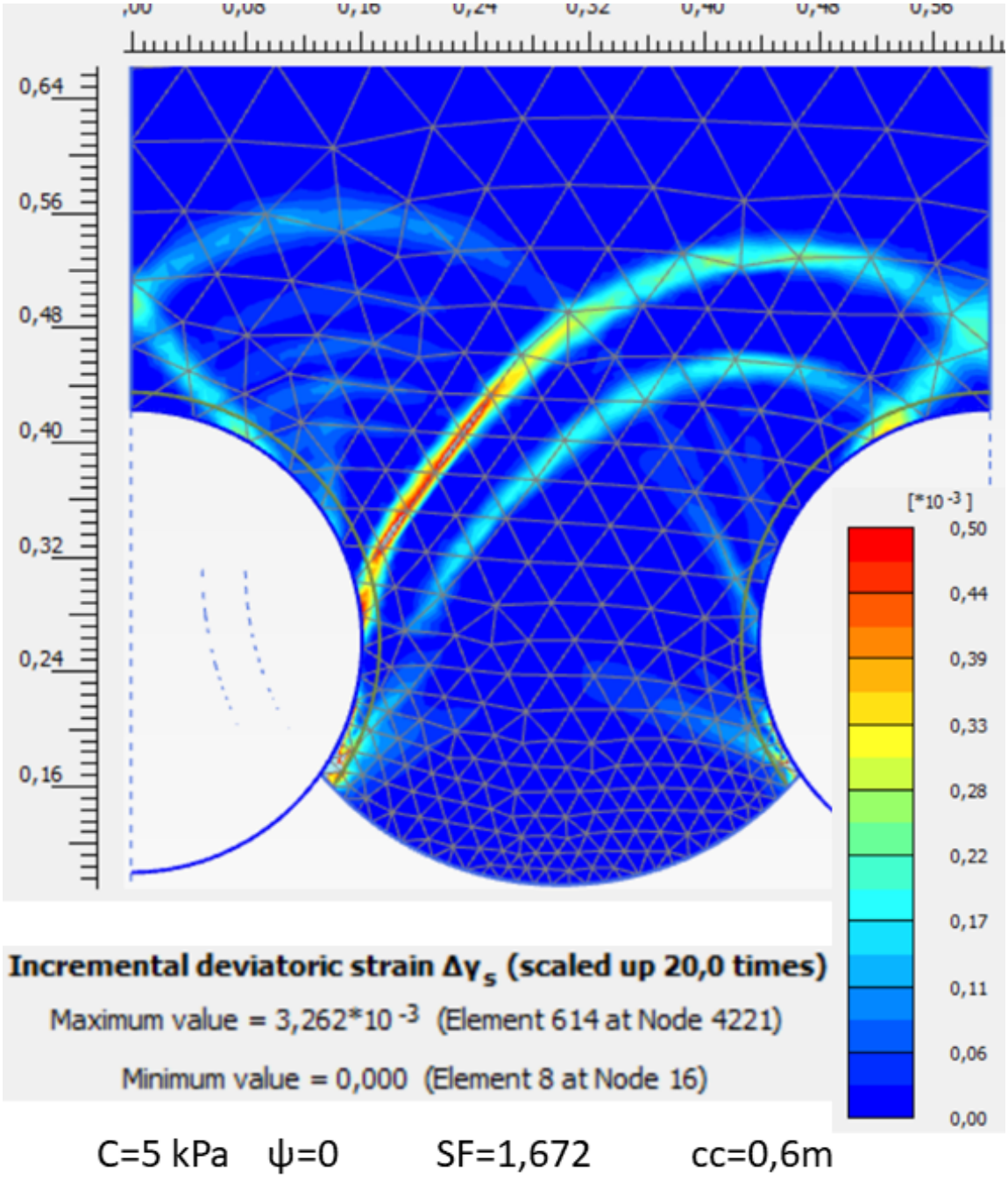

Figure A.2.2: Incremental strain for center distance 0,6 m with c=5 kPa and $\psi = 0$

A.2.2 Perfect arc excavation geometry for cc of 1 m.

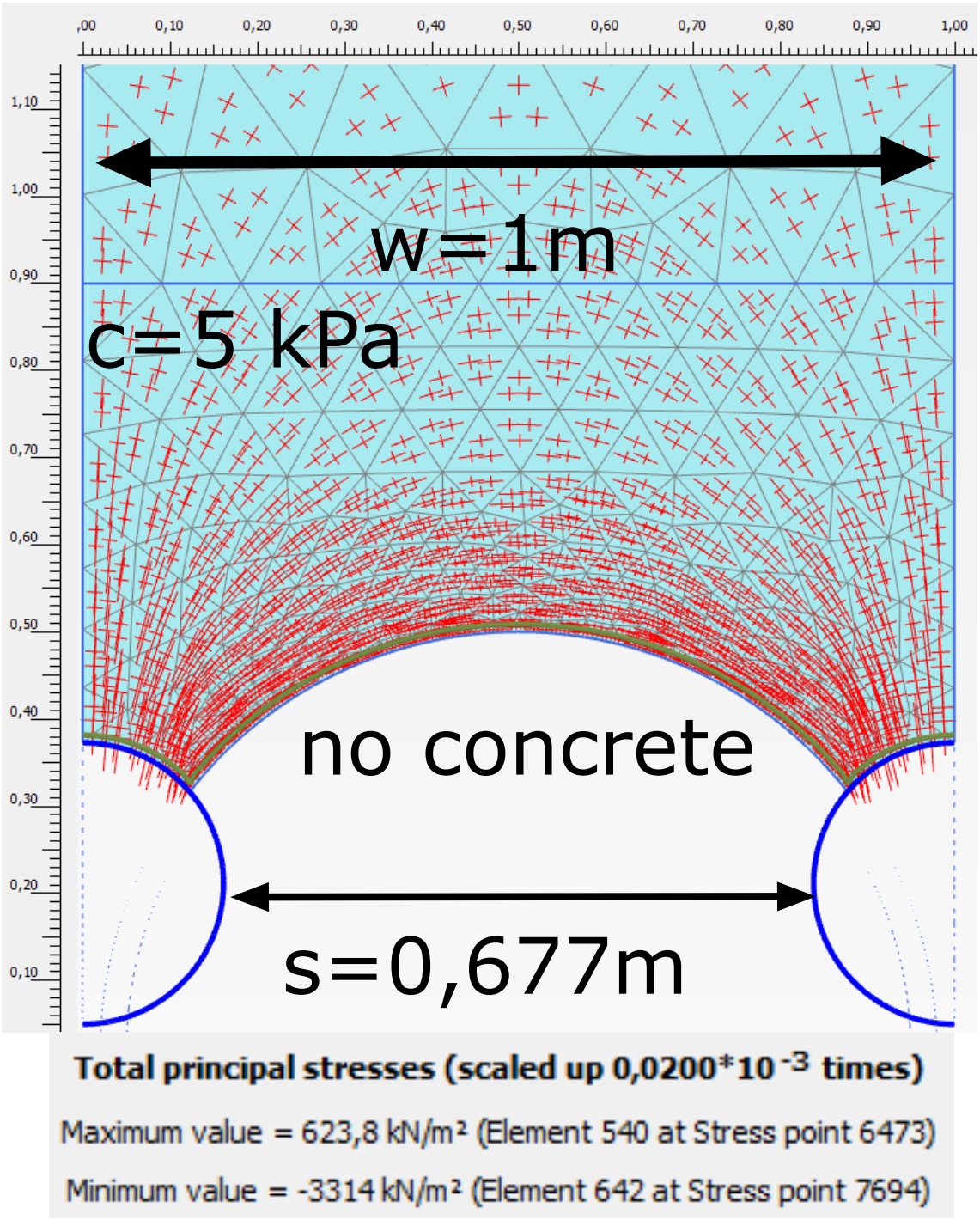

Figure A.2.3: Principal stress plot for 1 m center distance model. Safety calculation.

A.2.3 Perfect arc excavation geometry for cc of 0,6 m.

c=5kPa, S=0,277 m, D=0,323 m, $\psi = 0$, SF=1,101

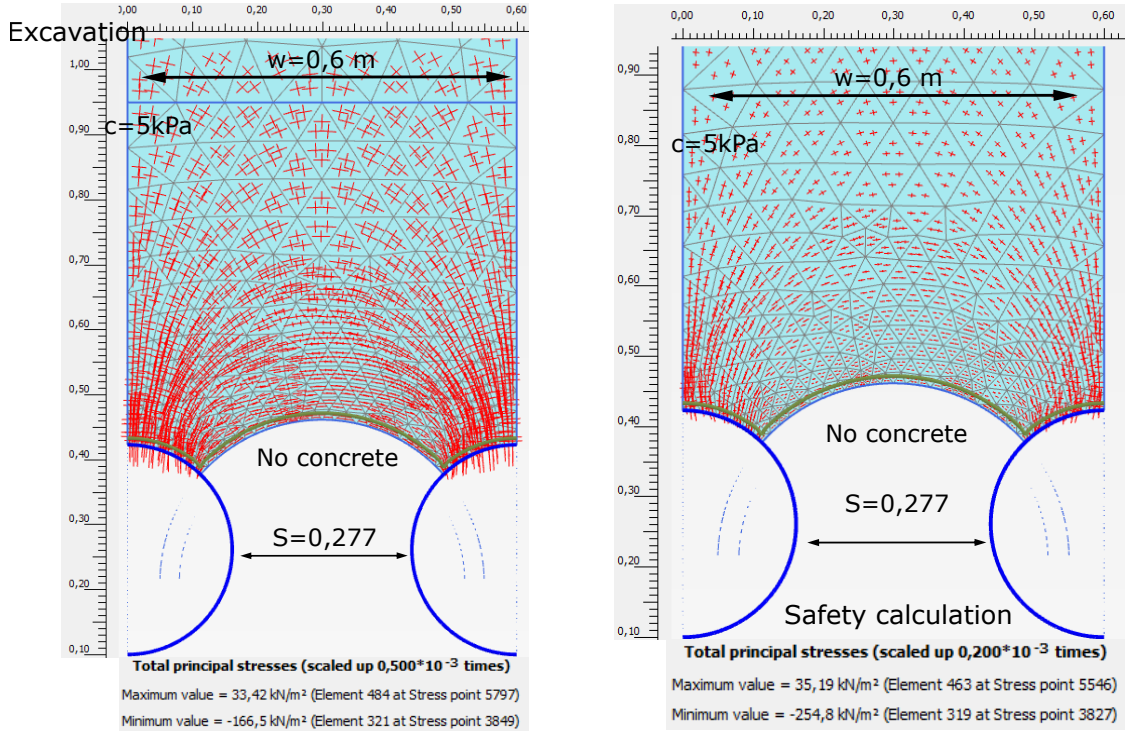

(a) (b)

Figure A.2.4: **a** Principal stress plot for 0,6 m center distance model. Excavation phase. **b** Principal stress plot for 0,6 m center distance model. Safety calculation.

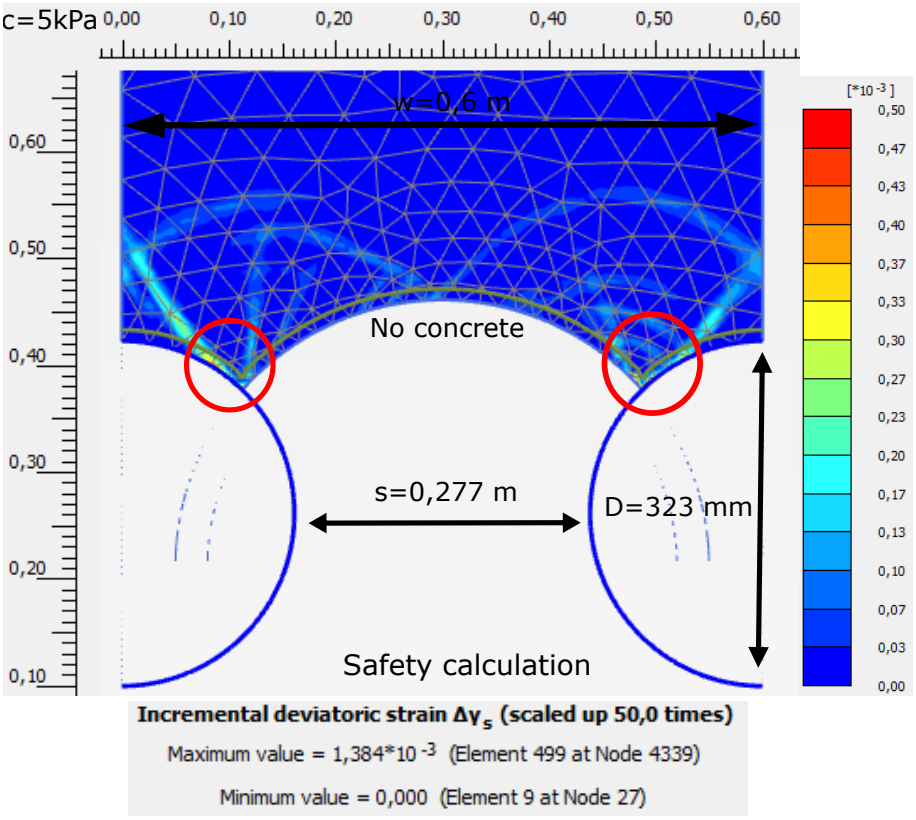
c=5kPa
0,00
0,10
0,20
0,30
0,40
0,50
0,60
w=0,6 m
No concrete
s=0,277 m
D=323 mm
Safety calculation
[*10 -3]
0,50
0,47
0,43
0,40
0,37
0,33
0,30
0,27
0,23
0,20
0,17
0,13
0,10
0,07
0,03
0,00
Incremental deviatoric strain Δγs (scaled up 50,0 times)
Maximum value = 1,384*10 -3 (Element 499 at Node 4339)
Minimum value = 0,000 (Element 9 at Node 27)

Figure A.2.5

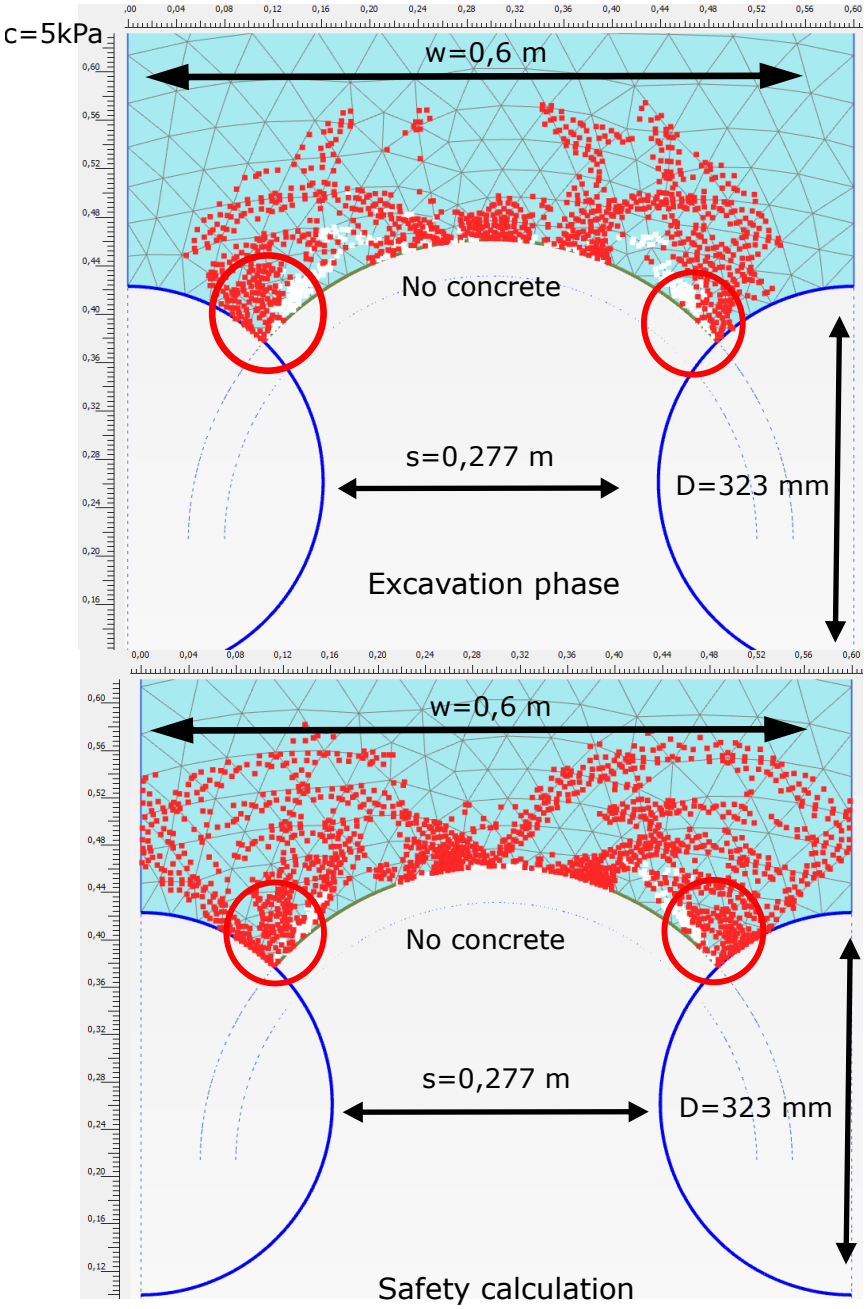
c=5kPa
w=0,6 m
No concrete
s=0,277 m
D=323 mm
Excavation phase
w=0,6 m
No concrete
s=0,277 m
D=323 mm
Safety calculation

Figure A.2.6

A.2.4 Bottom line

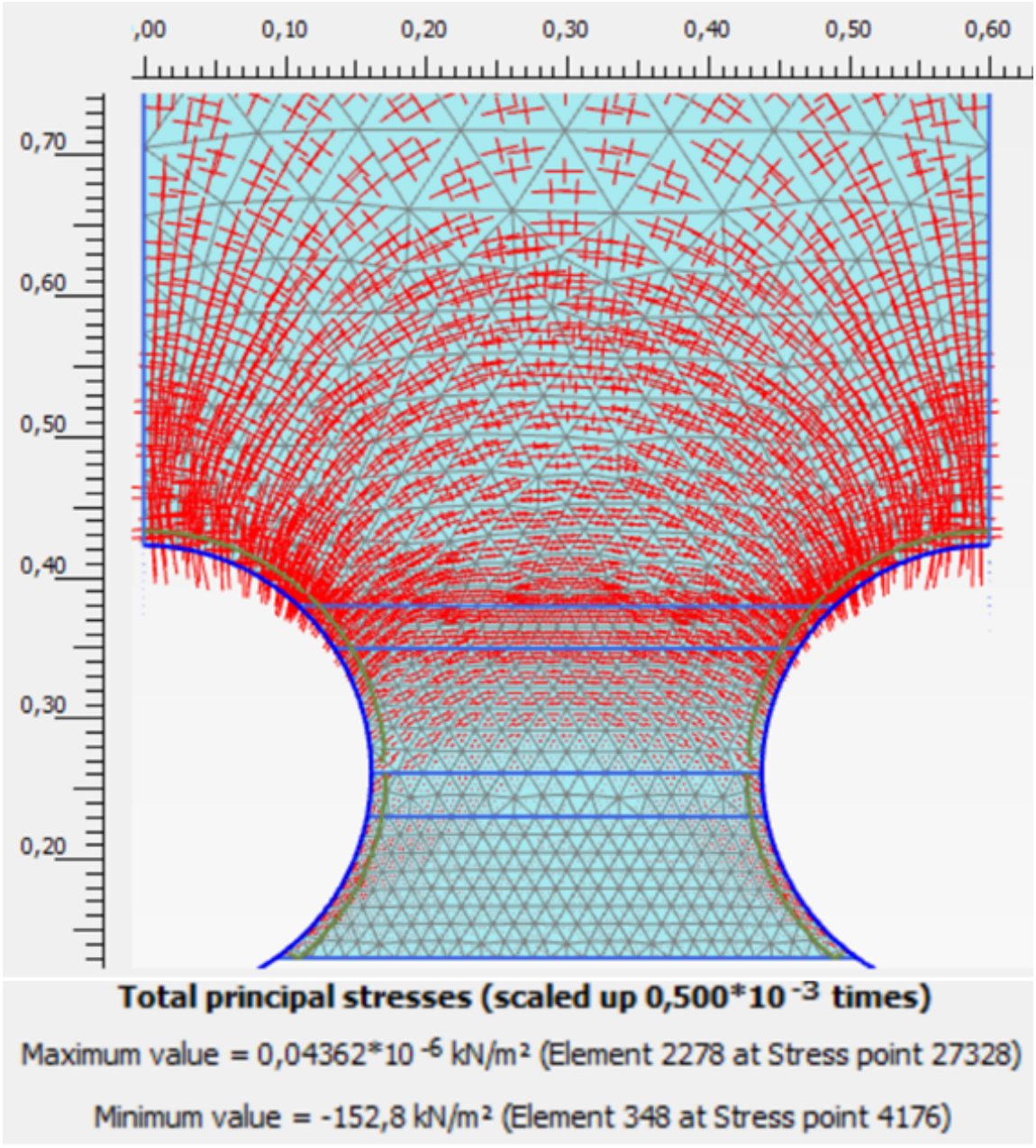

Figure A.2.7: Principal stress plot for center distance 0,6 m with c=0 kPa and $\psi = 0$

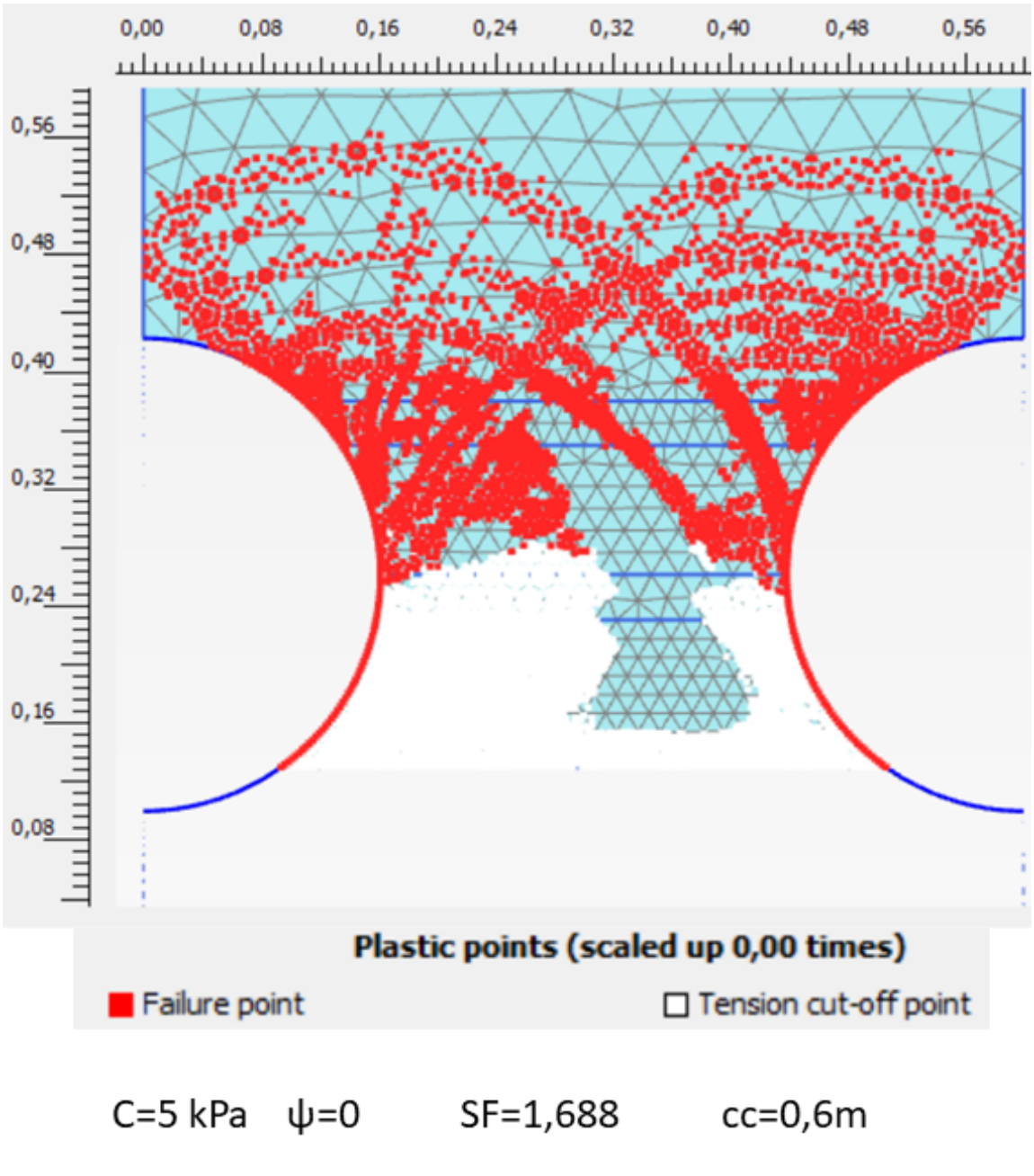

Figure A.2.8: Plastic points, center distance 0,6 m with c=5 kPa and $\psi = 0$

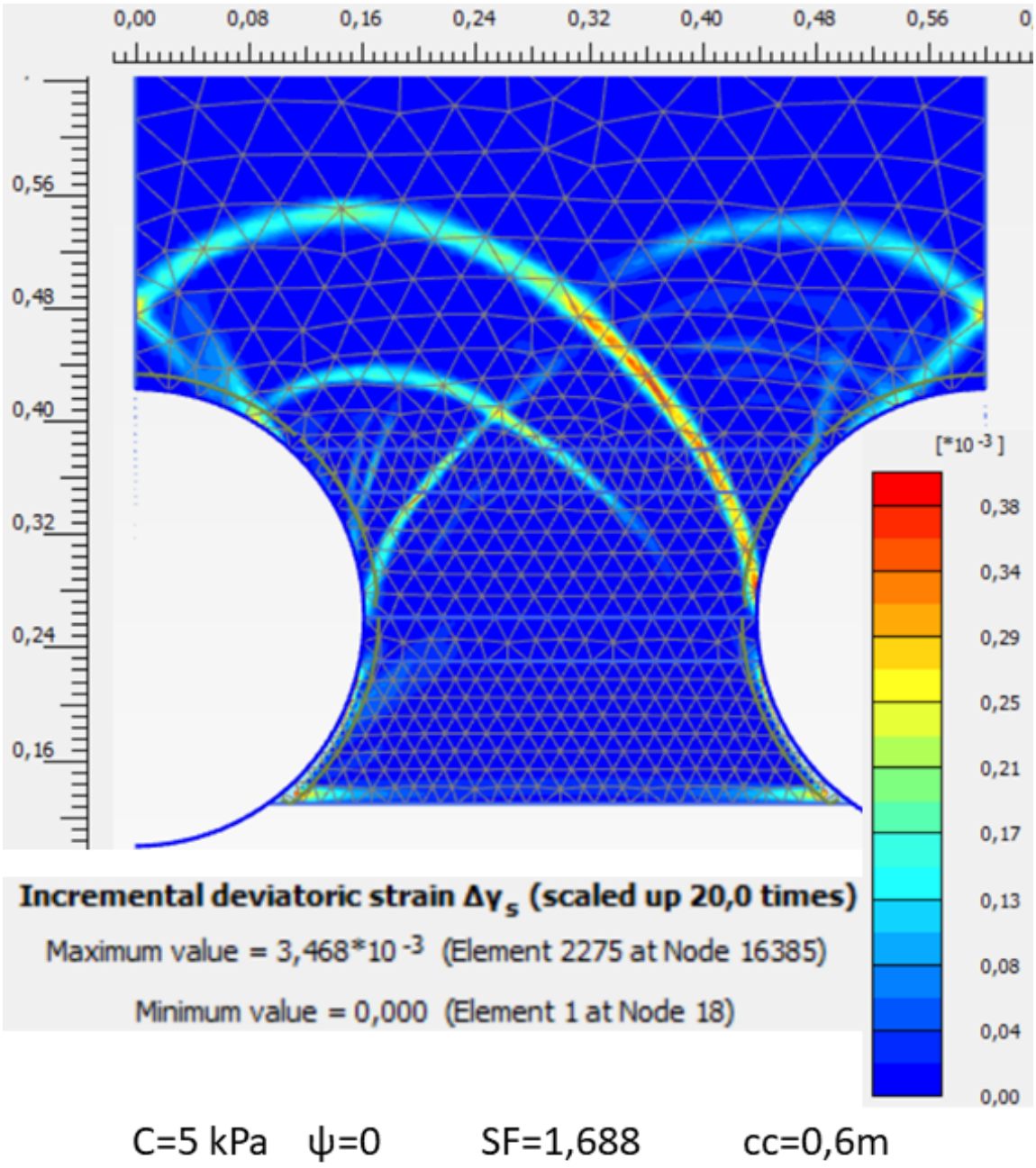

Figure A.2.9: Incremental strain plot for center distance 0,6 m with c=5 kPa and $\psi = 0$

A.2.5 Top line

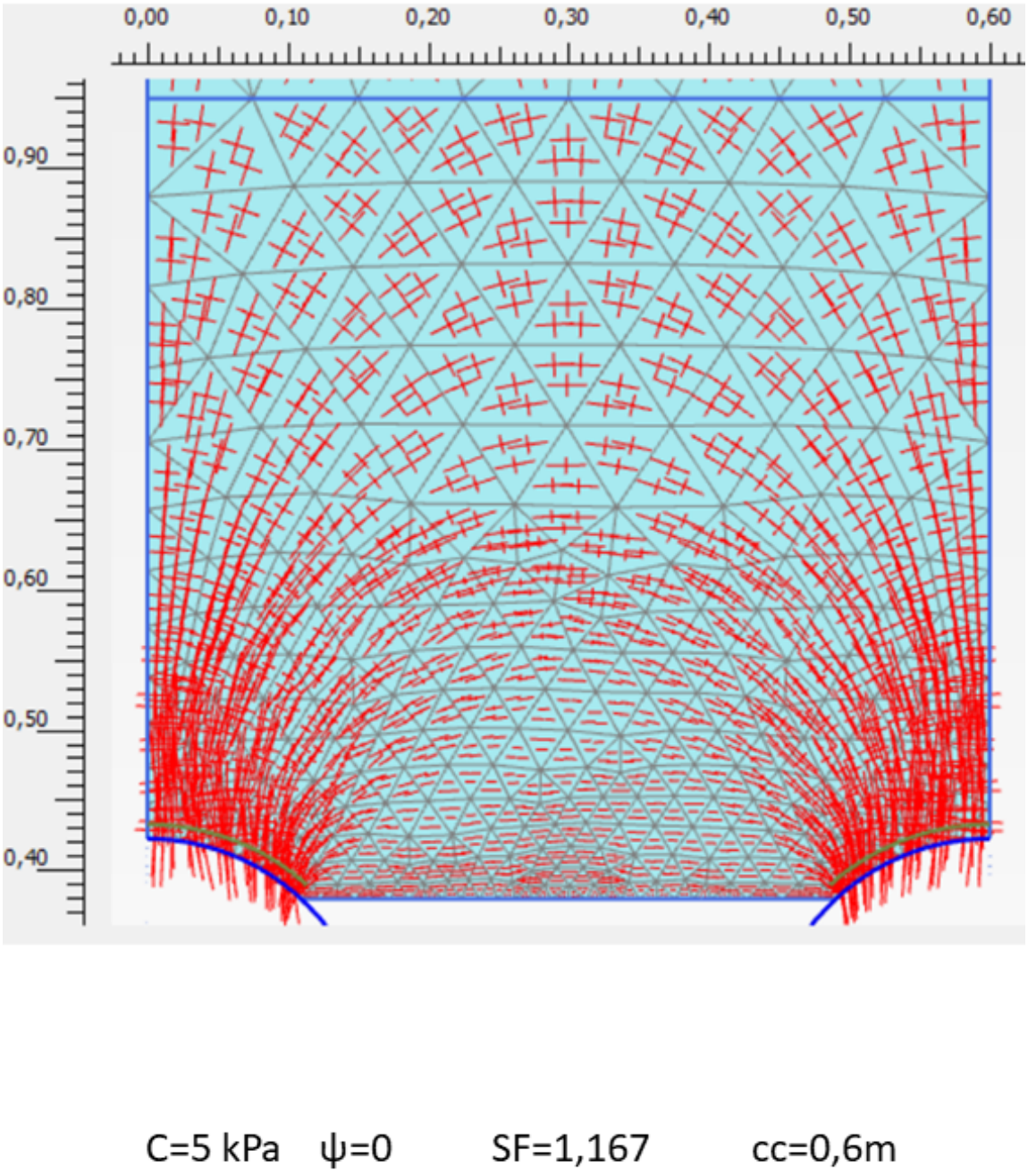

Figure A.2.10: Principal stress plot for center distance 0,6 m with c=5 kPa and $\psi = 0$

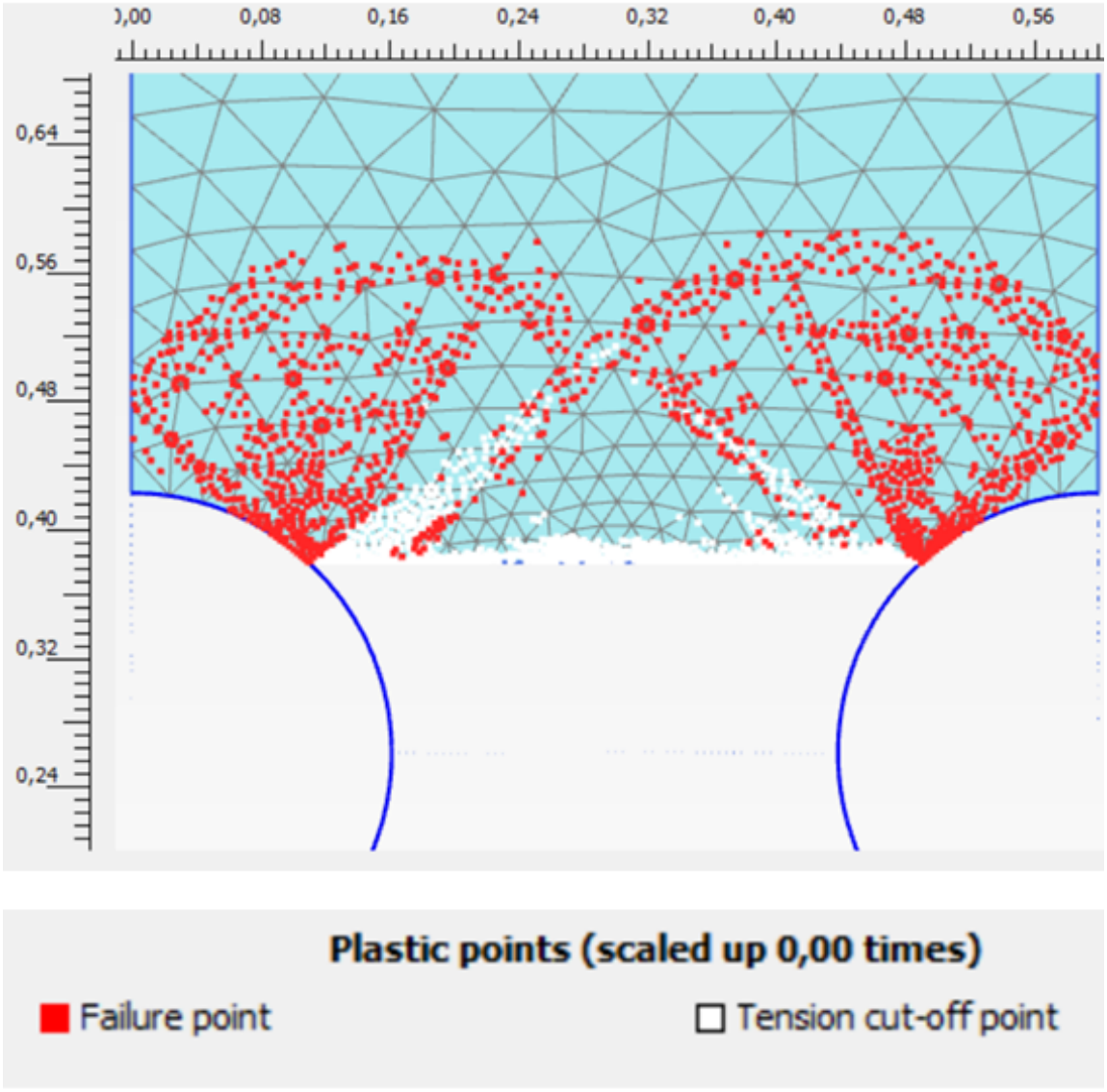

Figure A.2.11: Plastic points, center distance 0,6 m with c=5 kPa and $\psi = 0$

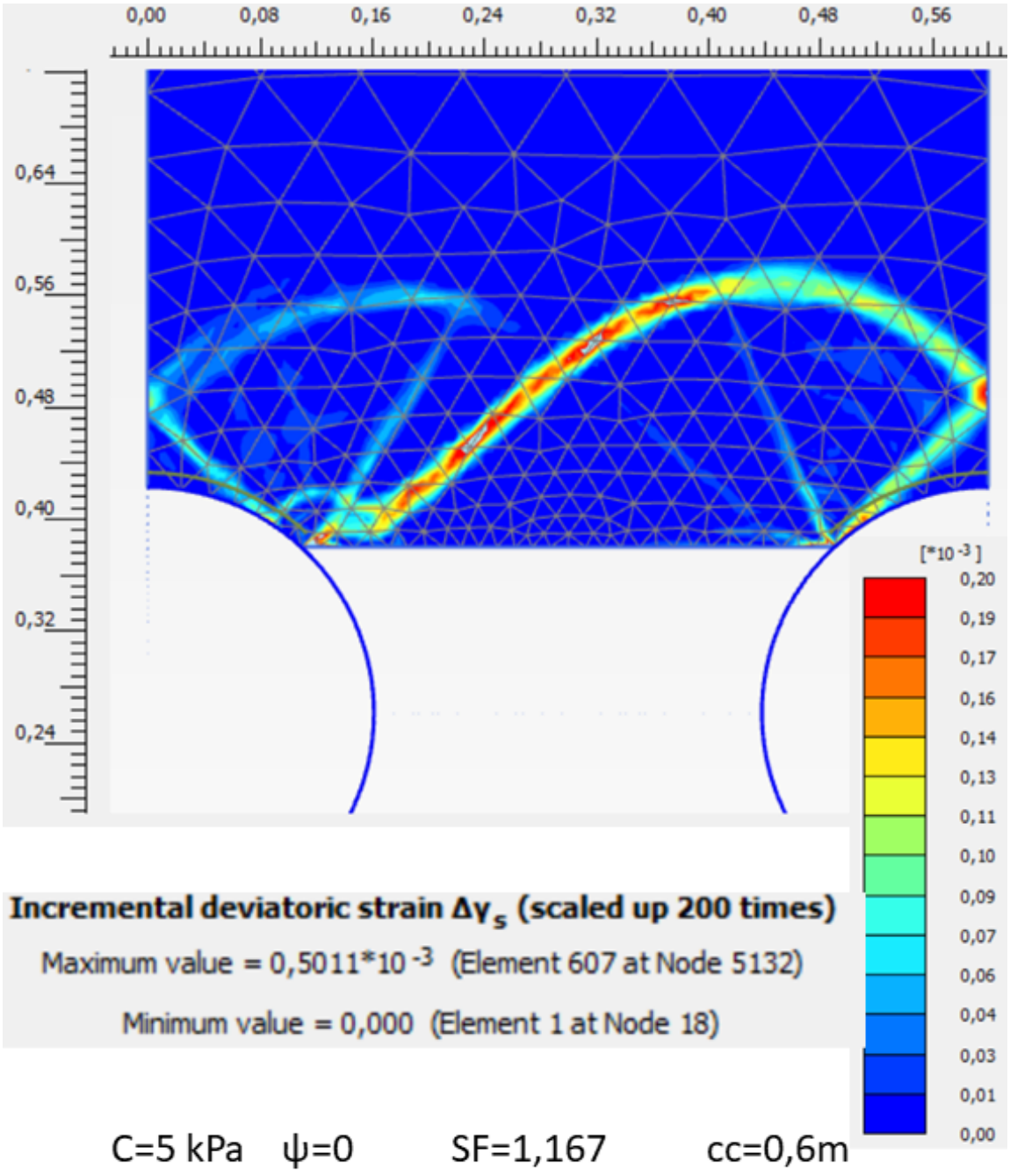

Figure A.2.12: Incremental strain plot for center distance 0,6 m with c=5 kPa and $\psi = 0$

Appendix B

Plaxis plots with concrete

B.1 Perfect pressure arc

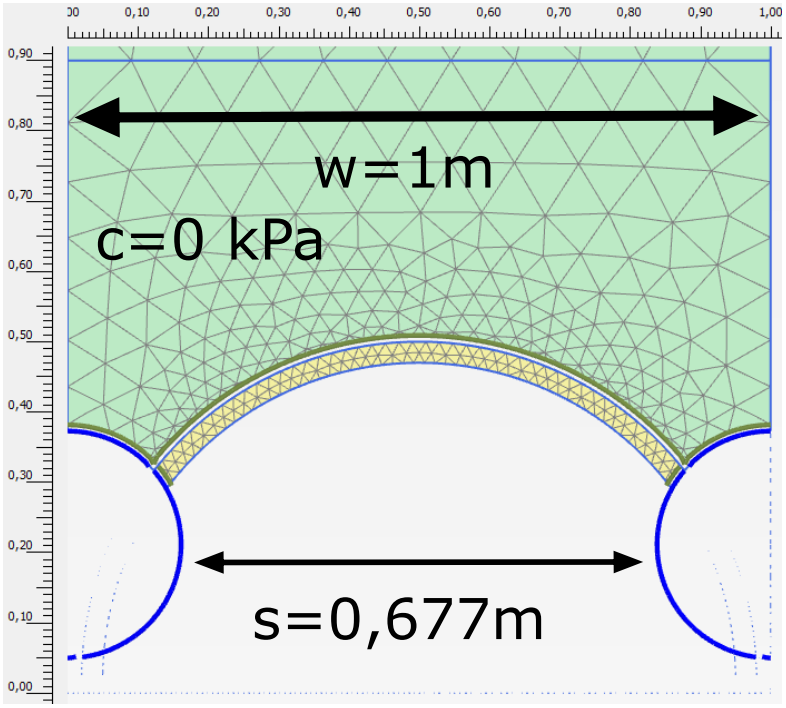

Figure B.1.1: Connectivity plot for the perfect geometry arc. In this phase the concrete is applied and the cohesion reduced.

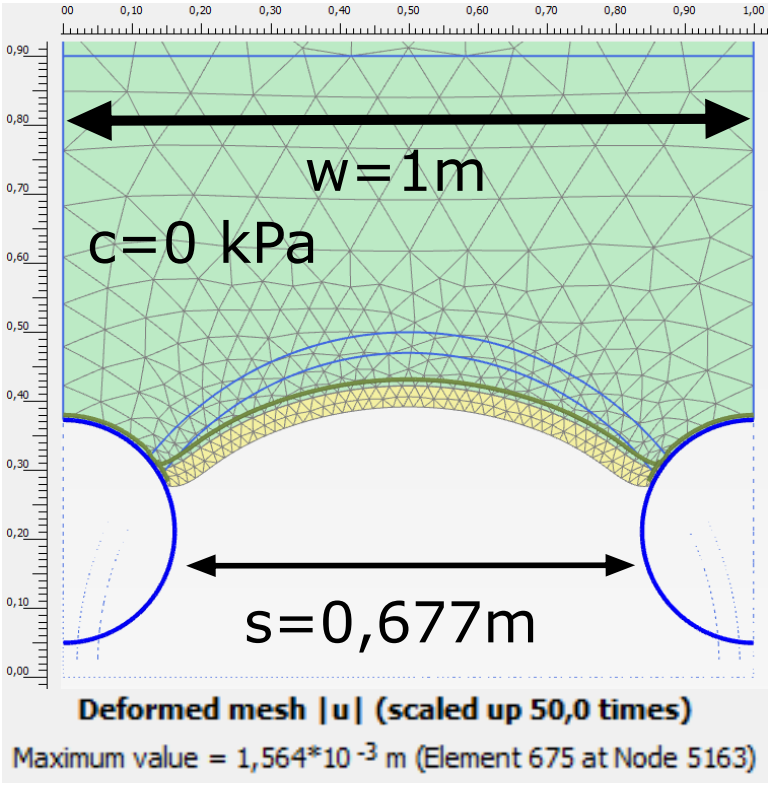

Figure B.1.2: Connectivity plot for the perfect geometry arc

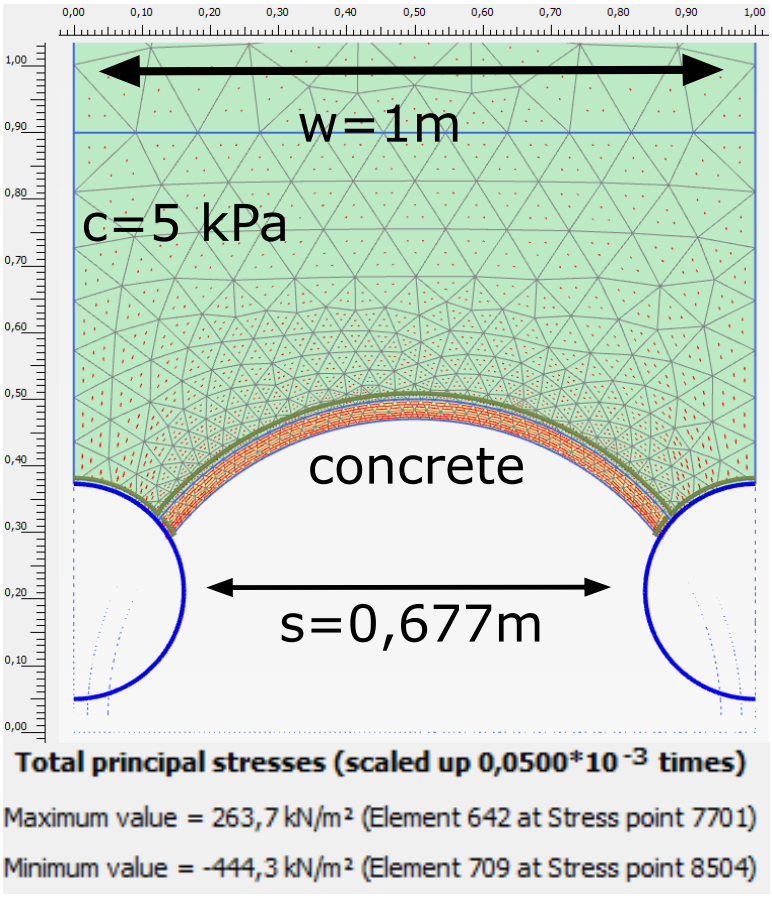

Figure B.1.3: Connectivity plot for the perfect geometry arc

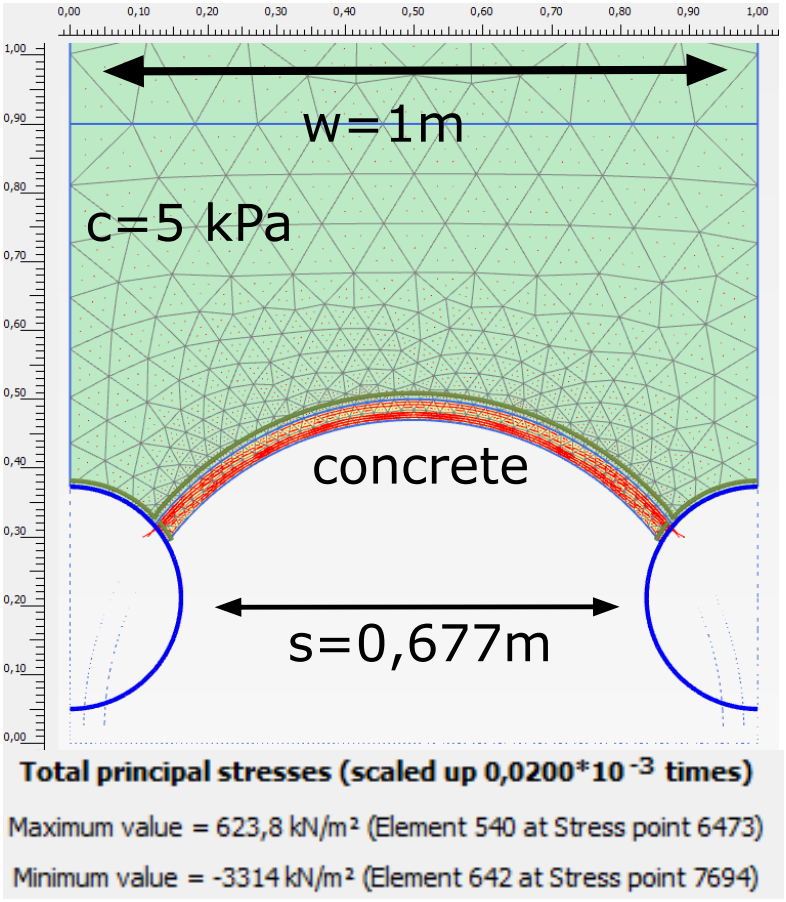

Figure B.1.4: Connectivity plot for the perfect geometry arc

B.2 Imperfect pressure arc

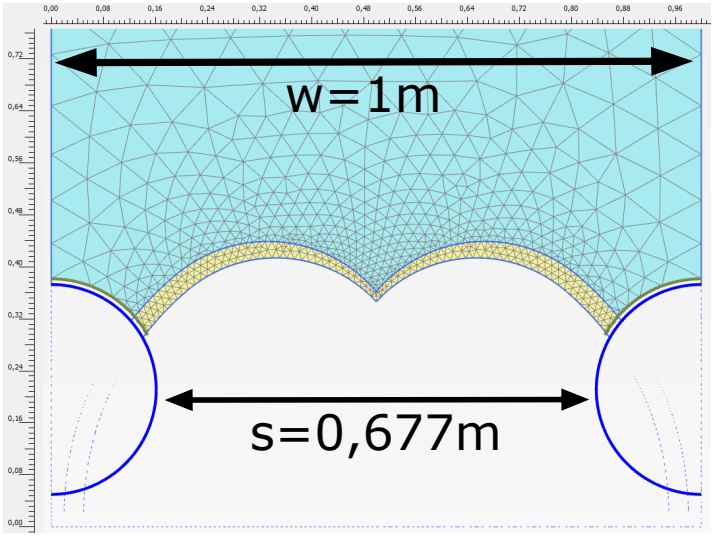

Figure B.2.1: Connectivity plot for imperfect arc for cc 1m

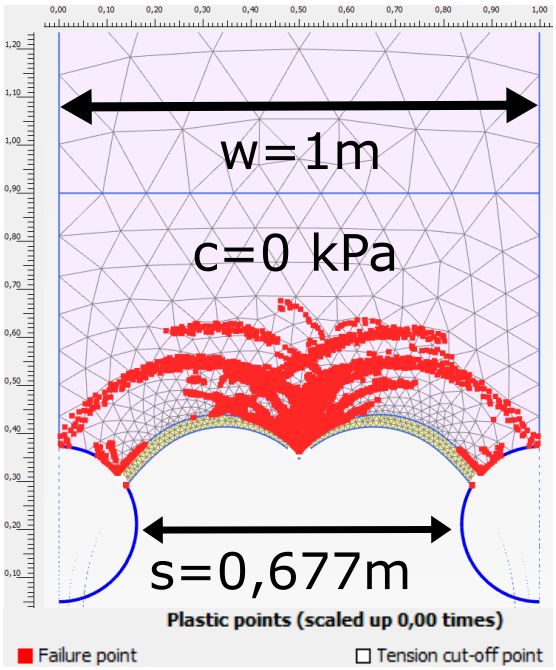

Figure B.2.2: Plastic point plot for imperfect arc cc 1m. There is a concentration of plastic points and tension cut-off points on the edge in the middle and at the steel-concrete interface.

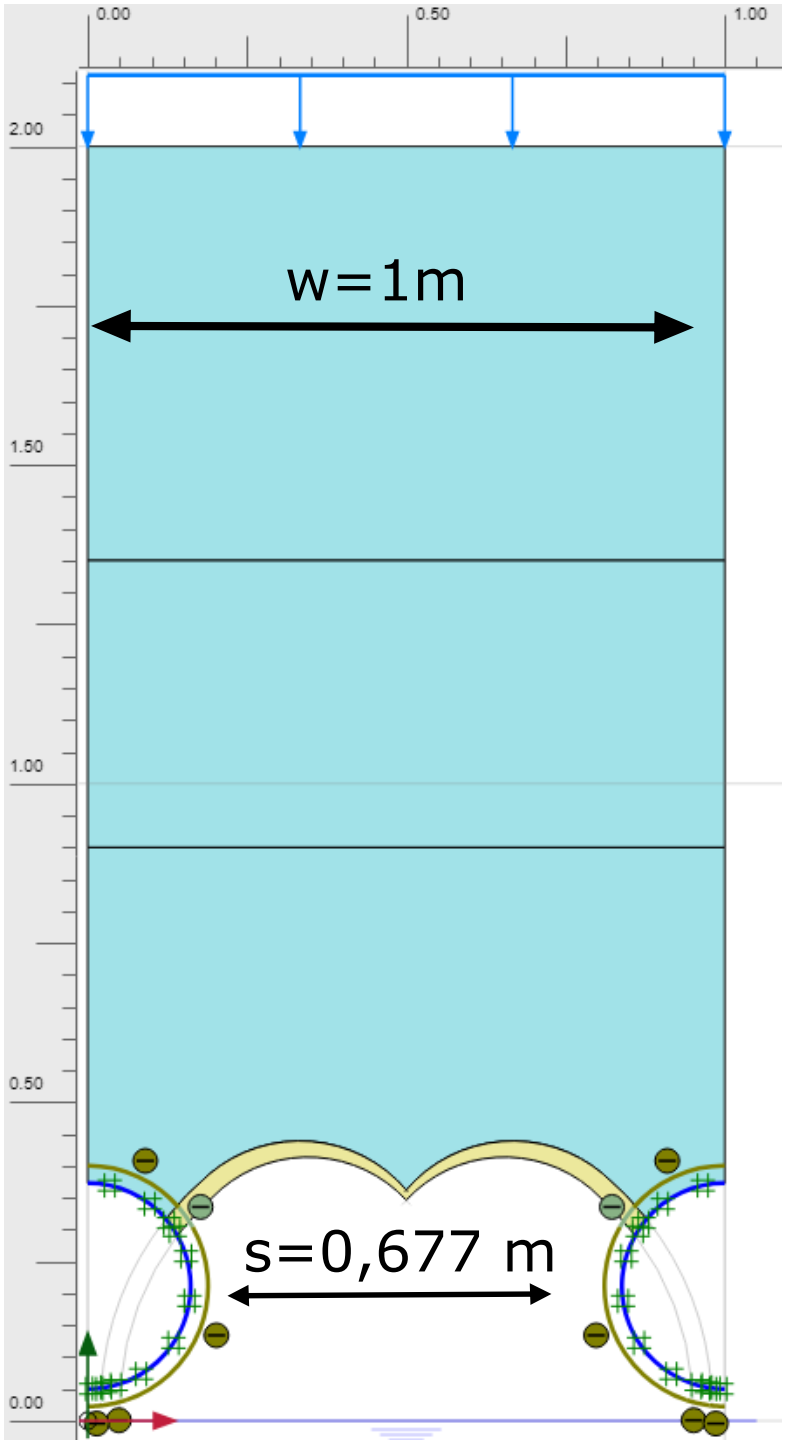

Figure B.2.3: Shows the model of the imperfect arc. With a soil-pipe interface value of $R_{int} = 0,65$ and a steel-concrete adhesion of 500 kPa.

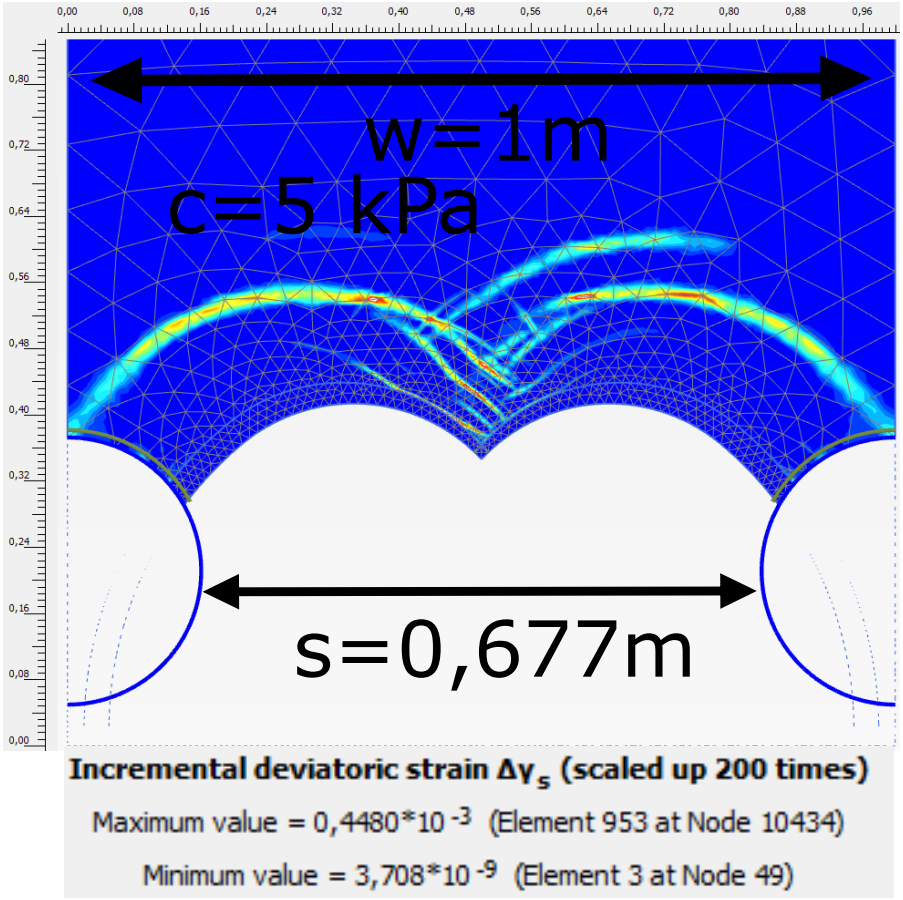

Figure B.2.4: Incremental strain for imperfect geometry with a center distance of 1 m.

B.3 Straight lines

The following plots show principal stresses, incremental strain and plastic points for straight concrete layer at the top part, bottom part and at the center of the pipes.

B.3.1 Middle line

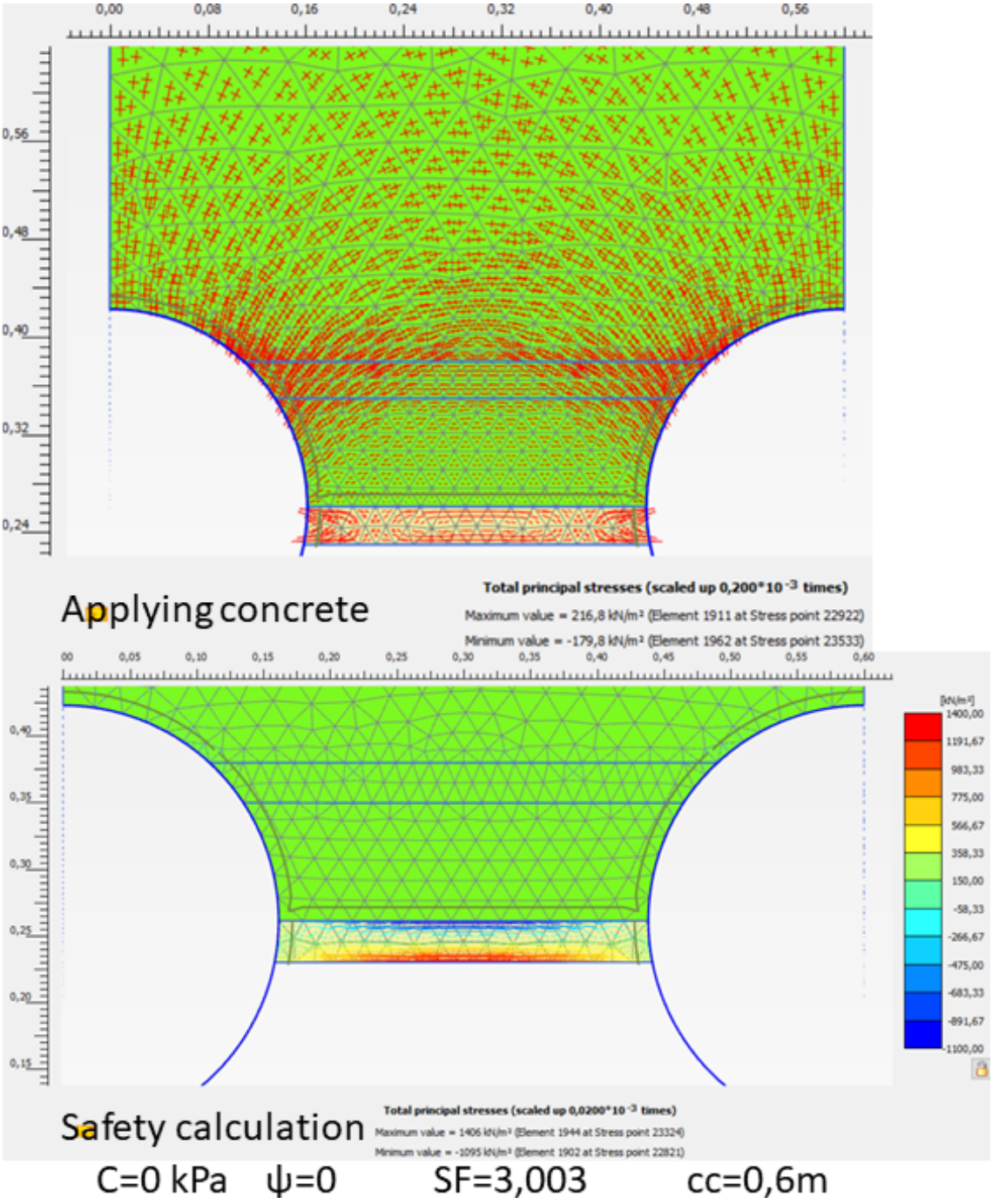

Figure B.3.1: Principal stress plot for center distance 0,6 m with c=0 kPa and $\psi = 0$. The first picture shows the principal stress after the concrete is applied and the cohesion reduced to 0, and the second picture shows the principal stress after $c\phi$-reduction

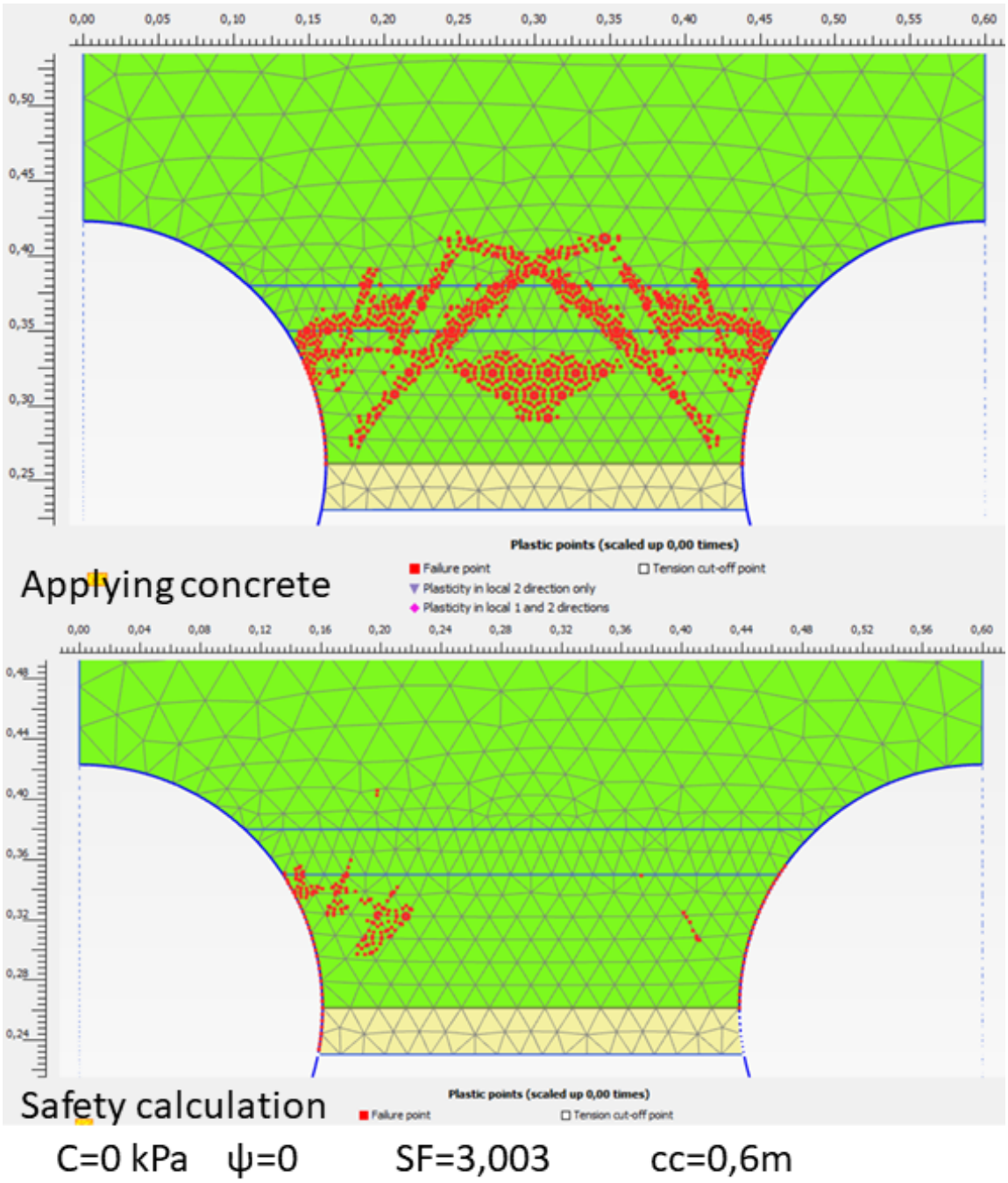

Figure B.3.2: Plastic points for center distance 0,6 m with c=0 kPa and $\psi = 0$. The first picture shows plastic points after the concrete is applied and the cohesion reduced to 0, and the second picture shows the plastic points after $c\phi$-reduction

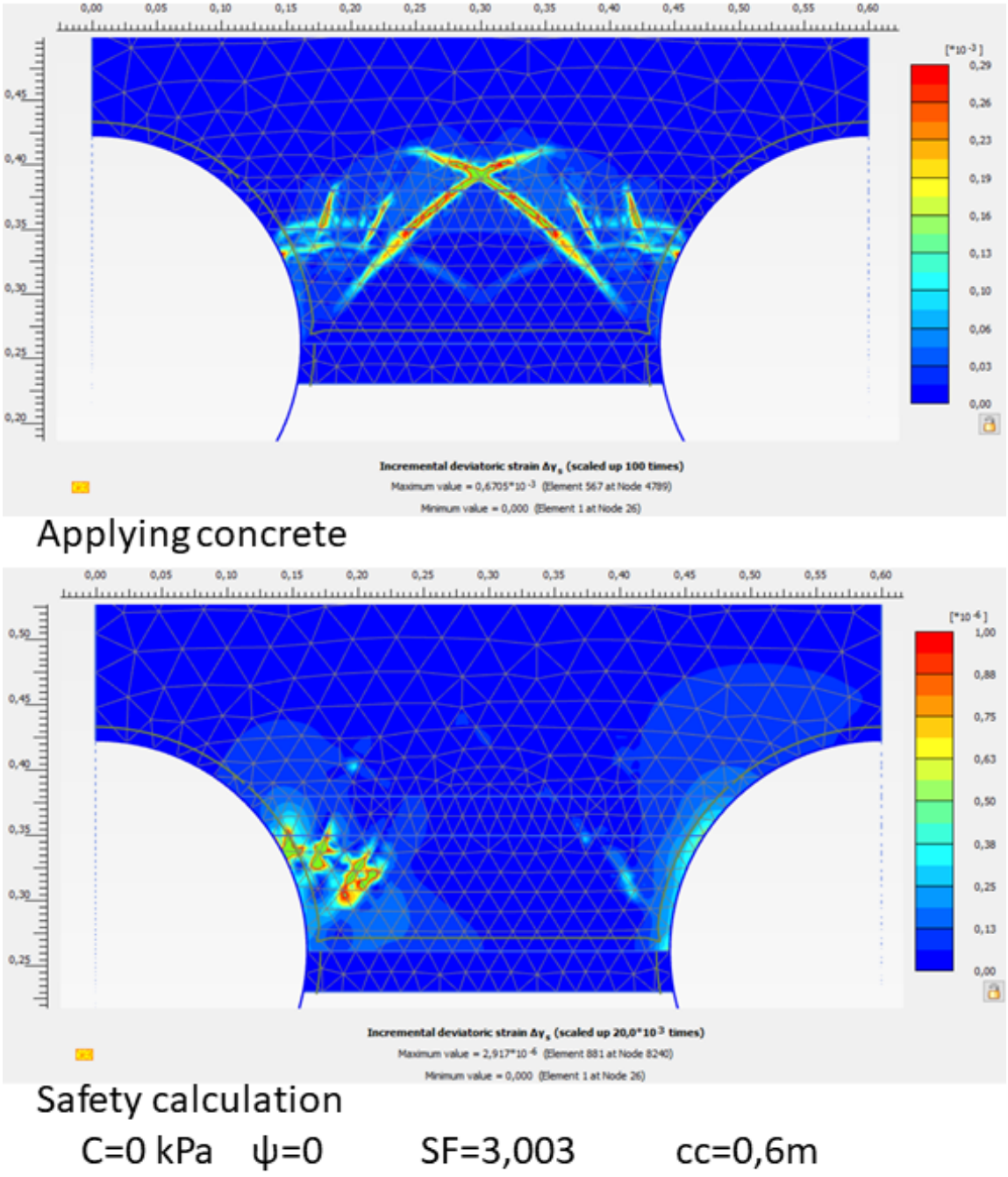

Figure B.3.3: Incremental strains for center distance 0,6 m with c=5 kPa and $\psi = 0$. The first picture shows incremental strains after the concrete is applied and the cohesion reduced to 0, and the second picture shows incremental strains after $c\phi$-reduction

B.3.2 Top line

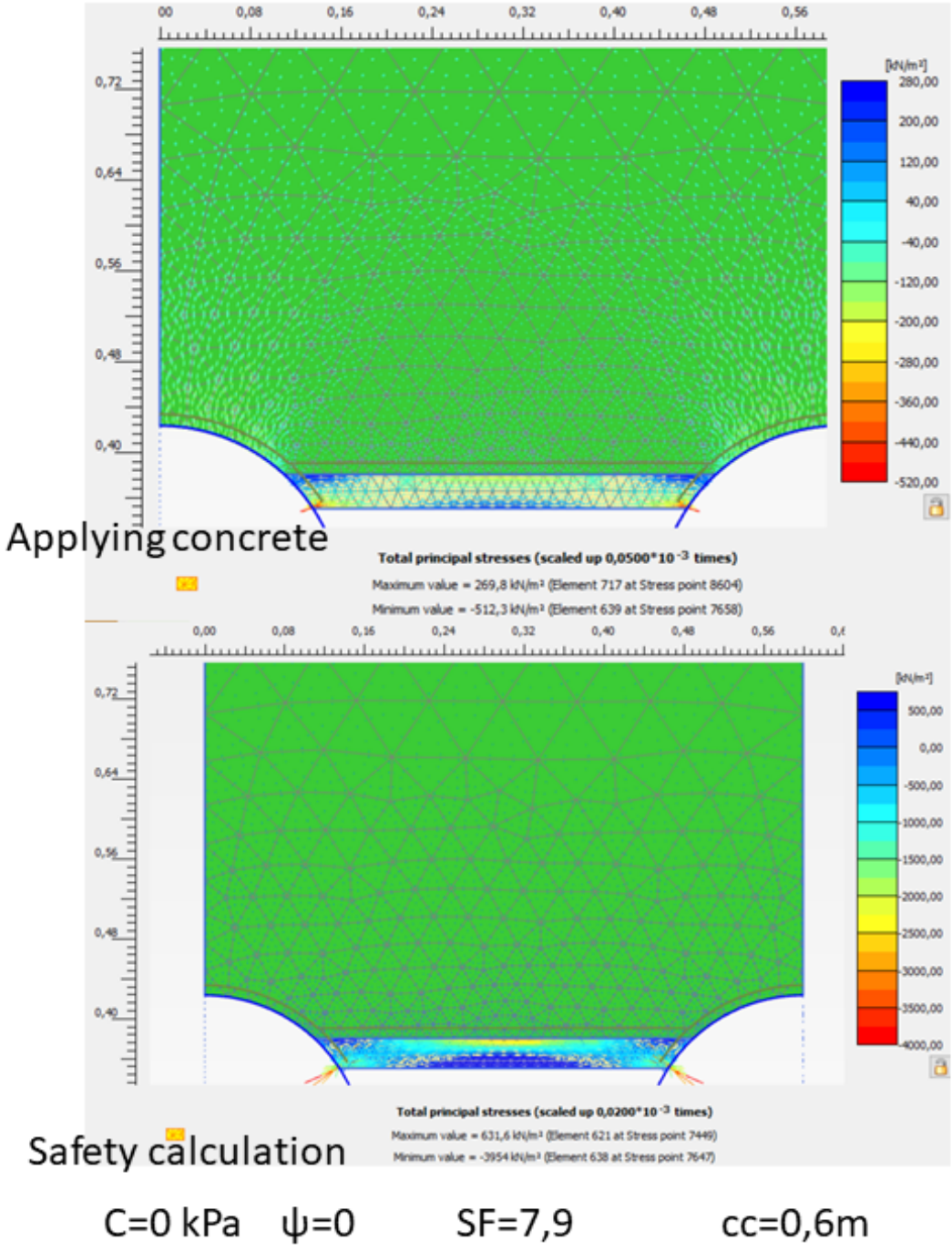

Figure B.3.4: Principal stress plot for center distance 0,6 m with c=0 kPa and $\psi = 0$. The first picture shows the principal stress after the concrete is applied and the cohesion reduced to 0, and the second picture shows the principal stress after $c\phi$-reduction.

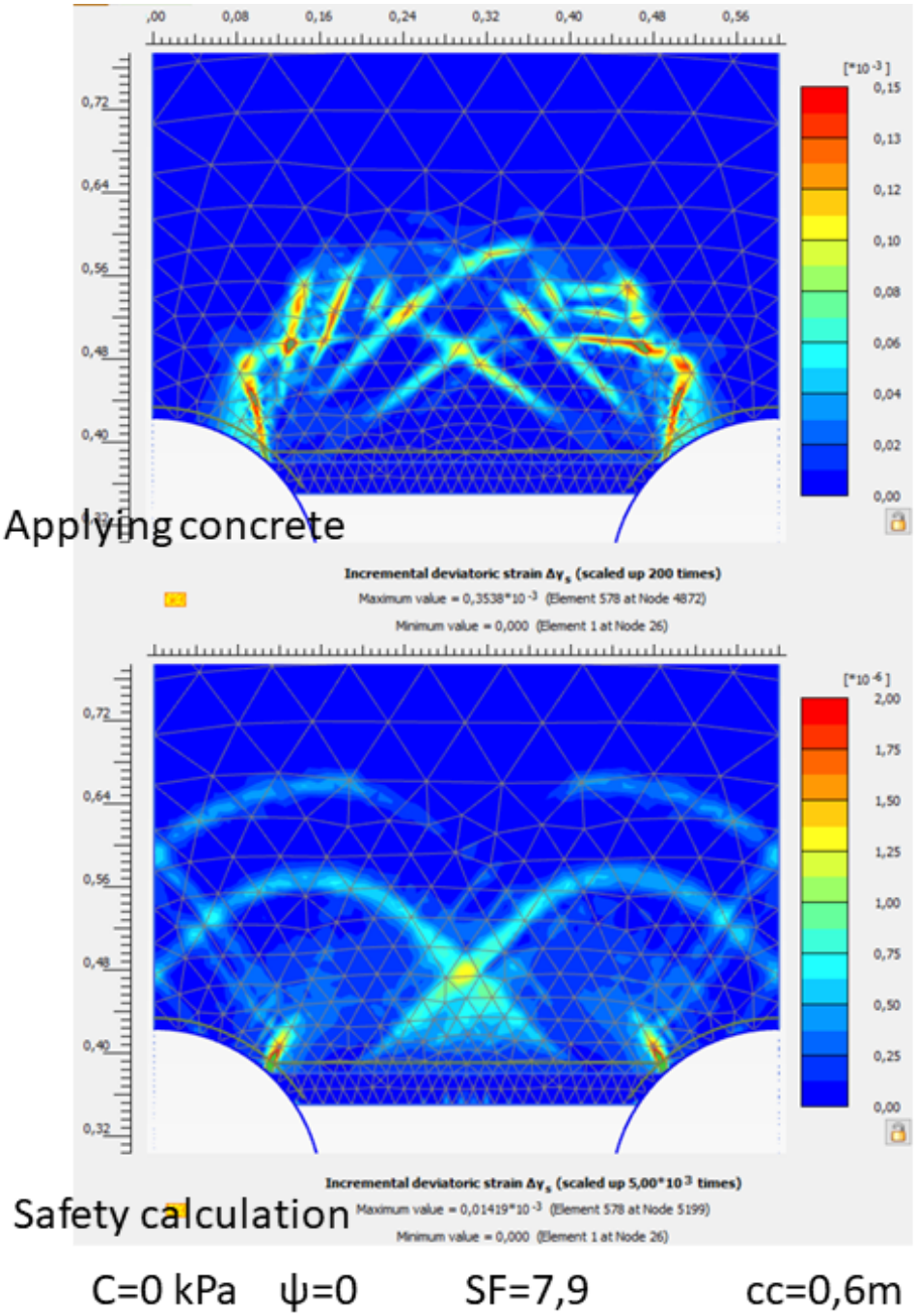

Figure B.3.5: Incremental strains for center distance 0,6 m with c=5 kPa and $\psi = 0$. The first picture shows incremental strains after the concrete is applied and the cohesion reduced to 0, and the second picture shows incremental strains after $c\phi$-reduction

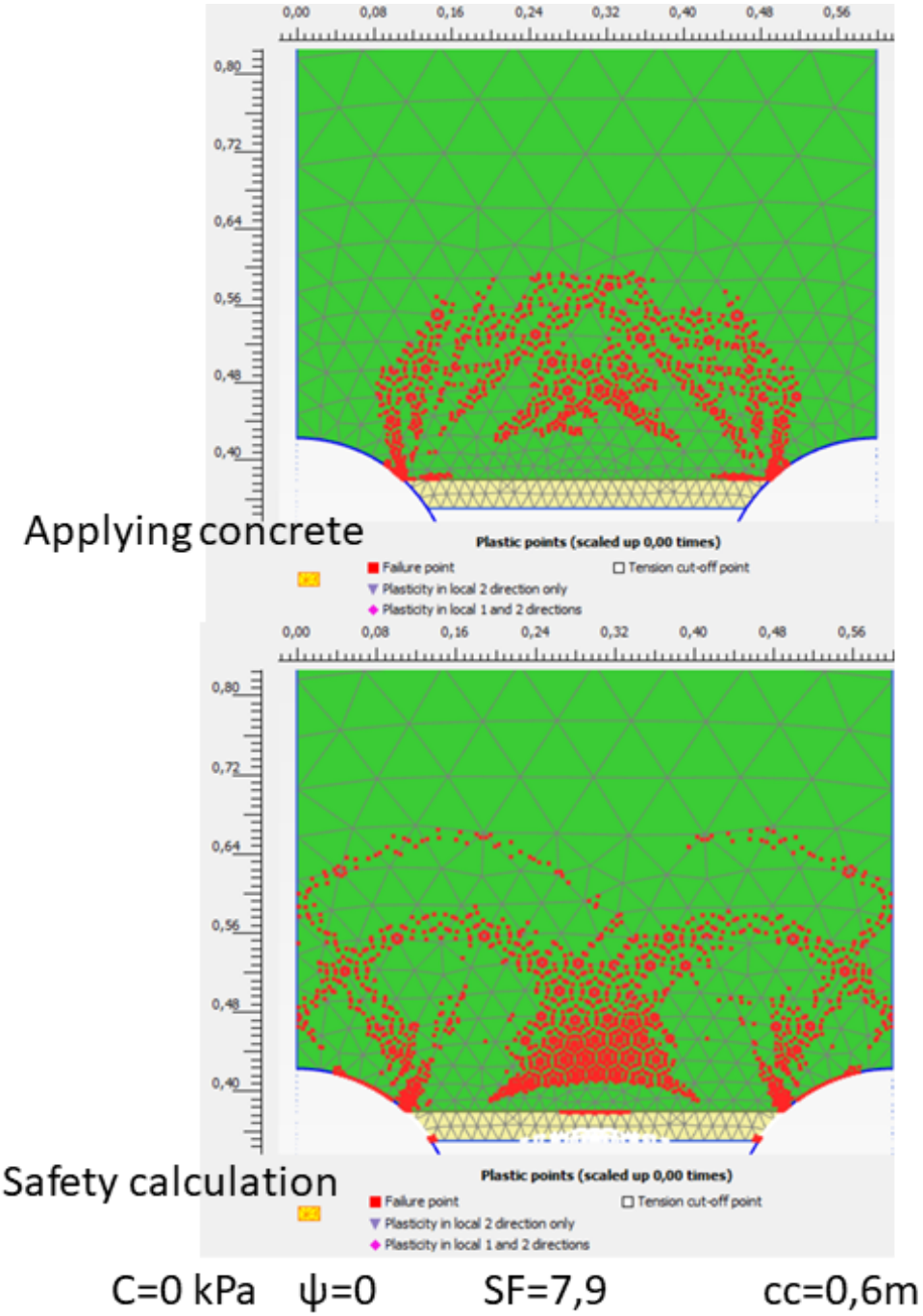

Figure B.3.6: Plastic points for center distance 0,6 m with c=0 kPa and $\psi = 0$. The first picture shows plastic points after the concrete is applied and the cohesion reduced to 0, and the second picture shows the plastic points after $c\phi$-reduction

B.3.3 Bottom line

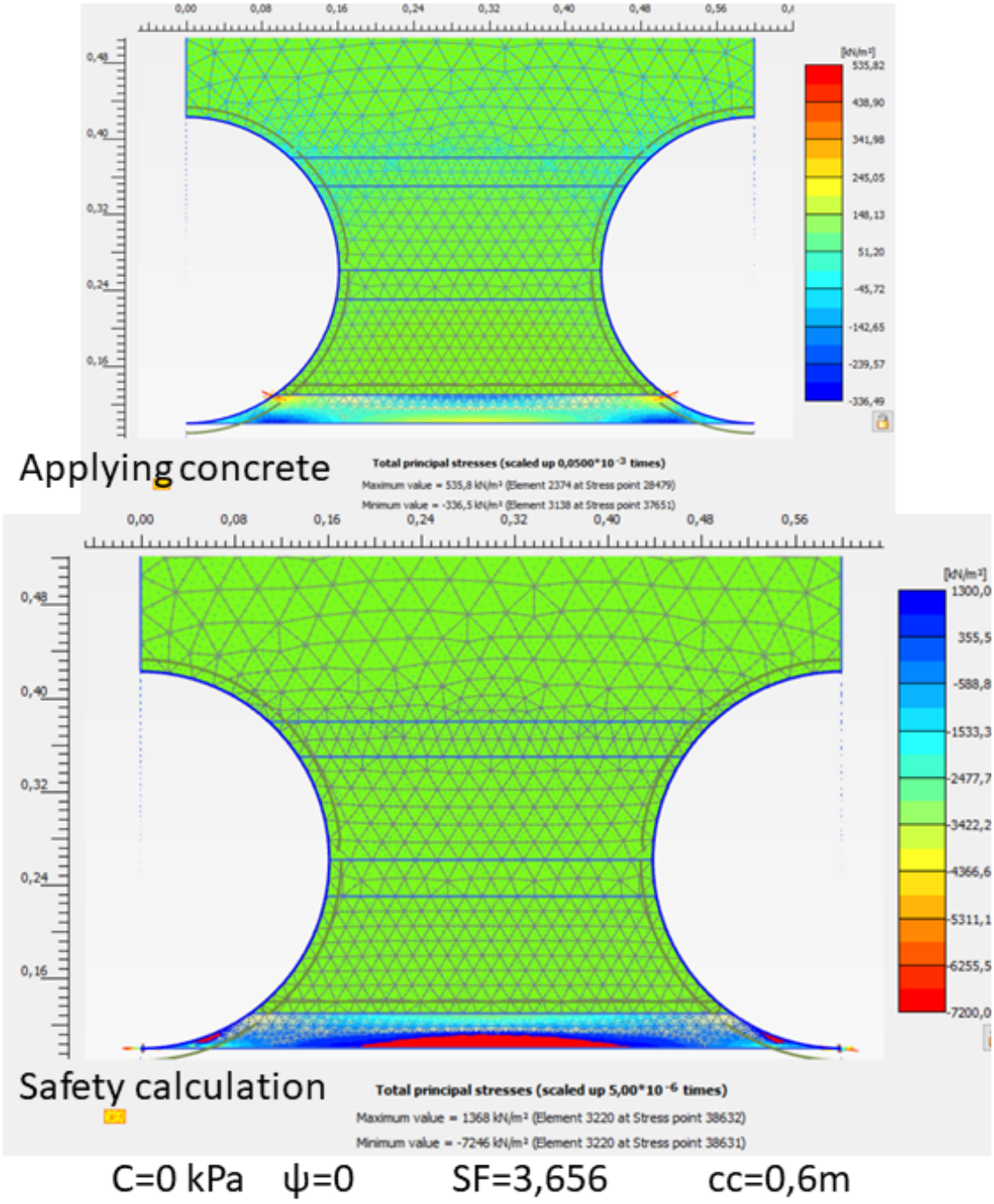

Figure B.3.7: Principal stresses for center distance 0,6 m with c=0 kPa and $\psi = 0$. The first picture shows the principal stress after the concrete is applied and the cohesion reduced to 0, and the second picture shows the principal stress after $c\phi$-reduction.

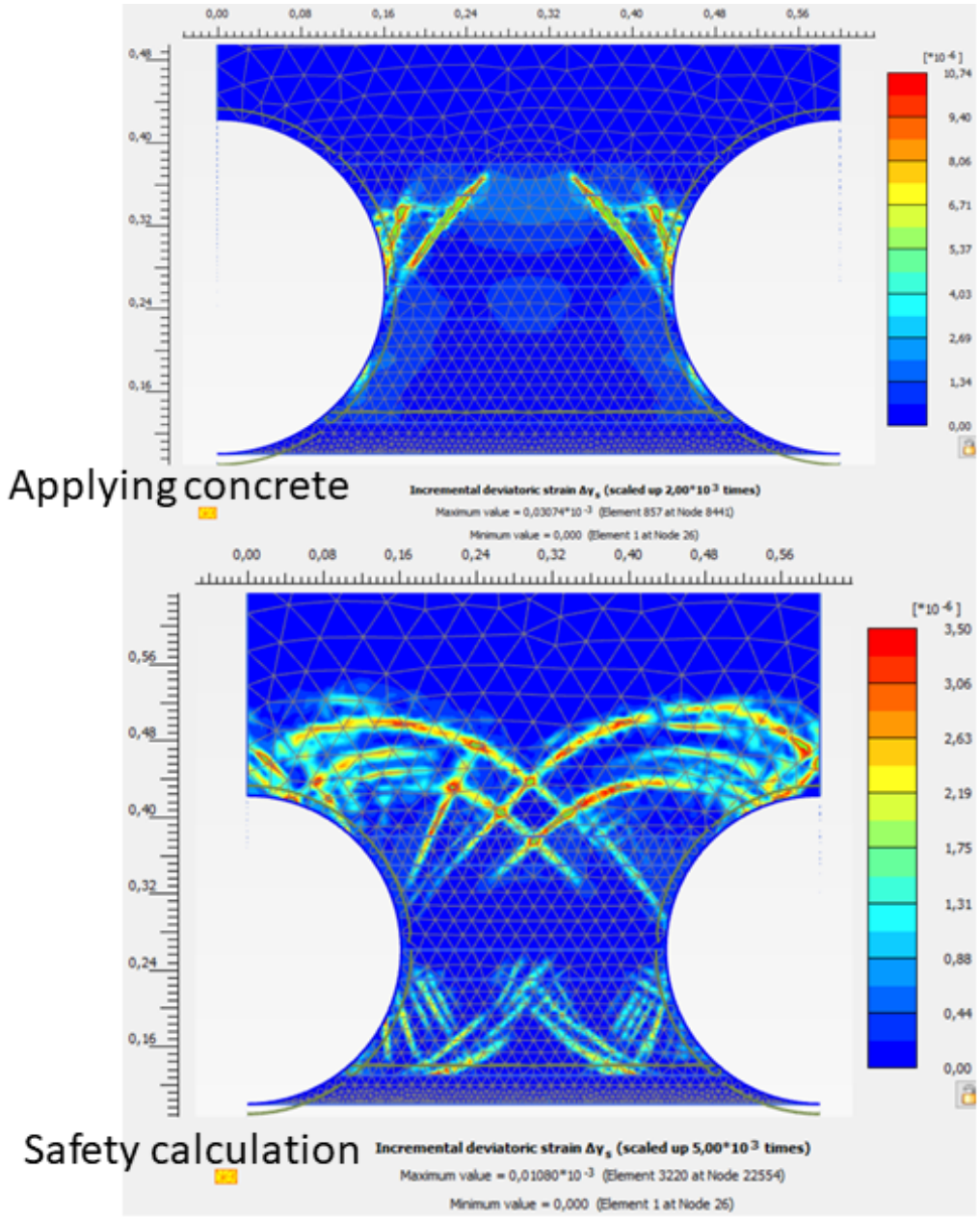

Figure B.3.8: Incremental strains plot for center distance 0,6 m with c=0 kPa and $\psi = 0$. The first picture shows incremental strains after the concrete is applied and the cohesion reduced to 0, and the second picture shows incremental strains after $c\phi$-reduction

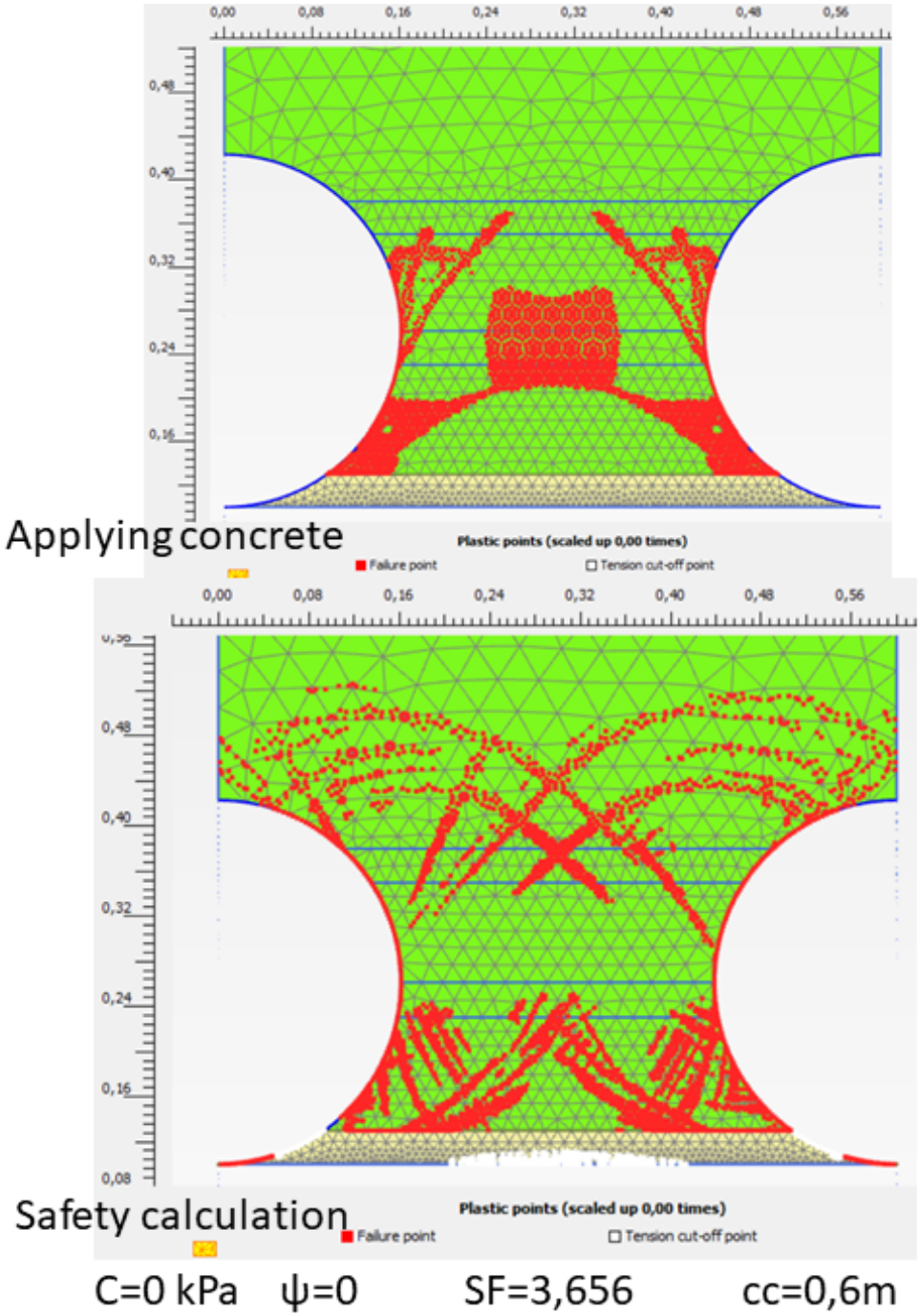

Figure B.3.9: Plastic points for center distance 0,6 m with c=5 kPa and $\psi = 0$. The first picture shows plastic points after the concrete is applied and the cohesion reduced to 0, and the second picture shows the plastic points after $c\phi$-reduction

Plastic points for straight line excavation, center distance of 1 m.

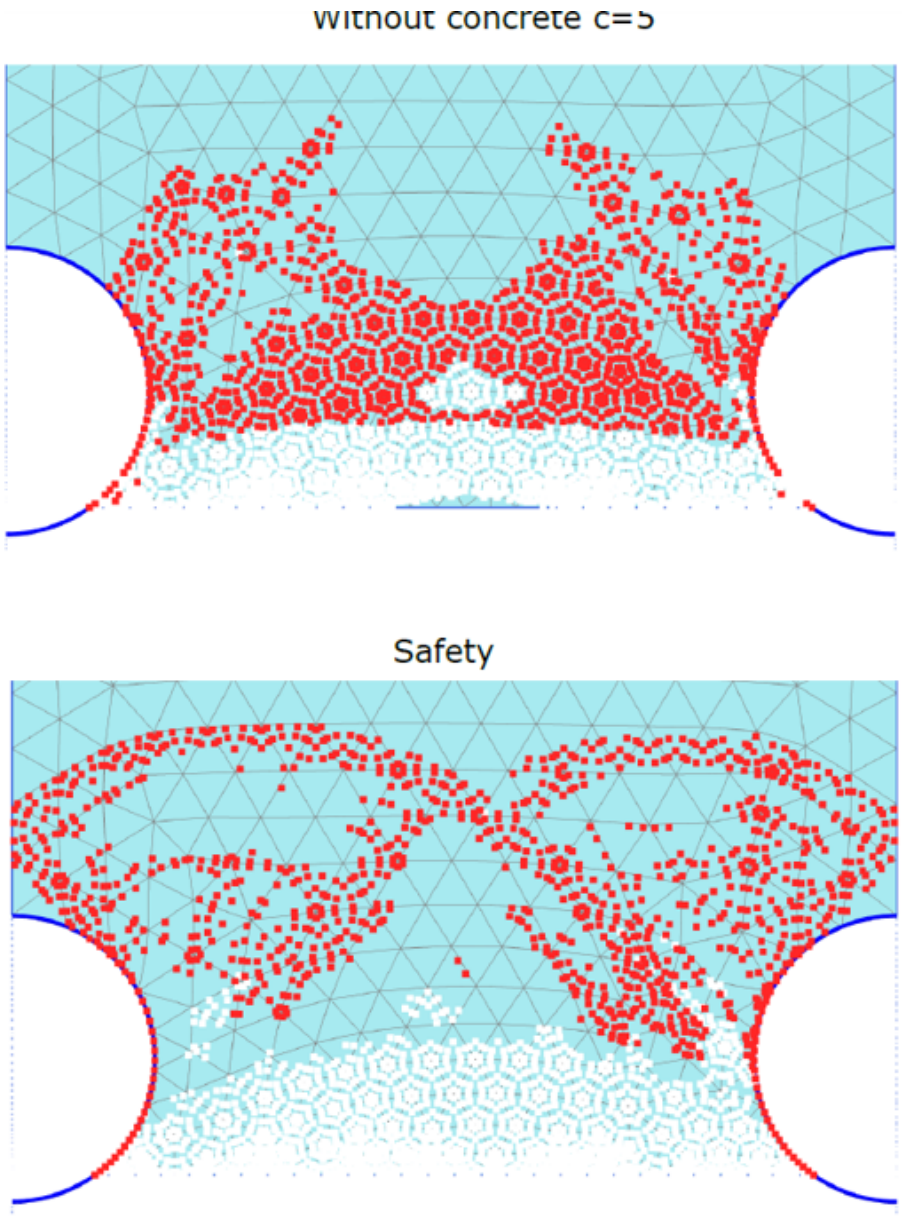

Figure B.3.10: Plastic points for straight excavation. First picture shows plastic points after excavation and second picture shows the plastic points after $c\phi$-reduction.

B.4 Sheet pile wall in Plaxis 2D

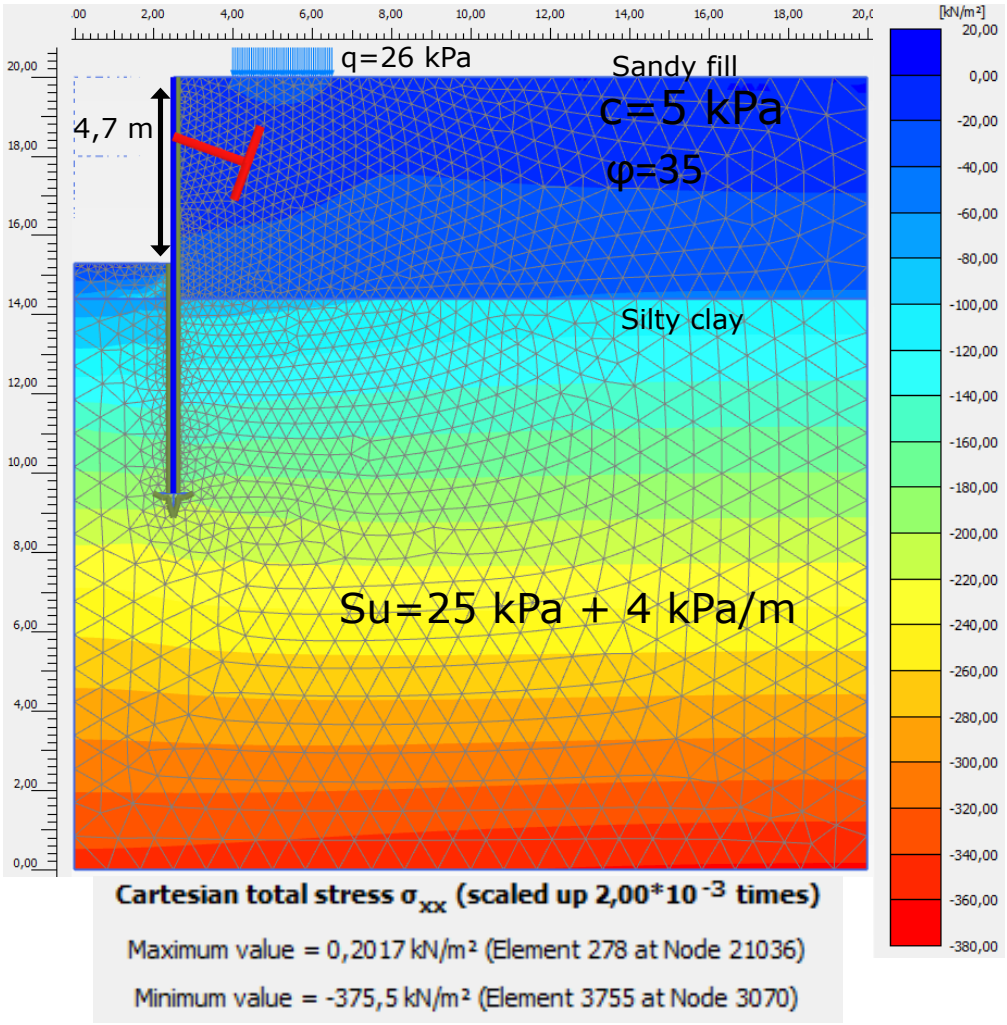

Figure B.4.1: Cartesian horizontal stresses after excavating to a depth of 4,7 meters.

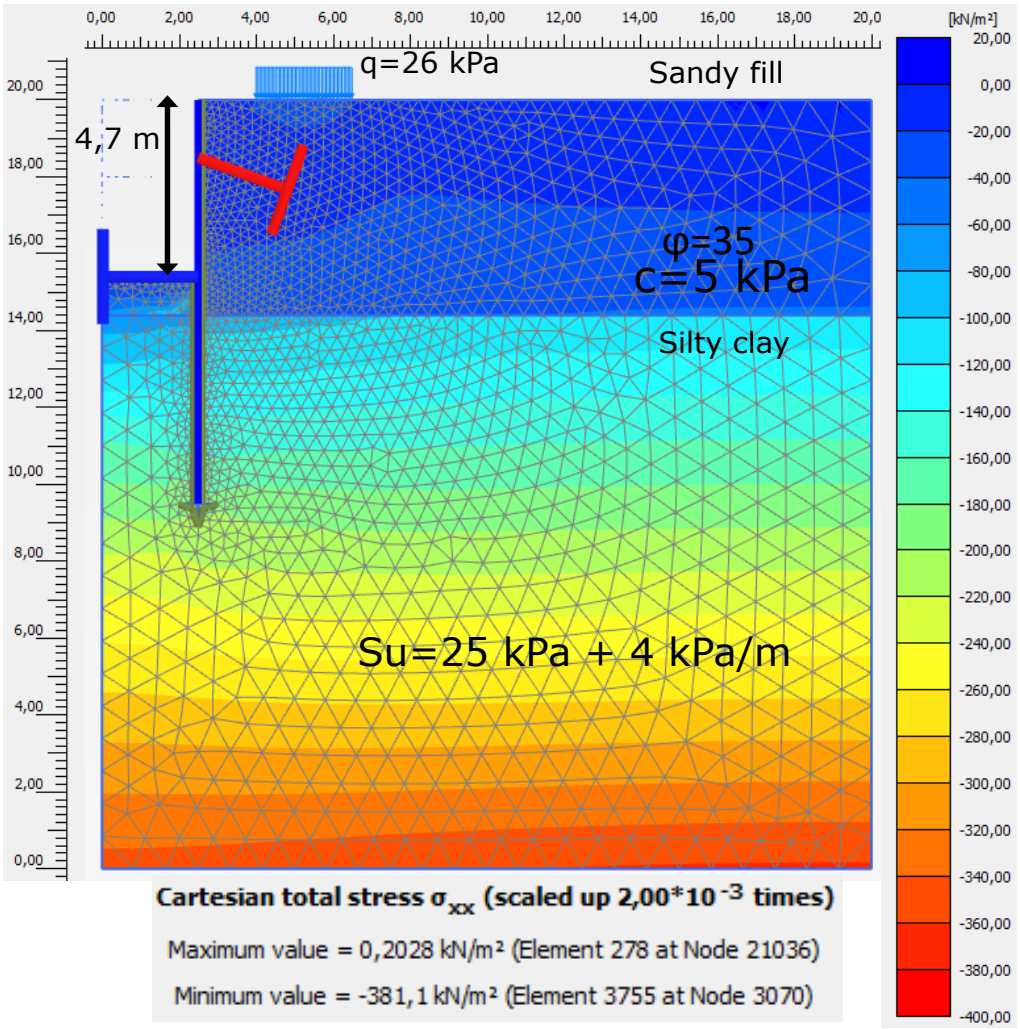

Figure B.4.2: Cartesian horizontal stresses after excavating to a depth of 4,7 meters and applying the second bracing consisting of H-beam struts.

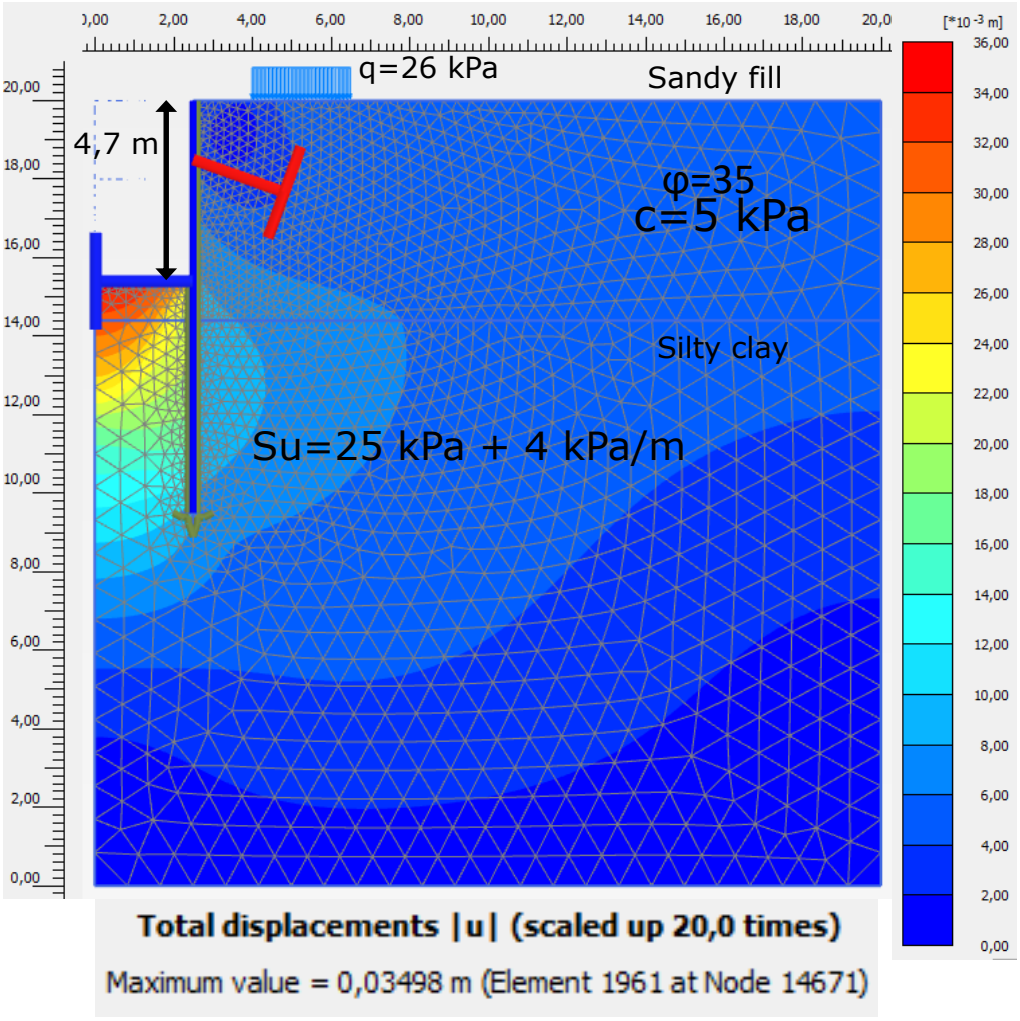

Figure B.4.3: Total displacements after activating the last strut for the pipe wall at Nordenga bridge.

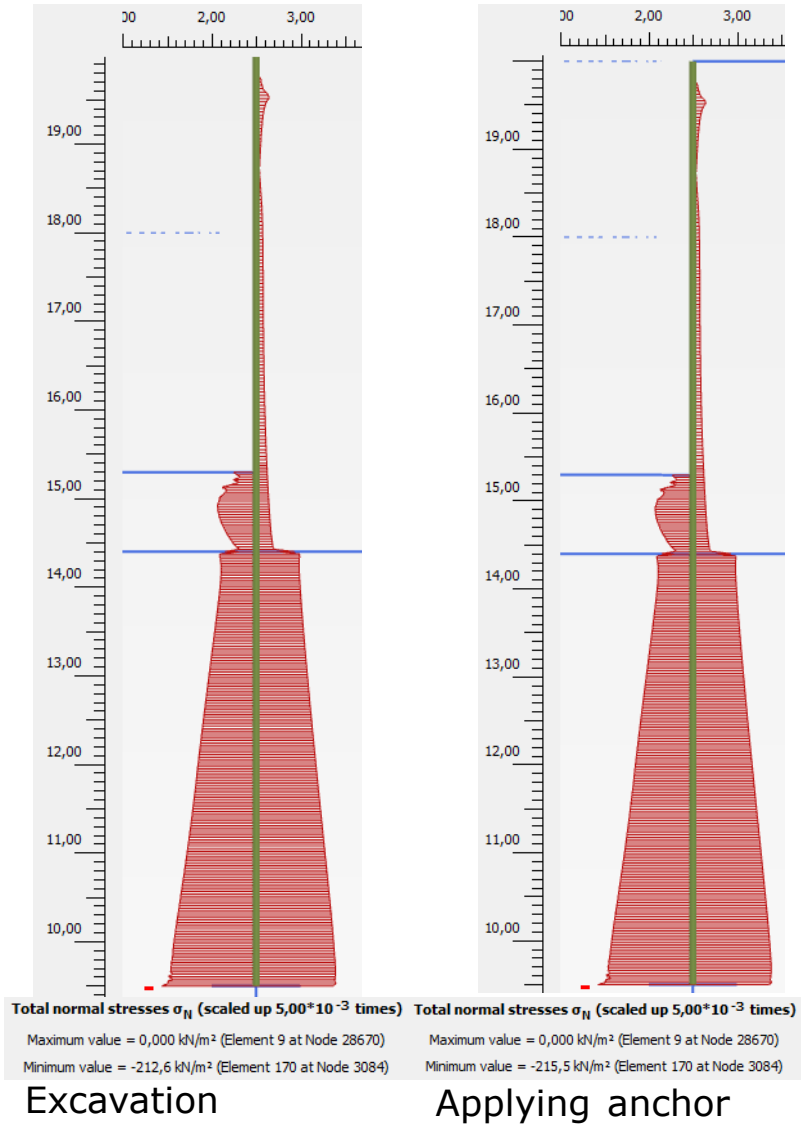

Figure B.4.4: Interface normal stresses from sandy fill sheet pile wall Plaxis calculation

B.5 Squeezing

Kevin Peter Cruz Sønsterud

Stability of Pipe Walls for Supporting Excavation in Cohesive Material and Clay

NTNU
Norwegian University of
Science and Technology